Analysis of the Role of Piwil2 gene in Tumorigenesis and Germline Stem Cell Metabolisms

Dissertation

zur Erlangung des Doktorgrades
der Mathematisch-Naturwissenschaftlichen Fakultät
der Georg-August-Universität zu Göttingen

vorgelegt von

Jae-Ho Lee

aus Seoul, Korea

Göttingen 2006

D7

Referent: Prof. Dr. W. Engel

Korreferentin: PD Dr. S. Hoyer-Fender

Tag der mündlichen Prüfungen:

INDEX

ABBREVIATIONS

a.a.	amino acids
ABI	Applied Biosystem Instrument
AP	Alkaline Phosphatase
APS	Ammonium peroxodisulfate
ATG	Translation intiation codon
ATP	Adenosintriphosphate
ATCC	American Type Culture Collection
AUAP	Abridged universal amplification primer
βa	β-actin promoter
BAC	Bacterial Artificial Chromosome
BCP	1-bromo-3-chloropropane
BFA	Brefeldin A
BPB	BromoPhenolBlue
β-gal	β-galactosidase
β-geo	a fusion gene between the β-galactosidase (β-gal) and neomycinphosphotransphearse (neo) genes
β-ME	β-Mercaptoethanol
bp	base pair
BSA	Bovine serum albumin
°C	Degree Celsius
CBF	Ciliary beat frequency
cDNA	complementary DNA
CIP	Calf intestine phosphatase
CMV	Cytomegalvirus
Cy3	indocarbocyanine
dATP	Desoxyriboadenosintriphosphate
dH2O	distilled Water
DAPI	Diamidino-2-phenylindole dihydrochloride

dCTP	Desoxyribocytosintriphosphate
DEPC	Diethylpyrocarbonate
DMEM	Dulbecco's Modified Eagle Medium
DMF	Dimethylformamide
DMSO	Dimethyl sulfoxide
DNA	Deoxyribonucleic acid
DNase	deoxyribonuclease
dNTP	deoxynucleotidetriphosphate
dpc	day post coitum
dsRNA	double-stranded RNA
dT	deoxythymidinate
DTT	Dithiothreitol
EDTA	Ethylene diamine tetraacetic acid
EGFP	Enhanced green fluorescence protein
EGL	External granular layer
ES	Embryonic stem
EST	Expressed sequenced tags
F	Filial generation
FCS	Fetal calf serum
FISH	Fluorescence in Situ Hybridisation
FITC	Fluorescence isothiocyanate
g	gravity
GFP	Green fluorescence protein
GITC	Guanidine-Isothiocyanate
gm	gram
hEF	Human Elongation Factor
HEPES	N-(-hydroxymethyl) piperazin,N'-3-propansulfoneacid
HPLC	High performance liquid chromatograpy
hr(s)	hour(s)
IGL	Internal granular layer
IFN	Interferon

IPTG	Isopropyl-ß-thiogalactopyranoside
IRES	Internal ribosomal entry sites
IVF	In vitro fertilisation
JL	Jackson Laboratory
kb	kilobase
kDa	kilodalton
LB	Luria-Bertrani
LIF	Recombinant leukaemia inhibitory factor
LPS	lipopolysaccharides
M	Molarity
Mbp	Mega base pair
MCS	Multicloning site
MEF	Mouse embryonic fibroblast
MeOH	Methanol
ML	Molecular layer
mRNA	messenger Ribonucleic acid
mg	milligram
µg	microgram
ml	milliliter
mM	millimolar
µl	microliter
µm	micrometer
µM	micromolar
min	minute
MW	Molecular Weight
N	Normal
NaAc	Sodium acetate
NaCl	Sodium chloride
NaOH	Sodium hydroxide
NBT	Nitro-blue tetrazolium
NCBI	National Center for Biotechnology Information

Neo	Neomycin(G-418)
ng	nanogram
NLS	Nuclear localisation sequence
nm	nanometer
nM	nanomolar
nt	Nucleotide
NTP	Nucleotidetriphospate
OD	Optimal density
ORF	Open Reading Frame
pA	polyadenylation signal
PAGE	Polyacrylamide Gel Electrophoresis
PCR	Polymerase chain reaction
pH	Preponderance of hydrogen ions
pmol	picomol
PBS	Phosphatebuffersaline
PBS-T	Phosphatebuffersaline + Tween 20
PCD	Primary ciliary dyskinesia
PI	Propidium iodide
PMSF	Phenylmethylsulfonyl fluoride
RACE	Rapid Amplification of cDNA Ends
RISC	RNA-induced silencing complex
RNA	Ribonucleic acid
RNAi	RNA interference
Rnase	Ribonuclease
rpm	revolution per minute
RT	Room temperature
RT-PCR	Reverse transcriptase-PCR
SDS	Sodium Dodecylsulfate
SDS-PAGE	SDS-Polyacrylamide Gel Electrophoresis
sec	second
siRNA	small interfering RNA

S.O.C medium	Sodium Chloride medium
SV 40	Simian Virus 40
Taq	Thermus aquaticus
TA	Thymidine-adenine
TBE	Tris-Borate-EDTA-Electrophoresis buffer
TE	Tris-EDTA buffer
TEMED	Tetramethylethylene diamine
Tris	Trihydroxymethylaminomethane
U	Unit
UAP	Universal amplification primer
UTR	Untranslated region
UV	Ultra violet
V	Voltage
v/v	volume/volume
w/v	weight/volume
WT	wild type
X-Gal	5-bromo-4-chloro-3-indolyl-ß-galactosidase
ZP	Zona pellucida

Symbols of amino acids

A	Ala	Alanine
B	Asx	Asparagine or Asparatic acid
C	Cys	Cysteine
D	Asp	Asparatic acid
E	Glu	Glutamic acid
F	Phe	Phenylalanine
G	Gly	Glycine
H	His	Histidine
I	Ile	Isoleucine
K	Lys	Lysine
L	Leu	Leucine
M	Met	Methionine
N	Asn	Asparagine
P	Pro	Proline
Q	Gln	Glutamine
R	Arg	Arginine
S	Ser	Serine
T	Thr	Threonine
V	Val	Valine
Z	Trp	Tryptophan
Y	Tyr	Tyrosine
W	Glx	Glutamine or Glutamic acid

Symbols of nucleic acid

A	Adenosine
C	Cytidine
G	Guanosine
U	Tymidine
T	Uridine

1. INTRODUCTION

1.1 *Piwi* Gene Family

Germ cells originate from primordial germ cells (PGC), a small population of cells set aside from other cell lineages very early in embryonic life. In *Drosophila,* gametes of both sexes are continuously produced from germline stem cells that are the progeny of PGCs (Lin, 1998). In mammals, the continuous production of male gametes similarly depends on stem cell system. PGCs differentiate into spermatogonia in testis through gonocytes during the development. In adult testis, sperms are produced from spermatogonia through spermatocyte and spermatid. One of the main issues in the study of germline stem cell system is the molecular mechanisms for the ability to self-renewal and the ability to produce numerous differentiated progeny like other stem cell systems such as hematopoietic stem cells and neural stem cells (Weissman, 2000). A fundamental question in stem cell biology, whose answer remains elusive, is whether there exists a universal molecular mechanism common to stem cell systems of various organisms or tissues. The gene family, including piwi, zwille and argonaute as family members, which is known to be involved in stem cell maintenance and differentiation, is likely a candidate. PIWI is a *Drosophila melanogaster* protein essential for maintaining germ-line stem cells (Cox et al., 1998, 2000). ZWILLE and ARGONAUTE are expressed in *Arabidopsis thaliana* and are necessary for stem cell division (Bohmert et al., 1998; Moussian et al., 1998; Lynn et al., 1999). PIWI and ZWILLE are involved in soma to germ cell signaling in *Drosophila* and *Arabidopsis*, respectively. RNA interference (RNAi) of *Caenorhabditis elegans* homologs of piwi, prg-1 and prg-2 resulted in depletion of germ line stem cells, indicating that prg-1 and prg-2 may also be involved in stem cell maintenance in nematodes (Cox et al., 1998). PIWI/ZWILLE homologs have a high degree of sequence similarity in their C-terminal regions; at least fifteen *C. elegans* genes contain this conserved region.

The *piwi* family genes encode basic proteins that contain a highly conserved PAZ domain of 110 amino acid residues in the middle region of the proteins and a 300 amino acid *piwi* domain in the C-terminal region (Cerutti et al., 2000). The *piwi* family gene play essential roles in stem cell self-renewal, gametogenesis and RNA interference in diverse organisms

ranging from *Arabidopsis* to human (Fig. 1.1). The name "PAZ domain" comes from the proteins **P**iwi, **A**rgonaut and **Z**wille. This domain is found in two families of proteins that are involved in post-transcriptional gene silencing. These are the *Piwi* family and the *Dicer* family (Fig. 1.2). The function of the domains is to bind the 2 nt 3'-overhang of the siRNA duplex and facilitates anchoring of this guide RNA into the effector complex (Ma et al., 2004).

In *Drosophila*, the loss of *piwi* function leads to the failure of germline stem cell self-renewal as well as downstream gametogenic functions such as germline cyst formation, egg polarity and possibly meiosis (Lin et al., 1997; Cox et al, 1998). Overexpression of *piwi* in somatic cells causes an increase both in the number of germline stem cells and the rate of their division. Thus, in *Drosophila*, *piwi* is a key regulator of stem cell division - its germline expression also contributes to promoting stem cell division in a cell-autonomous manner (Cox et al., 2000). Evolutionary relation was examined among 27 *Argonaute*-related genes from other species including mouse, rat, *Drosophila, C. elegans, Arabidopsis*, fission yeast and *N.crassa* (Fig. 1.3). In mammals, *piwi* genes are expressed specifically in testis and play a key role in spermatogenesis (Kuramochi-Miyagawa et al., 2001). In mouse genome, two *piwi* homologs have been identified (*Miwi* and *Mili* or *Piwil2*).

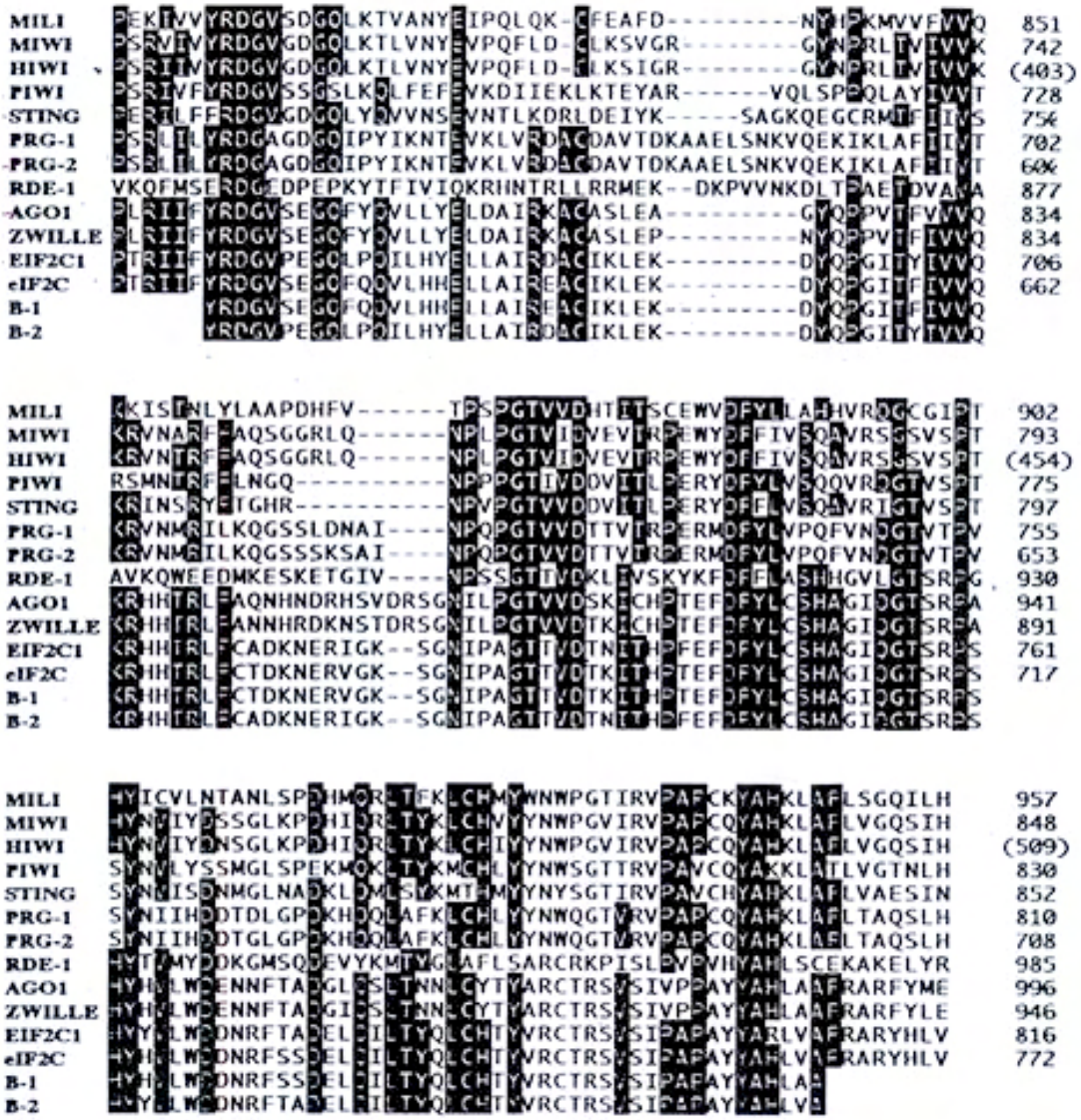

Figure 1.1: Alignment of the deduced amino acid sequences of MILI (Piwil2), MIWI (Piwil1), B-1 and B-2 with another ten proteins containing conserved PIWI regions. The sequences are MILI (mouse), MIWI (mouse), HIWI (human), PIWI (*Drosophila*), STING (*Drosophila*), PRG-1 (*C. elegans*), RDE-1 (*C. elegans*), AGO-1 (*Arabidopsis*), ZWILLE (*Arabidopsis*), EIF2C1 (human) and eIF2C (rabbit). The numbers indicate the amino acid positions. The highlighted sequences are identical at least in eight residues with solid boxes (adapted by Kuramochi-Miyagawa et al., 2001).

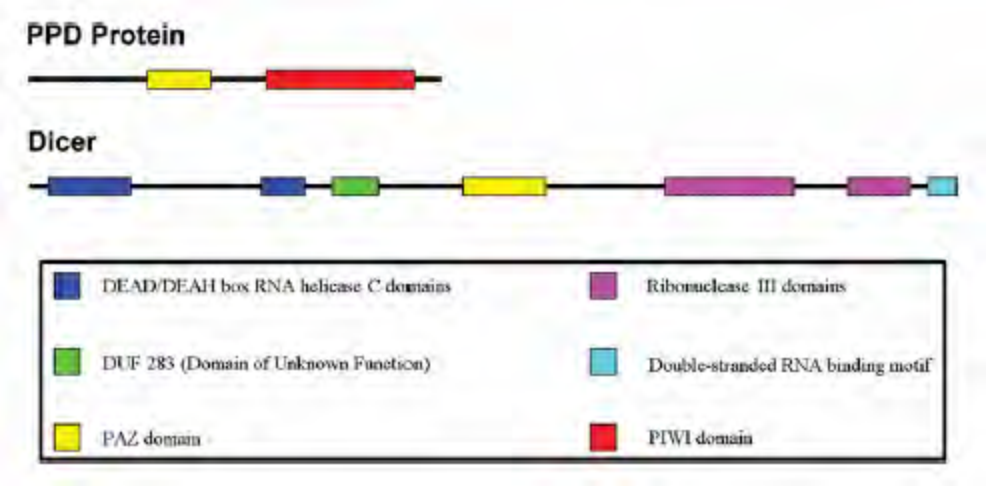

Figure 1.2: PPD protein and Dicer domain structures. PPD proteins are classically defined by the presence of PAZ and Piwi domains. The PAZ domain binds to siRNAs, whereas the Piwi domain serves as the binding site for Dicer. The Piwi domains of some PPD proteins possess endonuclease activity. The two ribonuclease III domains of Dicer dimerize to form the catalytic centre that is responsible for cleaving long dsRNA. Some Dicers, such as *Schiz. pombe* Dcr1, *A. thaliana* DCL4 and *D. melanogaster* Dcr1 do not have recognizable PAZ domains. One or more nuclear localization signals can be found in *A. thaliana* DCL1 and DCL4, *D. melanogaster* Dcr1, and mouse and human Dicers (adapted by Jaronczyk et al., 2005).

Miwi-null mice do not complete spermatogenesis. However, the arrest occurs at the beginning of the round spermatid stage and significantly downstream of the germline stem cell division stage (Deng et al., 2002). The *Piwil2*-null mice showed arrest of spermatogenesis at the spermatocyte stage, which is reminiscent of the phenotype of *Mvh* (mouse vasa homolog)-null mice (Kuramochi-Miyagawa et al., 2004).

In human, eight members of the *argonaute* family are identified. The *Argonaute* family was classified into two subfamilies: the *Piwi* subfamily, *Piwil1* (*hiwi*), *Piwil2* (*hili*), *Piwil3*,

Piwil4 (*hiwi2*) and the *eIF2C/AGO* subfamily. All four members of the *Piwi* subfamily are expressed mainly in testis (Sasaki et al., 2003).

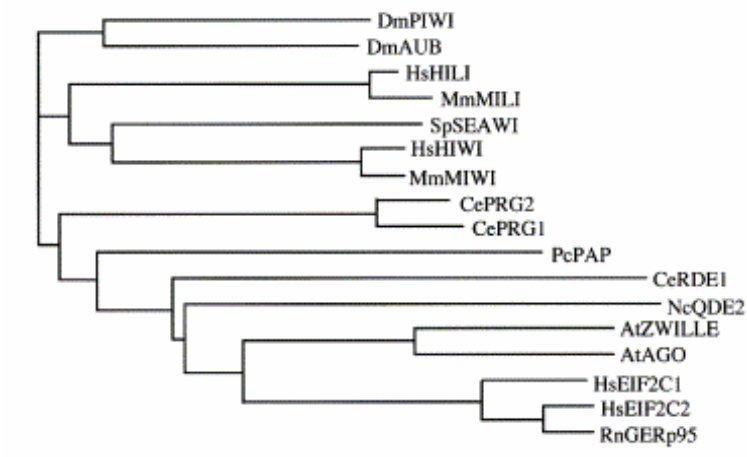

Figure 1.3: A phylogenetic tree of the representative members of the *piwi* family genes. MIWI (Piwil1) and MILI (Piwil2) from mice (gi 7416113), HIWI and HILI (gi 14042216) from humans, SEAWI from sea urchin (gi 12007643), PIWI and AUB from *Drosophila*, PRG-1 and PRG-2 from *C. elegans* and PAP from *Paramecium* (gi 6630673). Interestingly, most of these proteins are involved in the development of the germline or its equivalent. In addition, *piwi* shares significant homology to genes involved in RNA interference (*rde-1* in *C. elegans* and *qde-2* in *Neurospora*), meristem cell division (*Zwille* and *Agonaute* in *Arabidopsis*) and translational initiation (eIF2C1 and eIF2C2 in humans and GERp95 in rabbits) (adapted by Sasaki et al., 2003).

1.2 The role of *piwi* gene in tumorigenesis

In connection with tumors the issue of stem cells has been raised for several decades. Since tumor cells also exhibit self-renewal capacity, it seems plausible that their regulation is

similar to that of stem cells. Dysregulation of stem cell self-renewal is a likely requirement for the development of cancer. In addition, most cancers comprise a heterogenous population of cells with marked differences in their proliferative potential as well as the ability to reconstitute the tumor upon transplantation. Cancer stem cells are a minor population of tumor cells that posses the stem cell property of self-renewal. This new model for cancer will have significant ramifications for the way we study and treat cancer. In addition, through targeting the cancer stem cell and its dysregulated self-renewal, our therapies for treating cancer are likely to improve (Al-Hajj et al., 2004). It was reported that human *Piwil1* (*hiwi*) is specifically expressed in both normal and malignant male germ cells in a maturation stage-dependent pattern, in which it might function in germ cell proliferation (Qiao et al., 2002). It was also demonstrated that *Piwil1* (*hiwi*) is expressed in a variety of primitive hematopoietic cells and may play a role in determining or regulating hematopoietic stem cell development (Sharma et al., 2001). Altogether, the data from different organisms suggest a key role of *piwi* genes in stem cell division. The evidence that the piwi genes play essential roles in stem cell division is the basis of our hypothesis that overexpression of these genes leads to disturbance of cell division, causes tumors and therefore plays a role as dose-dependent oncogenic fate determinants.

Moreover, the chromosomal locus 12q24.33 that includes the *Hiwi* gene has been linked to testicular germ cell tumors (Skotheim et al., 2001; Summersgill et al., 2001). Conversely, deletion of this region is associated with hypogonadism (Sathya et al., 1999). Together, these observations are consistent with a scenario in which overexpression of certain PPD proteins is associated with increased mitosis in undifferentiated cells. The role of other PPD protein family members in this process is less clear. Paradoxically, there is evidence that some Argonaute proteins function as tumor suppressors. Specifically, chromosome 1 region p34-35, which is often lost in Wilms' tumors (Koesters et al., 1999; Dome et al., 2002), contains three human Argonaute genes (*hAgo1*, *hAgo3* and *hAgo4*) (Carmell et al., 2002). In addition, *miR15* and *miR16* are located in chromosome 13q14, a region lost in more than half of B-cell chronic lymphocytic leukaemias. Both genes are deleted or down-regulated in the majority of chronic lymphocytic leukaemia cases (Calin et al., 2002).

Finally, overexpression of *hAgo2* in a *Schizosaccharomyces pombe* strain lacking the *ago1* gene was shown to correct the cell cycle checkpoint deficiencies of this mutant (Carmichael

et al., 2004). These data suggest to a role for mammalian PPD proteins in enacting checkpoints in response to genotoxic stress.

In lower eukaryotes, the RNAi apparatus functions to maintain genome stability. Of course, it is not hard to imagine how RNAi effector proteins may indirectly affect cell cycle progression through their involvement in gene-silencing pathways that regulate expression of transcription factors and other proteins. However, it has recently become evident that PPD proteins and Dicer also function in siRNA-independent pathways that regulate cell cycle events (Carmichael et al., 2004). Accordingly, it is important to consider the aberrant expression of PPD proteins and Dicer in human cancers.

There is compelling, but indirect evidence that Dicer may also have a role in human cancer development. For example, in yeast lack of Dicer function results in chromosome segregation defects (Volpe et al., 2002; Provost et al., 2002) as well as failure to enact S-M cell cycle checkpoints (Carmichael et al., 2004). Both of these defects would be expected to contribute to the development of cancer in humans. Human Dicer can partially complement the loss of Dcr1 activity in yeast (Provost et al., 2002) and thus it is possible that the human enzyme also functions in cell-cycle regulation. Interestingly, human Dicer is also known to bind to 5-lipoxygenase (Provost et al., 1999), an enzyme whose activity is deregulated in pancreatic tumors (Ding et al., 2003). Lipoxygenase inhibitors are a promising new class of anticancer reagents (Kennedy et al., 2003) that have been shown to prevent lung tumors in mice and slow progression of adenomas to carcinomas (Gunning et al., 2002). Unfortunately, it is not known if or how Dicer affects the activity of lipoxygenase. In addition, the Burkitt lymphoma-derived cell line, EB-3, was found to possess 4-fold higher expression of Dicer mRNA than normal human lymphocytes and 2-fold higher activity of RNA polymerase III (Kaul et al., 2004). It is also important to note that Burkitt's lymphoma is characterized by increased activity of c-myc, a transcription factor that regulates genes involved in cell cycle progression and apoptosis (Hecht et al., 2000). These observations suggest that RNA polymerase III, whose promoter sequences are present in exon1/intron1 of the c-*myc* gene (Hecht et al., 2000), produces siRNAs that silence the negative-regulatory elements of c-myc expression (Kaul et al., 2004). Finally, the core RNAi proteins undoubtedly play a role in signaling and cancer that can be attributed to miRNA-regulated alteration of transcription factor expression (Lewis et al., 2003).

Altogether, the data from different organisms suggest a key role of *piwi* genes in stem cell division and tumorigenesis.

1.3 Function of *piwi* gene in spermatogenesis

Genes belonging to the *piwi* family are required for stem cell self-renewal in diverse organisms. The deduced amino acid sequences of mouse homologs MIWI (Piwil1) and MILI (Piwil2) show that each contains a well-conserved C-terminal PIWI domain and that each shares significant homology with PIWI and their human counterparts HIWI and HILI. *Piwil2* is found in germ cells of adult testis, suggesting that these genes may function in spermatogenesis. Furthermore, *Piwil2* is expressed in primordial germ cells (PGCs) of developing mouse embryos and may therefore play a role during germ cell formation. The data suggest that *Piwil2* regulates spermatogenesis and primordial germ cell production (Kuramochi-Miyagawa et al., 2001). Subcellular localization analysis of Piwi shows that it is a nucleoplasmic protein. This implies two things: *Piwi* may be involved in post-transcriptional mRNA processing in the nucleus or, alternatively, *Piwi* may be involved in nuclear functions indirectly related to gene expression. However, Piwil2 proteins are localized in cytoplasm. These data suggest that the proteins are involved in post-transcriptional regulation of mRNA in cytoplasm. Although circumstantial, these data raise the possibility that some of the family members may be involved in RNA post-transcriptional processing or translational regulation (Kuramochi-Miyagawa et al., 2001). Based on the notion that *Piwil2* may be involved in RNA processing, the RNA binding activity of these proteins was analysed, but RNA binding activity of Piwil2 could not be detected. Nevertheless, the possibility of the RNA binding activity of Piwil2 cannot be excluded. To further reveal the function of the mammalian homolog of *piwi*, mice with targeted mutations in the *Piwil2* gene, which is one of the two mouse homologs of *piwi*, were produced and analysed. Spermatogenesis in the Piwil2-null mice is blocked completely at the early prophase of the first meiosis, from the zygotene to early pachytene, and the mice are sterile. However, primordial germ cell development and female germ cell

production are not disturbed. Furthermore, Piwil2 binds to MVH, an essential factor during the early spermatocyte stage. The similarities in the phenotypes of the Piwil2- and MVH-deficient mice and in the physical binding properties of Piwil2 and MVH indicate a functional association of these proteins in post-transcriptional regulation. These data indicate that Piwil2 is essential for the differentiation of spermatocytes (Kuramochi-Miyagawa et al., 2004).

1.4 Objectives of this study

The aims and experimental approaches devised in this study can be placed in several categories, which are described below:

1) Expression analysis of *Piwil2* in different normal tissues and during germ cell development.

2) Expression analysis of *Piwil2* in tumor cell lines and tissues.

3) Characterization of potential molecular downstream targets of *Piwil2* in cell culture model related to tumorigenesis and in vitro stem cell metabolism.

4) Determination of the role of *Piwil2* in an in vivo “gain of function” transgenic model.

5) Establishment of an in vitro “gain of function” model and characterization of differentially regulated genes by using stem cell array.

2. MATERIALS AND METHODS

2.1 Materials

2.1.1 Chemicals

Acrylamide/Bisacrylamide	Roth, Karlsruhe
Acetic acid	Merck, Darmstadt
Agar	Roth, Karlsruhe
Agarose	Invitrogen, Karlsruhe
Ammonium acetate	Fluka, Neu Ulm
Ampicillin	Sigma, Deisenhofen
Ampuwa	Fresenius, Bad Homburg
Bacto-tryptone	Roth, Karlsruhe
Bacto-Yeast-Extract	Roth, Karlsruhe
BCIP	Applichem, Darmstadt
Blocking powder	Roth, Karlsruhe
Boric acid	Scharlau Chemie, Barcelona
BSA	Biomol, Hamburg
Cell culture media	Invitrogen, Karlsruhe
Clonfectin	BD Clontech, Palo Alto
Coomasie G-250	Sigma, Deisenhofen
Chloroform	Merck, Darmstadt
Crystal violet	Sigma, Deisenhofen
Vectashield (DAPI)	Vector, Burlingame
Diethyl pyrocarbonate (DEPC)	Sigma, Deisenhofen
Dulbecco's Modified Eagle Medium (DMEM)	PAN, Aidenbach
Dimethyl sulfoxid (DMSO)	Merck, Darmstadt

Dithiothreitol	Sigma, Deisenhofen
DNA Markers	Invitrogen, Karlsruhe
dNTPs (100 mM)	Invitrogen, Karlsruhe
Dye Terminator Mix	Applied Biosystems
EDTA	Sigma, Deisenhofen
Ethanol	Baker, Deventer, NL
Ethidium bromide	Roth, Karlsruhe
Ficoll 400	Applichem, Darmstadt
FCS	Invitrogen, Karlsruhe
Formaldehyde	Merck, Darmstadt
Formamide	Sigma, Deisenhofen
Glutaraldehyde	Serva, Heidelberg
Glycerol	Invitrogen, Karlsruhe
Glycine	Biomol, Hamburg
HBSS medium	Sigma, Deisenhofen
Horse serum	Sigma, Deisenhofen
HCl	Roth, Karlsruhe
H_2O_2	Merck, Darmstadt
HEPES	Merck, Darmstadt
Ionophore A23187	Calbiochem, Bad Soden
IPTG	Biomol, Hamburg
Isopropanol	Merck, Darmstadt
IVF Media	Medicult, Berlin
1 kb DNA Ladder	Gibco BRL, Karlsruhe
0.24-9.5 RNA Ladder	Gibco BRL, Karlsruhe
KCl	Merck, Darmstadt
M16 medium	Sigma, Deisenhofen
Methanol	Merck, Darmstadt
$MgCl_2$	Merck, Darmstadt
MOPS	Applichem, Darmstadt
β-Mercaptoethanol	Serva, Heidelberg

Mineral oil	Sigma, Deisenhofen
Na azide	Sigma, Deisenhofen
Na acetate	Merck, Darmstadt
Na citrate	Merck, Darmstadt
Na deoxycholate	Merck, Darmstadt
NaCl	Merck, Darmstadt
Na_2HPO_4	Merck, Darmstadt
NaH_2PO_4	Merck, Darmstadt
NaN_3	Merck, Darmstadt
NaOH	Merck, Darmstadt
NBT	Applichem, Darmstadt
Neomycin(G-418)	PAN, Aidenbach
NuPAGE LDS sample buffer (4x)	Invitrogen, Karlsruhe
NuPAGE MOPS SDS running buffer	Invitrogen, Karlsruhe
Orange G	Sigma, Deisenhofen
OPTI-MEM I	Invitrogen, Karlsruhe
Penicillin/Streptomycin	PAN, Aidenbach
PBS	Invitrogen, Karlsruhe
Phosphoric acid	Merck, Darmstadt
Picric acid	Fluka, Neu Ulm
Phenol	Biomol, Hamburg
Proteinase K	Applichem, Darmstadt
Protein marker	Invitrogen, Karlsruhe
Radioactive substances: $[\gamma^{32}P]$-ATP $[\alpha^{32}P]$-dCTP	Amersham, Braunschweig
Rediprime™ II	Amersham, Freiburg
RNase Inhibitor	Boehringer, Mannheim
RNA length standard	Invitrogen, Eggenstein
RNA reagent	Biomol, Hamburg
RNAse away	Biomol, Hamburg
Saccharose	Roth, Karlsruhe

Salmon sperms DNA	Sigma, Deisenhofen
SDS	Serva, Heidelberg
S.O.C Medium	Invitrogen, Karlsruhe
siRNA of Piwil2(mouse,human)	Eurogentec, Belgium
Luciferase double strand RNA	Eurogentec, Belgium
Triton X-100	Serva, Heidelberg
Tris	Sigma, Deisenhofen
Tween-20	Promega, Mannheim
X-Gal	Biomol, Hamburg
Xylol	Merck, Darmstadt

All those chemicals, which are not mentioned above, were ordered from Merck, Darmstadt or Roth, Karlsruhe.

2.1.2 Solutions, buffers and media

2.1.2.1 Agarose gel electrophoresis

5x TBE buffer	450 mM Trisbase 450 mM Boric acid 20 mM EDTA (pH 8.0)
Glycerol loading buffer -I	10 mM Tris/HCl (pH 7.5) 10 mM EDTA (pH 8.0) 0.025% Orange G 30% Glycerol

2.1.2.2 SDS-PAGE

40% Acrylamide stock solution	Acrylamide 29.2% (w/w) Bis-acrylamide 0.8% (w/w) 10% Ammonium persulfate solution in H_20
NuPAGE gel SDS sample buffer (4x)	10% Glycerol 62.5 mM Tris/HCl (pH 6.8) 2% SDS 0.01 mg/ml BPB
Running buffer (5x)	25 mM Tris/HCl (pH 8.3) 192 mM Glycine 0.1% SDS
Stacking gel buffer (4x)	0.5 M Tris/HCl (pH 6.8) 0.4% SDS
Separating gel buffer (4x)	1.5 M Tris/HCl (pH 8.3) 0.4% SDS

2.1.2.3 Frequently used buffers and solutions

AP buffer	100 mM Tris-HCl (pH 9.5) 100 mM NaCl 50 mM $MgCl_2$
BCIP-Solution	50 mg/ml BCIP 70% Dimethyl formamide
Blocking solution (immunostaining)	60 µl of horse serum,

	150 µl of 10%Triton X-100 2790 µl o PBS
Bouin's solution	15 volume of picric acid (in H_2O) 5 volume 37% formaldehyde 1 volume acetic acid
Carrier DNA	Sonicated salmon sperm DNA, 5 mg/ml
Denaturation solution	1.5 M NaCl 0.5 M NaOH
Depurination solution	0.25 M HCl
E-buffer (10x)	300 mM NaH_2PO_4 50 mM EDTA
Elution buffer	1.5 M NaCl 20 mM Tris/HCl (pH 7.5) 1 mM EDTA
Ligation buffer (10x)	600 mM Tris/HCl (pH 7.5) 80 mM $MgCl_2$ 100 mM DTT
Lysis buffer I	100 mM Tris/HCl (pH 8.0) 100 mM NaCl 100 mM EDTA 0.5% SDS
Lysis-buffer II	100 mM Tris/HCl (pH 8.0)

	5 mM EDTA 200 mM NaCl 0.2% SDS 100 µg/ml proteinase K
10x MOPS buffer	41.8 g MOPS 16.6 ml 3 M Sodium acetate 20 ml 0.5 M EDTA In 1 liter of DEPC Water Adjust pH to 6.75
NBT- solution	75 mg/ml NBT 70% Dimethyl formamide
Neutralisation solution	1.5 M NaCl 1 M Tris/HCl (pH 7.0)
PBS buffer	130 mM NaCl 7 mM $Na_2 HPO_4$ 4 mM $NaH_2 HPO_4$
Protein lysis buffer	150 mM NaCl 10 mM EDTA 50 mM Tris/HCl pH7.6 1% Triton X-100 1% sodium deoxycholate
Semidry transfer buffer (1x)	25 mM Tris pH 8.3 150 mM Glycin 10 % Methanol

SSC (20x)	3 M NaCl 0.3 M Na_3 citrate (pH 7.0) Stop-Mix 15% Ficoll 400 200 mM EDTA 0.1% Orange G
TE-buffer	10 mM Tris/HCl (pH 8.0) 1 mM EDTA
Washing solution I	2x SSC 0.1% SDS
Washing solution II	0.2x SSC

2.1.3 Laboratory materials

The laboratory materials, which are not listed here, were bought from Schütt and Krannich (Göttingen).

Cell culture flasks	Greiner, Nürtingen
Dialysis hoses	Serva, Heidelberg
Disposable filter Minisart	NMI Sartorius, Göttingen
Filter paper 0858	Schleicher and Schüll, Dassel
Hybond - C	Amersham, Braunschweig
Hybond - N	Amersham, Braunschweig
Microcentrifuge tubes	Eppendorf, Hamburg
Petri dishes	Greiner, Nürtingen
Pipette tips	Eppendorf, Hamburg
Roti-plast paraffin	Roth, Karlsruhe

Superfrost slides	Menzel, Gläser
Culture slides	Lab-Tek/Nalge, Nunc, IL, USA
Whatman blotting paper (GB 002, GB 003 and GB 004)	Schleicher and Schüll, Dassel
X-ray films	Amersham, Braunschweig

2.1.4 Sterilisation of solutions and equipments

All solutions that are not heat sensitive were sterilised at 121°C, 10^5 Pa for 60 min in an autoclave (Webeco, Bad Schwartau). Heat sensitive solutions were filtered through a disposable sterile filter (0.2 to 0.45 µm pore size). Plastic wares were autoclaved as above. Glassware were sterilised overnight in an oven at 220°C.

2.1.5 Media, antibiotics and agar-plates

2.1.5.1 Media for bacteria

LB Medium (pH 7.5):	1% Bacto-tryptone 0.5% Yeast extracts 1% NaCl
LB-Agar:	1% Bacto-trypton 0.5% Yeast extracts 1% NaCl 1.5% Agar

The LB medium was prepared with distilled water, autoclaved and stored at 4°C.

2.1.5.2 Media for cell culture

NIH3T3 fibroblasts	DMEM 10% fetal calf serum (FCS), 1% glutamine (200mM), 1% penicillin / streptomycin
GC-1	DMEM containing 15 mM HEFES, 0.45% glucose (w/w), 10% FCS, 2% penicillin(50units/ml)/ streptomycin(50µg/ml)
MDA-MB-231	DMEM supplemented with sodium pyruvate (1 mM), 10% FCS, 2% penicillin/ streptomycin
HeLa cell	(DMEM) containing 10% heat-inactivated FCS 2 mM L-glutamine, 100 U/ml penicillin, 100 µg/ml streptomycin

For long time storage of the cells in liquid nitrogen, the following freezing media were used:

NIH3T3 fibroblasts	90% culture media 10% DMSO
GC-1, MDA-MB-231, HeLa cell	95% culture media 5% DMSO

2.1.5.3 Antibiotics

Stock solutions were prepared for the antibiotics. The stock solutions were than filtered through sterile disposable filters and stored at -20°C. When antibiotics were needed, in each

case it was added after the autoclaved medium has cooled down to a temperature lower than 55°C.

	Master solution	Solvent	Final concentration
Ampicillin	50 mg/ml	H_2O	50 µg/ml
Kanamycin	25 mg/ml	H_2O	50 µg/ml
G 418	40 mg/ml	PBS	400 µg/ml
Gancyclovir	100 mM	PBS	2 µM
Mitomycin C	1 mg/ml	PBS	10 µg/ml
Zeocin	100 mg/ml	HEPES	1000 µg/ml
Blasticidin	10 mg/ml	H_2O	6-12 µg/ml

2.1.5.4 IPTG/X-Gal plates

LB-agar with 50 µg/ml ampicillin, 100 µM IPTG and 0.4% X-Gal was poured into Petri dishes. The dishes were stored at 4°C.

2.1.6 Bacterial strains

E. coli	DH5α	Invitrogen

2.1.7 Plasmids

pBluescript SK (+/-)	Stratagene, Amsterdam
pBluescript KS (+/-)	Stratagene, Amsterdam
pCDNA	BCCM/LMBP Plasmid collection, Belgium

pEF-BOS	BCCM/LMBP Plasmid collection, Belgium
pGEM-T Easy	Promega, Mannheim
pEGFP 1	Clontech, Palo Alto
pEGFP-N1	Clontech, Palo Alto

2.1.8 Synthetic oligonucleotide primers

The synthetic oligonucleotide primers used in this study were obtained either from Eurogentec (Köln) or Roth (Karlsruhe) and dissolved in water to a final concentration of 100 pmol/µl.

EGFP F2	5'-CTG AAG TTC ATC TGC TGC ACC AAA-3'
EGFP R2	5'-TTG AAG TCG ATG CCC TTC AGC-3'
EGFP TG 1R	5'-TGG TGC AGA TGA ACT TCA GG-3'
EGFP TG 1F	5'-GAA CAC TGC AAA TCT GAG CC-3'
EGFP TG 2R	5'-CCG ATT TCG GCC TAT TGG TT-3'
hEF-1a TG 1F	5'-CCA GCT TGG CAC TTG ATG TA-3'
Piwil2 TG 1R	5'-TGT CCT TGC GGA CCA TGT TA-3'
hCMV 1F	5'-CCA TTG ACG TCA ATG GGA GT-3'
f1 ORI 1R	5'-CGT GAA CCA TCA CCC TAA TC-3'
pEGFPN 1F	5'-CGG TGG GAG GTC TAT ATA AGC-3'
pEGFPN 1R	5'-CTG AAC TTG TGG CCG TTT ACG-3'
T7	5'-TAA TAC GAC TCA CTA TAG GG-3'
T3	5'-ATT AAC CCT TCA CTA AAG-3'
SP6	5'-AGG TGA CAC TAT AGA ATA C-3'
Blastidin F	5'-CCT TTG TCT CAA GAA GAA TCC A-3'
Blastidin R	5'-CCC TCC CAC ACA TAA CCA GAG G-3'
Zeocin F	5'-CGC GAC GTC GCC GGA GCG GTC G-3'
Zeocin R	5'-CGG AGG CGT CCC GGA AGT TCG T-3'

Piwil2 2F(mouse)	5’-GCA CAG TCC ACG TGG TGG AAA -3’
Piwil2 2R(mouse)	5’-TCC ATA GTC AGG ACC GGA GGG -3’
Piwil2 2F (human)	5’-CAG GCA GAG GCC ATG TAT TT-3’
Piwil2 2R (human)	5’-AAC ATG CCG ACC TCA TGC T-3’
Cyclin D1 F(mouse)	5’-TGA CAC CAA TCT CCT CAA CG-3’
Cyclin D1 R(mouse)	5’-AGC TTG TTC ACC AGA AGC AG-3’
Stat3 F(mouse)	5’-TAG CCG ATT CCT GCA AGA GT-3’
Stat3 R(mouse)	5’-AGC CAG CTC TTA TCA GTC A-3’
Akt F (mouse)	5’-TAT TGG CTA CAA GGA AGG C-3’
Akt R (mouse)	5’-TCT TCA TGG CAT AGT AGC AA-3’
Bcl-X_L F (mouse)	5’-TCG AAG AGA ATA GGA CTG AG-3’
Bcl-X_L R (mouse)	5’-TCA AAG CTC TGA TAC GCG GT-3’
Bcl-X_L F (human)	5’-ATC AAT GGC AAC CCA TCC TG-3’
Bcl-X_L R (human)	5’-GTA AGT GGC CAT CCA AGC TG-3’
Cyclin D1 F(human)	5’-TGC ATG TTC GTG GCC TCT AA-3’
Cyclin D1 R(human)	5’-CAG TCT GGG TCA CAC TTG AT-3’
Akt F (human)	5’-ACG CCA TGA AGA TCC TCA AG-3’
Akt R (human)	5’-TTA ATG TGC CCG TCC TTG TC-3’
Stat3 F (human)	5’-ATT GAC CAG CAG TAT AGC CG-3’
Stat3 R (human)	5’-TTC CAG CTG CTG CAT CTT CT-3’
GAPDH F (mouse)	5’-CAC CAC CAA CTG CTT AGC C-3’
GAPDH R (mouse)	5’-CGG ATA CAT TGG GGG GTA GG-3’
GAPDH F (human)	5’-CCA GCA AGA GCA CAA GAG GAA GAG-3’
GAPDH R (human)	5’-AGC ACG GGA TAC TTT ATT AGA TG-3’
piwil2 siRNA Forward	5’-ACA CAG CAU UCC GGC CUC CUU CAA A-3’
piwil2 siRNA Reverse	5’-UUU GAA GGA GGC CGG AAU GCU GUG U-3’
Pdgfrb F(mouse)	5’-AGG TCA TTG AGT CTG TGA GC-3’
Pdgfrb R(mouse)	5’-ATC GGC AGT ATT CCG TGA TG-3’
Slc2a1 F(mouse)	5’-TGT CAC CTA CAG CTC TAC GT-3’
Slc2a1 R(mouse)	5’-TGA AGG CCG TGT TGA CGA TA-3’
Gja7 F(mouse)	5’-CTG TAT GGC TTC CAA GTC CA-3’

Gja7 R(mouse)	5’-GTT CCT GAG CCA TTC TGA TC-3’
Thy-1 F(mouse)	5’-AAC TCT TGG CAC CAT GAA CC-3’
Thy-1 R(mouse)	5’-TCC AGG ATG TGT TCT GAA CC-3’
Itga6 F(mouse)	5’-AAC ATC AGA GAC AAG CTG CG-3’
Itga6 R(mouse)	5’-CTC AGT TCT CTG TAA GCG GA-3’
Itgb1 F(mouse)	5’-CCT ACT TCT GCA CGA TGT GA-3’
Itgb1 R(mouse)	5’-CAC CTT CTG GAG AAT CCA AG-3’
Egr3 F(mouse)	5’-GTG ACC ATG AGC AGT TTG CT-3’
Egr3 R(mouse)	5’-GGT ACA GGT TGT AGT CAG GT-3’
Stra8 F(mouse)	5’-TCA CAG CCT CAA AGT GGC AGG-3’
Stra8 R(mouse)	5’-GCA ACA GAG TGG AGG AGG AGT-3’
CD9 F (mouse)	5’-TGC AGT GCT TGC TAT TGG AC-3’
CD9 R (mouse)	5’-GTT CAT CCT TGC TCC GTA AC-3’
Hsp90a F (mouse)	5’-ATC TCC AAT TCA TCG GAC GC-3’
Hsp90a R (mouse)	5’-TAT CTG CAC CAG CCT GCA AA-3’

2.1.9 cDNA probes for Northern blotting

Akt	generated in present study
Bcl-X_L	generated in present study
Cyclin D1	generated in present study
Egr3	generated in present study
Ets2	generated in present study
Gja7	generated in present study
hEF	generated in present study
Itga6	generated in present study
Itgb1	generated in present study
GFP	generated in present study
NFkB2	generated in present study

Pdgfrb	generated in present study
Piwil2	generated in present study
RelA	generated in present study
Slc2a1	generated in present study
Stat2	generated in present study
Stat3	generated in present study
Thy-1	generated in present study

2.1.10 Eukaryotic cell lines

RI mouse embryonic stem cell line (Passage 11)	Dr. A. Nagi, Toronto, Canada
NIH 3T3	Institut für Humangenetik, Göttingen
MDA-MB-231	ATCC, Rockville, USA
GC-1	ATCC, Rockville, USA
HeLa	ATCC, Rockville, USA

2.1.11 RNA samples of human and mouse

2.1.11.1 Total RNAs from normal human tissues (BD Clontech, Palo Alto, CA, USA)

Human total RNAs from colon, bone marrow, brain, small intestine, fetal brain, fetal liver, heart, kidney, spinal cord, lung, placenta, prostate, salivary gland, skeletal muscle, spleen, testis, stomach, thyroid, trachea and uterus were purchased from BD Biosciences.

2.1.11.2 Total RNAs from human cancer tissues

Human cancer tissues RNA from colon cancer (n=2), ovarian dysgerminoma (n=2), malignant mixed mullerian tumor (MMMT) of the endometrium (n=2), clear cell renal cell carcinoma (n=2), gastrointestinal stromal tumor (n=4), stromal sarcoma of endometrium (n=2), adenocarcinoma of endometrium (n=2), squamous cell carcinoma of pancreas (n=1), adenocarcinoma of pancreas (n=1), ovarian cancer (n=4), prostate carcinoma (n=4), mamacarcinoma (n=7) and lymphatic gland tumors (n=5) were isolated for RT-PCR analysis.

2.1.11.3 Total RNAs from human cancer cell lines

Cell lines of PC3 (prostate cancer), MDA-MB-231 (breast cancer), LNCAP (prostate cancer), HeLa (cervical cancer), Jurkat (T cell leukaemia), MCF-7 (breast adenocarcinoma), Daudi (Burkitt's lymphoma), 2102EP (embryonal carcinoma), DU-145 (prostate cancer) and H12.1 (embryonal carcinoma) were used for isolation of RNA and RT-PCR analysis.

2.1.11.4 Total RNAs from wild type mouse tissues

Each RNAs from spleen, lung, heart, brain, kidney, skeletal muscle, ovary, liver, testis, breast, cerebellum and from testes of W/W^v, olt/olt, qk/qk, Ley $^{-/-}$ and Tfm/y were isolated for RT-PCR analysis.

2.1.11.5 Total RNAs from mouse cancer tissues

Mouse breast cancer tissues (n=2), rhabdomyosarcoma (n=3) and meduloblastoma (n=3) were obtained from Prof. Dr. H. Hahn.

2.1.11.6 Total RNAs from mouse tumor cell lines

Cell lines from transformed germ cells (GC-1 and GC-2), transformed Leydig cell line (MA-10), teratocarcinoma cell line F9, non-transformed spermatocytes (GC-4) and Sertoli

cell (15P-1) line and non-testicular tumor cell lines PTC (pituitary gland), BT (breast tumor) and NS 20Y (neuroblastoma) were used for isolation of RNA and RT-PCR analysis.

2.1.11.7 Total RNAs from human bloods

Normal woman blood (n=4).

2.1.12 Mouse strains

Mouse strains C57BL/6J, 129X1/SvJ, C3H/J and DBA/2J were initially ordered from Charles River Laboratories, Wilmington, USA and further bred in Animal facility of Institute of Human Genetics, Göttingen.

2.1.13 Antibodies

Rabbit anti rabbit Piwil2 peptide Antibody	Eurogentec, Belgium
Goat anti mouse Itga6 Antibody	Santa Cruz Biotechnology, Heidelberg
Mouse anti mouse Stra8 Antibody	Eurogentec, Belgium
Mouse anti mouse CD9 Antibody	Santa Cruz Biotechnology, Heidelberg
Mouse anti mouse α-tubulin Antibody	Sigma, Deisenhofen
Mouse anti mouse Stat3 Antibody	Biomol, Hamburg
Rabbit anti goat Hsp90a Antibody	Santa Cruz Biotechnology, Heidelberg
Goat anti rabbit IgG FITC and Cy3-conjugated Antibody	Sigma, Deisenhofen

Sheep anti mouse IgG Cy3-conjugated Antibody	Sigma, Deisenhofen
Goat anti rabbit IgG alkaline phosphatase conjugated Antibody	Sigma, Deisenhofen

2.1.14 Enzymes

Alkaline phosphatase	New England Biolabs, Frankfurt am Main
Platinum Taq polymerase	Invitrogen, Karlsruhe
Proteinase K	Sigma, Deisenhofen
Restriction enzymes (with supplied buffers)	Invitrogen, NEB, Karlsruhe, Frankfurt am Main
RNase A	Qiagen, Hilden
RNase H	Invitrogen, Karlsruhe
RNase inhibitors	Invitrogen, Karlsruhe
Superscript-II	Invitrogen, Karlsruhe
Taq Polymerase	Invitrogen, Karlsruhe
T4 DNA ligase	Promega, Mannheim
T4 RNA ligase	Invitrogen, Karlsruhe
Trypsin	Invitrogen, Karlsruhe

2.1.15 Kits

ApoAlert DNA fragmentation kit	BD Clontech, Palo Alto
Cancer PathwayFinder Gene Array	SuperArray, Hamburg
CLONfectin	Clontech, Palo Alto

Dye Terminator Cycle Sequencing-Kit	Applied Biosystem
DYEnamic ET-Terminator mix	Amersham Pharmacia
Endo Free Plasmid Maxi Kit	Qiagen, Hilden
Human Cancer Profiling ArrayII	Clontech, Palo Alto
Lipofectamine 2000	Invitrogen, karlsruhe
Megaprime DNA Labeling Kit	Amersham Pharmacia, Braunschweig
Maxi Plasmid Kit	Qiagen, Hilden
Mega Plasmid Kit	Qiagen, Hilden
Mini Plasmid Kit	Qiagen, Hilden
Mouse stem cell gene array	SuperArray, Hamburg
QIAEX II	Qiagen, Hilden
QIAquick Gel Extraction Kit	Qiagen, Hilden
QIA shredder kit	Qiagen, Hilden
Quantos cell proliferation assay	Stratagene, Amsterdam
Rediprime™ II Random Prime Labeling System	Amersham Pharmacia, Braunschweig
RNeasy Minikit	Qiagen, Hilden

2.1.16 Instruments

ABI PRISM 377 DNA Sequencer	Applied Biosystem, Braunschweig
ABI 3100 Genetic Analyser	Applied Biosystem, Braunschweig
Autoclave	Webeco, Bad Schwartau
Centrifuge 5415 D	Eppendorf, Hamburg
Centrifuge 5417 R	Eppendorf, Hamburg

Biophotometer	Eppendorf, Hamburg
Biofuge 13	Heraeus, Hanau
FACStar Plus	Becton Dickinson, Heidelberg
FACScan	Becton Dickinson, Heidelberg
GeneAmp PCR System 9700	Perkin Elmer, Rodgau - Jügesheim
Histocentre 2 embedding machine	Shandon, Karlsruhe
Inverted Microscope IX81	Olympus, Planegg
Megafuge 1.0 R	Heraeus, Hanau
Microscope BX60	Olympus, Planegg
Microtom Hn 40 Ing.,	Nut hole
Microplate-Reader, Model 450	BioRad, München
Neubauer cell chamber	Schütt Labortechnik, Göttingen
Pipette	Eppendorf, Hamburg
Power supply	Gibco BRL, Karlsruhe
Refrigerated Superspeed Centrifuge RC-5B	Sorvall, Langenselbold
Semi-Dry-Blot Fast Blot	Biometra, Göttingen
Spectrophotometer Ultraspec 3000	Amersham Pharmacia, Braunschweig
SpeedVac concentrator SVC 100H	Schütt Labortechnik, Göttingen
Thermomixer 5436	Eppendorf, Hamburg
Turboblotter™	Schleicher & Schüll, Dassel
UV Stratalinker™ 1800	Leica, Bensheim
X-Ray Automatic Processor Curix 60	Agfa, Köln

2.2 Methods

2.2.1 Isolation of nucleic acids

2.2.1.1 Isolation of plasmid DNA

(Sambrook et al., 1989)

2.2.1.1.1 Small-scale isolation of plasmid DNA

A single *E.coli* colony was inoculated in 5 ml of LB medium with the appropriate antibiotic and incubated in a shaker for 16 hrs at 37°C with a vigorous shaking. 0.5 ml of this culture was used for making glycerol stock (0.5 ml of culture and 0.5 ml of glycerol) and rest was centrifuged at 2000 x g for 10 min. The pellet was resuspended in 100 µl of solution P1. The bacterial cells were lysed with 200 µl of P2 solution and then neutralised with 150 µl of P3 solution. The precipitated solution was centrifuged at 10000 x g at 4°C. The supernatant was transferred into a new tube and centrifugation was done again. The supernatant was transferred into a new tube and 1 ml of 100% ethanol was added to precipitate the DNA. It was then stored on ice for 15 min, centrifuged at full speed for 20 min and finally the pellet was washed with 70% ethanol and after air-drying was dissolved in 30 µl of sterile water.

P1	50 mM Tris-Cl, pH 8 10 mM EDTA 100 µg/ ml RNase A
P3	200 mM NaOH, 1% SDS
P2	3.0 M Potassium acetate, pH 5.5

2.2.1.1.2 Large-scale preparation of plasmid DNA

A single clone was inoculated in 2 ml LB medium with appropriate antibiotic as a pre-culture for 8 hrs in 37°C shaker. This pre-culture was added in a dilution of 1:100 fold into 100 ml LB medium with appropriate antibiotic and incubated overnight at 37°C with shaking. The culture was centrifuged then at 6000 x g for 15 min. The pellet was resuspended in 4 ml of solution P1 and cells were then lysed with 4 ml of P2 and incubated on ice for 5 min. 4 ml of P3 buffer was added, mixed and incubated on ice for 15 min. The precipitated solution was centrifuged at 20000 x g for 30 min at 4°C. Meanwhile, the column (Qiagen-tip) that was provided with the midi preparation kit was equilibrated with 10 ml of QBT solution. After centrifugation the lysate was poured into this equilibrated column thus allowing the DNA to bind with the resin present in the bed of the column. The column was then washed twice with 10 ml of solution QC. Finally, the DNA was eluted with 5 ml of QF solution. To precipitate the DNA, 3.5 ml of isopropanol was added, mixed thoroughly and centrifuged at 14000 x g for 30 min at 4°C. The DNA pellet was washed with 70% ethanol and dissolved in 100 µl of TE buffer.

QBT	750 mM Sodium chloride
	50 mM MOPS (pH 7.0)
	15% Ethanol
	0.5% Triton X-100
QF	1 mM Sodium chloride
	50 mM MOPS (pH 7.0)
	15% Ethanol
QC	1.25 M Sodium chloride
	50 mM Tris/HCl (pH 8.5).

2.2.1.1.3 Endotoxin free preparation of plasmid DNA

Endotoxins, also known as lipopolysaccharides (LPS), are cell membrane components of Gram-negative bacteria (e.g. *E.coli*). During lysis of bacterial cells for plasmid preparations, endotoxin molecules are released from the outer membrane into the lysate. Endotoxins strongly influence transfection of DNA into primary cells and cultured cells like embryonic stem (ES) cells. Increased endotoxin levels lead to sharply reduced transfection efficiencies. Endofree plasmid preparation kit integrates endotoxin removal into standard plasmid preparation procedure. The neutralised bacterial lysate was filtered through a QIAfilter cartridge (provided in kit) and incubated on ice with a specific Endotoxin Removal buffer (patented by Qiagen). The endotoxin removal buffer prevents LPS molecules from binding to the resin in the columns (QIAGEN-tips), thus allowing purification of DNA containing less than 0.1 endotoxin unit per µg plasmid DNA.

2.2.1.2 Isolation of genomic DNA from mouse tail samples

(Laird et al., 1991)

Lysis buffer I	100 mM Tris/HCl (pH 8.0)
	100 mM NaCl
	100 mM EDTA
	0.5% SDS

The method was performed according to Laird et al. (1991). 1 to 2 cm of mouse tail was incubated in 700 µl of lysis buffer I containing 30 µl Proteinase K (10 µg/µl) at 55°C for overnight in Thermomixer 5436. To the tissue lysate, equal volume of phenol was added, mixed by inverting several times and centrifuged at 10000 x g at RT for 5 min. After transferring the upper aqueous layer into a new tube, the same procedure was repeated, first with 1:1 ratio of phenol and chloroform and then with chloroform alone. Finally, the DNA was precipitated with 700 µl of isopropanol, washed with 500 µl of 70% ethanol, dissolved in 100-200 µl of sterile water and incubated at 60°C for 10-20 min. DNA was then stored at 4°C.

2.2.1.3 Isolation of total RNA from tissue samples and cultured cells

(According to Chomczynski and Sacchi, 1987).

Total RNA isolation reagent (Biomol) is an improved version of the single-step method for total RNA isolation described first by Chomczynski and Sacchi (1987). The composition of reagent includes phenol and guanidine thiocyanate in a monophase solution. In order to avoid any RNase activity, homogeniser used for RNA isolation was previously treated with RNase away and DEPC water and special RNase free Eppendorf cups were used during the procedure. 100 mg tissue sample was homogenised in 1 ml of RNA reagent by using a glass-teflon homogeniser. The sample volume should not exceed 10% of the volume of reagent used for the homogenisation. The homogenate was vortexed and incubated on ice for 5 min to permit the complete dissociation of nucleoprotein complexes. Then, 0.2 ml of chloroform was added, vortexed and incubated on ice for 5 min. After centrifuging at 800 x g for 15 min at 4°C, the colourless upper aqueous phase was transferred into a new tube. 500 µl of isopropanol was added, solution was mixed by vortexing and RNA was precipitated by centrifugation at 10000 x g for 1 min. Finally, the pellet was washed with 75% ethanol and dissolved in 50-100 µl DEPC-H_2O. The RNA was stored at -80°C. To isolate total RNA from cultured cells, 350 µl of reagent was added to the 6 cm diameter Petri dish. Cells were collected with a rubber stick and the lysate was transferred into a QIA shredder in 2 ml cup. Probe was then centrifuged for 2 min at 10000 x g in order to homogenise. 350 µl of 70% ethanol was added and mixed. Mixture was put in RNeasy mini spin column, centrifuged for 15 sec at 60 g and washed with 700 µl of washing buffer I. Filter was put into new cup, 500 µl of RPE was added and centrifuged for 2 min at 6000 x g. After removing of supernatant, washing buffer II was repeated. Finally filter was put into new 1.5 ml cup, 30-50 µl of DEPC treated H_2O was added and centrifuged for 1 min at 6000 x g.

2.2.2 Determination of nucleic acid concentrations

The concentration of nucleic acids was determined spectrophotometrically by measuring absorption of the samples at 260 nm. The quality of nucleic acids, i.e. contamination with salt and protein was checked by the measurements at 230, 280 and 320 nm. The concentration was calculated according to the formula:

C = (E 260 – E 320) fc
C = concentration of sample (µg/µl)
E 260 = ratio of extinction at 260 nm
E 320 = ratio of extinction at 320 nm
f = dilution factor
c = concentration (standard) / absorption (standard)
For double stranded DNA: c = 0.05 µg/µl
For RNA: c = 0.04 µg/µl
For single stranded DNA: c = 0.03 µg/µl

2.2.3 Gel electrophoresis

Gel electrophoresis is the technique by which mixture of charged macromolecules, especially nucleic acids and proteins are separated in an electrical field according to their mobility which is directly proportional to macromolecule's charge to mass ratio.

2.2.3.1 Agarose gel electrophoresis of DNA

Agarose gels are used to electrophorese nucleic acid molecules from as small as 50 base pairs to more than 50 kilobases, depending on the concentration of the agarose and the precise nature of the applied electrical field (constant or pulse). Usually, 1 g of agarose was added in 100 ml 0.5x TBE buffer and boiled in the microwave to dissolve the agarose, then cooled down to about 60°C before adding 3 µl ethidium bromide (10 mg/ml). This 1% agarose gel was poured into a horizontal gel chamber. 0.5x TBE buffer was used also as

electrophoresis buffer. Before loading the samples about 0.1 volumes of loading buffer was added and mixed. The samples were then loaded into the wells of the gel and electrophoresis was carried out at a steady voltage (50-100 V). Size of the DNA fragments on agarose gels was determined using 1 kb DNA ladder, which was loaded with samples in parallel slots. DNA fragments were observed and photographed under UV light.

2.2.3.2 Agarose gel electrophoresis of RNA

(Hodge, 1994)

Single-stranded RNA molecules often have complementary regions that can form secondary structures. Therefore, RNA was run on a denaturing agarose gel that contained formaldehyde and before loading, the RNA was pre-treated with formaldehyde and formamide to denature. 2 g of agarose was added to 20 ml of 10x MOPS buffer and 148 ml of DEPC water and dissolved by heating in microwave oven. After cooling it to about 50°C, 33.2 ml of formaldehyde (37%) was added, stirred and poured into a horizontal gel chamber. RNA samples were prepared as follows:

10-20 µg RNA
2 µl 10x MOPS Buffer
3 µl Formaldehyde
7 µl Formamide (40%)
1 µl Ethidium bromide
5 µl Loading buffer

Samples were denatured at 65°C for 10 min and chilled on ice before loading into the gel. The gel was run at 30 V at 4°C overnight. To determine the size of the nucleic acid fragments on agarose gels, molecular weight ladder (0.24-9.5 RNA ladder) was loaded with samples in parallel slots.

2.2.3.3. SDS-PAGE of proteins

(Laemmli, 1970)

SDS-Page (Sodium Dodecylsulfate-Polyacrylamide Gel Electrophoresis) gel electrophoresis can be used for separating proteins for analysis and molecular weight determination. The proteins are denatured and rendered monomeric by boiling in the presence of reducing agents (β-mercaptoethanol or dithiothreitol) and negatively charged detergent (SDS). The proteins, which normally differ according to their charges, are all coated with the SDS molecules, which are negatively charged. Hence, all the proteins in the sample become negatively charged and achieve constant charge to mass ratio. In this way, the separation is according to the size of the proteins. A SDS-PAGE consists of two gels; firstly, a 10-12% separating gel was poured. In order to achieve a smooth boundary between separating and stacking gel, the separating gel was covered with a layer of water. After polymerisation of the separating gel, a 4% stacking gel was poured over it. The samples were heated in 70°C in NuPage SDS sample buffer for 10 min before loading into the gel. The gel was run in NuPage MOPS SDS running buffer at 15 mA for 1 hr, then at a constant current of 30 mA.

2.2.4 Isolation of DNA fragments from agarose gel

2.2.4.1 Glass silica method

(Vogelstein and Gillespie, 1979)

For the isolation of DNA fragments of 300-4000 base pairs (bp) in length from agarose gels, the QIAEX II Gel Extraction System kit from Qiagen was used. The principle of this method depends on the binding capacity of DNA to silica in high salt concentrations and elution in low salt solutions. After separation of DNA on an agarose gel, the DNA fragment to be isolated was excised with a razor blade and weighed. DNA isolation was performed according to protocol in QIAEXII handbook supplied with the kit.

2.2.4.2 QIAquick gel extraction method

This method is designed to extract and purify DNA of 70 bp to 10 kilobase pairs (kb) in length from agarose gels. Up to 400 mg agarose can be processed per spin column. The principle of this method depends on selective binding of DNA to uniquely designed silica-gel membrane. Excised DNA fragment in agarose was isolated as described in QIAquick Spin Handbook supplied by producer (Qiagen).

2.2.5 Enzymatic modifications of DNA

2.2.5.1 Digestion of DNA using restriction enzymes

Restriction enzymes are class of bacterial enzymes that cut DNA at specific sites. In bacteria their function is to destroy foreign DNA, such as that of bacteriophages. This attribute of restriction endonucleases is widely utilized in molecular biology. Restriction enzyme digestions were performed by incubating double-stranded DNA with an appropriate amount of restriction enzyme in its respective buffer as recommended by the supplier and at the optimal temperature for that specific enzyme. Standard digestions include 2-10 U enzyme per microgram of DNA. These reactions were usually incubated for 1-3 hrs to ensure complete digestion at the optimal temperature for enzyme activity, which was typically 37°C. However, for genomic DNA digestion the reaction solution was incubated overnight at 37°C.

2.2.5.2 Ligation of DNA fragments

The ligation of an insert DNA into a vector (digested with appropriate restriction enzyme) was carried out in the following reaction mix:

30 ng vector DNA (digested)
50-100 ng insert DNA (1:3, vector: insert ratio)
1 µl ligation buffer (10x)

1 µl T4 DNA ligase (5U/µl)
In a total volume of 10 µl

Blunt-end ligations were carried out at 16°C for overnight, whereas overhang-end ligations were carried out at 4°C overnight.

2.2.5.3 Phenol-chloroform extraction and ethanol precipitation

Protein impurities were removed by vigorous shaking of nucleic acid solution with an equal volume of phenol/chloroform/isoamyl alcohol mixture (25:24:1). The emulsion was then centrifuged for 1min, 10000 x g, at RT and the upper aqueous phase was collected, mixed with an equal volume of chloroform and centrifuged (1 min, RT, 10000 x g). Finally, the upper aqueous phase was collected for precipitation. Nucleic acids were precipitated by addition of NaAc (final conc. 0.3 M) and 2.6 volume of absolute ethanol. The mixture was then vortexed and centrifuged (5 min, 4°C, 10000 x g). The pellet was washed with 70% ethanol and centrifuged (5 min, RT, 10000 x g). After washing, the supernatant was aspirated and the pellet was air dried. The dried pellet was redissolved in sterile RNase free water or TE buffer.

2.2.5.4 TA-Cloning

(Hu, 1993)

Taq and other polymerases have a terminal transferase activity that results in the non-template addition of a single nucleotide to the 3' ends of PCR products. In the presence of all 4 dNTPs, dATP is preferentially added. This terminal transferase activity is the basis of the TA-cloning strategy. For cloning of PCR products, pGEM-T Easy vector systems that have 5’ T overhangs were used. The followings were mixed:

50 ng of pGEM-T Easy Vector
PCR product (1:3, vector to insert ratio)
1 µl T4 DNA Ligase 10x buffer

1 µl T4 DNA Ligase
In a total volume of 10 µl

The content was mixed with pipetting and the reaction was incubated for 1 hr at RT. For transformation of the ligation reaction, DH5α competent cells were used (Invitrogen).

2.2.5.5 Filling-up reaction

(Costa and Weiner, 1994)

To make blunt-end from overhang-end 0.1-4 µg of digested DNA was mixed with 0.05 mM dNTPs and 1-5 U of Klenow fragment with reaction buffer in a total volume of 50 µl. The reaction was incubated at 37°C for 15 min and then stopped by heating at 75°C for 10 min.

2.2.6 Transformation of competent bacteria

Transformation of the bacteria was done by gently mixing one aliquot of competent bacteria (50 µl) with 10 µl of ligation reaction. After incubation for 35 min on ice, bacteria were heat shocked for 20-60 sec at 42°C and cooled down for 2 min on ice. After adding 600 µl of S.O.C. medium, bacteria were incubated at 37°C with shaking for 1 hr to allow recovery of heat shocked bacteria. They were then plated out on LB-agar plates containing appropriate antibiotic (50µg/ml) and whenever required 1 mM IPTG and X-Gal 40 mg/ml were added for "Blue-White" selection.

2.2.7 Polymerase Chain Reaction (PCR)

The polymerase chain reaction (PCR) is one of the most important techniques in the field of molecular biology. It is a very sensitive and powerful technique (Saiki et al., 1988) that is

widely used for the exponential amplification of specific DNA sequences in vitro by using sequence specific synthetic oligonucleotides (primers). The general principle of PCR starts from a pair of oligonucleotide primers that are designed so that a forward or sense primer directs the synthesis of DNA towards a reverse or antisense primer and vice versa. During the PCR, the *Taq* DNA polymerase (a heat stable polymerase) (Chien et al., 1976) catalyses the synthesis of a new DNA strand that is complementary to a template DNA from the 5' to 3' direction by a primer extension reaction, resulting in the production of the DNA region flanked by the two primers. It allows the rapid and unlimited amplification of specific nucleic acid sequences that may be present at very low concentrations in very complex mixtures.

2.2.7.1 PCR amplification of DNA fragments

The amplification cycles were performed in an automatic thermocycler. The PCR reaction contains the following substances:

1 µl DNA
1 µl forward primer (10 pmol)
1 µl reverse primer (10 pmol)
1 µl 10 mM dNTPs
5 µl 10x PCR buffer
1.5 µl 50 mM $MgCl_2$
1 µl *Taq* DNA polymerase (5U/µl)
Up to 50 µl H_2O

The reaction mixture was placed in a 200 µl reaction tube and placed in a thermocycler. A standard PCR program is shown here:

Initial denaturation	95°C	5 min	
Elongation	95°C	30 sec (denaturation)	30-35 cycles
	55°C - 65°C	30-45sec (annealing)	
	72°C	1-2 min (extension)	
Final extension	72°C	10 min	

2.2.7.2 Reverse transcription PCR (RT-PCR)

RT-PCR is a technique, which generates cDNA fragments from RNA templates and thereafter amplifies it by PCR. It is very useful to determine the expression of genes in specific tissues or in different development stages. 1-5 µg of total RNA was mixed with 1 µl of oligo $(dT)_{18}$ primer (10 pmol/µl) and sterile water was added to total volume of 12 µl. To avoid the possible secondary structure of the RNA, which might interfere with the synthesis, the mixture was heated to 70°C for 10 min and then quickly chilled on ice. After a brief centrifugation, the followings were added to the mixture:

4 µl 5x First strand buffer
2 µl 0.1 M DTT
1 µl 10 mM dNTPs

The content of the tube was mixed gently and incubated at 42°C for 2 min. Then, 1 µl of reverse transcriptase enzyme (Superscript II) was added and further incubated at 42°C for 50 min for the first strand cDNA synthesis. Then, the reaction was inactivated by heating at 70°C for 15 min. One µl of the first strand reaction was used for the PCR reaction (as described above).

2.2.8 Blotting techniques

2.2.8.1 Southern blotting of DNA to nitrocellulose filters

(Southern, 1975)

In Southern blotting, the transfer of denatured DNA from agarose gels to nitrocellulose membrane is achieved by capillary flow. 20x SSC buffer, in which nucleic acids are highly soluble, is drawn up through the gel into the nitrocellulose membrane, taking with it the single-stranded DNA that becomes immobilised in the membrane matrix. After electrophoresis of DNA, the gel was treated for 20 min with 0.25 M HCl for depurination. It was followed by denaturation solution for 45 min and 1 hr in neutralization solution. The transfer of the DNA to the nitrocellulose membrane was done in a Turbo-Blot-apparatus (Schleicher & Schuell, Dassel). About 20 Whatman filter papers (GB 003) were layered on a Stack Tray followed by 4 Whatman filter papers (GB 002) and 1 Whatman filter paper GB 002 soaked with 2x SSC. The equilibrated nitrocellulose filter that was also soaked with 2x SSC was laid on the top. The agarose gel, which was treated as described above, was placed on the filter and was covered with 3 Whatman filter papers GB 002 soaked with 2x SSC. The buffer tray was placed and filled with 20x SSC. Finally a wick, which was soaked with 20x SSC and the wick cover were put on the top of the blot. The transfer was carried out for overnight. Finally, after disassembling of the blot, the filter was washed briefly in 2x SSC, dried on air and the DNA was fixed onto the filter by either baking it at 80°C for 2 hrs or by UV-crosslinking in UV Stratalinker 1800.

2.2.8.2 Northern blotting of RNA onto nitrocellulose filters

For the transfer of RNA onto a nitrocellulose filter, the same procedure as described above (2.2.11.1) was performed. In this case, however, the gel does not need to be denatured, but was transferred directly onto the nitrocellulose filter, as described in section 2.2.11.1.

2.2.8.3 Western blotting of protein onto PVDF membrane

(Gershoni and Palade, 1982)

Semi-dry transfer buffer (1x): 25 mM Tris pH 8.3

150 mM Glycin
10% Methanol

After the electrophoresis of proteins on a SDS-PAGE, the gel and the PVDF membrane, which was cut at the size of the gel, were first moistened with methanol and then equilibrated in semidry transfer buffer. Six pieces of GB004 Whatman filter paper were also cut at the size of the gel. First, three papers soaked with transfer buffer were placed on semi dry transfer machine's lower plate and then equilibrated membrane was placed over them. Next the gel was placed avoiding any air bubbles. Another three Whatman paper soaked with transfer buffer were placed over to complete the sandwich model. The upper plate was placed over this sandwich and the transfer was carried out at 10 W (150-250 mA, 39 V) for 1 hr. For protein dot blot, specified amounts of protein solution in different concentrations were poured onto PVDF membrane. Membrane was air-dried and used for incubation with antibodies. To confirm transfer efficiency of proteins onto nitrocellulose membranes, the gel was incubated for 30 min in Coomassie blue solution at RT.

2.2.8.4 Incubation of protein-bound membranes with antibodies

The membrane was first incubated in P1 buffer with 5% non-fat dry milk for 1 hr at RT in order to block unspecific binding sites, followed by incubation with 2% milk in P1 buffer for 5 min. Membrane was then incubated with a primary antibody at the recommended antibody dilution in P1 buffer with 2% non-fat dry milk for overnight at 4°C. Then, the membrane was washed 4 times in P1 buffer with 2% dry milk for 5 to 10 min and then incubated with the alkaline phosphatase conjugated secondary antibody in P1 buffer with 2% non-fat dry milk for 1 hr at RT. After this step, the membrane was washed 4 times in P1 with 2% dry milk, one time in P1 without dry milk and one time in AP buffer for 5 min at RT. Finally, the proteins on the membrane were visualized by an incubation step in the dark with 10 ml of staining solution (alkaline phosphatase substrate solution) for 15 min and rinsed with water to stop the reaction.

P1 buffer: 1.5 M NaCl

	1 M Tris/HCl pH 7.5
AP buffer:	100 mM Tris-HCl (pH 9.5) 100 mM NaCl 50 mM $MgCl_2$
Staining Solution:	66 µl NBT 33 µl BCIP In 5 ml of AP buffer

2.2.9 The atlas human cancer profiling array II

To identify genes that are differentially expressed in normal and tumor tissues, The cancer profiling array II includes normalized cDNAs from 154 tumors and corresponding normal tissues from individual patients, amplified using BD SMART™ technology. Hybridization controls, positive controls and cDNA from nine cancer cell lines are also included. The human tumor array is a premade array of known and novel human cDNAs that were found to be up- or down-regulated in human tumors using Clontech PCRSelectTM cDNA subtraction. This array contains immobilized cDNAs of differentially expressed genes from human tumors, breast, ovary, colon, stomach, lung, kidney, bladder, vulva, prostate, uterus, cervix, rectum, thyroid gland, testis, skin, small intestine, pancreas, trachea and liver. This array provides a high-throughput format for analysing differential gene expression. After identifying a differentially expressed gene with atlas arrays, the cancer profiling array can be used to view the distribution of a differentially expressed gene across many samples. Some samples represent different stages of malignancy for one type of the tumor, therefore a particular tumor stage can be correlated with distinctive gene expression patterns. Amplified full-length cDNA accurately preserves the relative abundance of mRNA in a sample, making the array suitable for detecting differential expression of a gene across many different samples. The quantitative profiling of gene expression on the array is

normalized to three different house-keeping genes. The cancer profiling array was used to determine the role of a particular gene (*Piwil2*) in a broad range of cancer cell types. The cDNA fragment for *Piwil2* was labeled as described above in section 2.2.9.1 and the labeled probe was hybridized to the cancer profiling array as described in paragraph 2.2.9.6. The signals were scanned after a 1 day exposure by using a Molecular Imager FX (Bio-Rad GmbH, Munich, Germany) and analysed by using the Quantity one software (Bio-Rad).

2.2.9.1 Overview of the atlas array procedure

(Chalifour et al., 1994)

Identical membranes are included with each purchase, so the expression profiles of different mRNA populations can be compared side-by-side. The first step was to synthesize probe mixtures by reverse transcribing each RNA population using the cDNA Synthesis (CDS) Primer Mix included in the kit and [α-^{32}P] dATP. The CDS Primer Mix is a mixture of primers specific for different type of atlas array. These primer mixes ensure that cDNAs are only synthesized for the genes on a particular atlas array. Each radioactively labeled probe mix was then hybridized to separate atlas arrays. After a high-stringency wash, the hybridization patterns were analysed by autoradiography and quantified by phosphorimaging. The relative expression levels of a given cDNA from two different RNA populations were assessed by comparing the signal obtained with a probe from one RNA source to that obtained with a probe from another source.

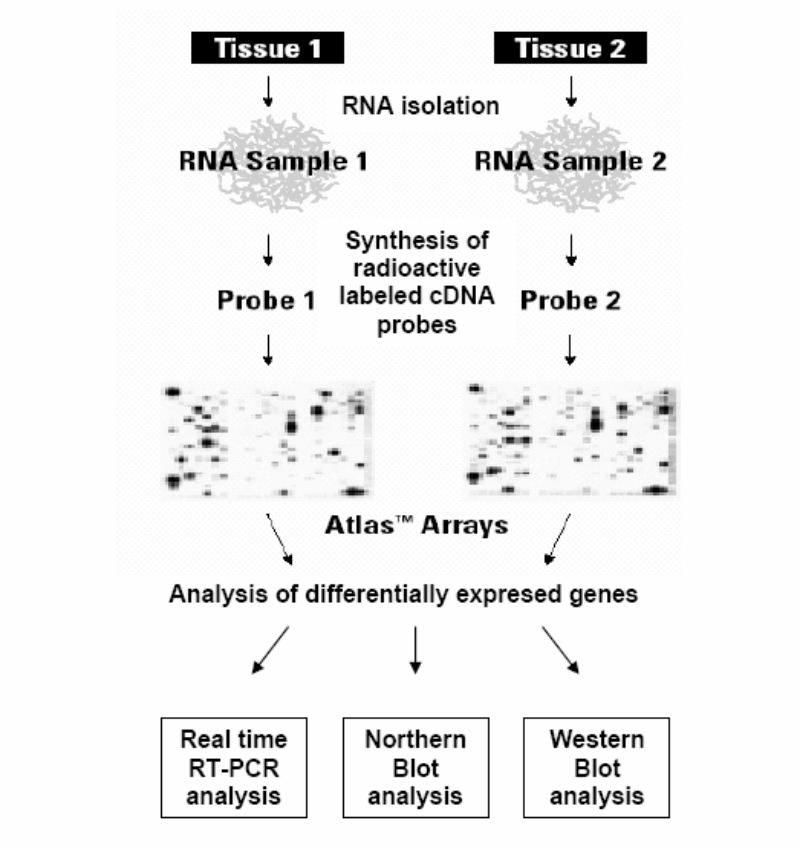

Figure 2.1: Schematic representation of the broad-scale expression profiling with atlas™ arrays. Side-by-side hybridizations with radioactive labeled cDNA probes prepared from two different RNA populations allowed the simultaneous comparison of the expression levels of all the cDNAs on the array. Furthermore, the expression of identified genes was verified by Northern blot, quantitative RT-PCR and Western blot analysis, respectively.

2.2.9.2 Preparation of whole cDNA probes from total RNA

To analyse gene expression patterns using the arrays described above, cDNA probes were generated from total RNA samples. The Atlas™ Pure Total RNA Labeling System (Clontech) was used in conjunction with reagents supplied with the atlas arrays to synthesize highly sensitive atlas cDNA probes directly from total RNA. The key

components in the Atlas Pure System are streptavidin-coated magnetic beads and biotinylated oligo (dT), which allow to carry out both poly (A)+-RNA enrichment and probe synthesis in a single procedure. This simplicity is possible because probes are synthesized while poly (A)+-RNA remains bound to the magnetic beads, eliminating potentially troublesome intermediate poly (A)+-RNA purification steps. By using this procedure, atlas probes made from total RNA produce results that are just as reliable as those from pure poly (A)+-RNA, a clear advantage when only small amounts of tissues or cells are available.

2.2.9.3 DNase treatment of total RNA

First, total RNA (50 µg) was treated with RNase-free DNase I (Clontech) according to the user manual where the following reagents were combined: 100 µl of total RNA (1 mg/ml), 20 µl 10x DNase I buffer, 10 µl DNase I (1 unit/ml), 70 µl deionized water, mixed and incubated at 37°C for 30 min. Next, 20 µl of 10x termination mix was added and the RNA samples were purified by phenol/ chloroform extraction and ethanol precipitation. The air dried pellet was dissolved in 50 µl RNase-free water and 4 µl of the RNA mixture was checked on a denaturing agarose gel to verify RNA yield and purity.

2.2.9.4 Whole cDNA probe synthesis

Master mix for all labeling reactions was prepared plus one extra reaction by combining the following in a 0.5 ml microcentrifuge tube at RT.

5x reaction buffer	4 µl
10x dNTP Mix (for dATP label	2 µl
[α-^{32}P]dATP (10 µCi/µl)	5 µl
DTT (100 mM)	0.5 µl
Total volume	11.5 µl

To the resuspended beads 4 µl of CDS Primer Mix was added, mixed well by pipetting and

incubated in the preheated thermal cycler at 65°C for 2 min. Then, the temperature of the thermal cycler was reduced to 50°C and the samples were incubated for 2 min. During this incubation step, 2 µl MMLV Reverse Transcriptase per reaction was added to the Master mix (6 µl MMLV RT for the 3-reaction Master mix). After completion of the 2 min incubation at 50°C, 13.5 µl of Master Mix was added to each reaction tube. The samples were incubated at 50°C for 25 min and then 2 µl of 10x Termination Mix was added and labeled probes were purified with column chromatography.

2.2.9.5 Purification of labeled cDNA probes by column chromatography

To purify the labeled cDNA from nonincorporated ^{32}P-labeled nucleotides and small (<0.1kb) cDNA fragments, the following procedure for each reaction tube was used. The atlas cDNA probe synthesis reactions were diluted to 200 µl total volume with buffer NT2, mixed well by pipetting and pipetted into a NucleoSpin Extraction Spin Column placed in a 2 ml collection tube and centrifuged at 10000 x g for 1 min. Then, the NucleoSpin column was inserted into a fresh 2 ml Collection Tube, centrifuged at 10000 x g for 1 min and the flow-through was discarded. This washing step with NT3 buffer was repeated twice. Next, the NucleoSpin column was transferred to a clean 1.5 ml microcentrifuge tube, 100 µl of buffer NE was added and the column was allowed to soak for 2 min. After completion of the 2-min incubation step, the column was centrifuged at 10000 x g for 1 min to elute the purified probe. The radioactivity of the probe was checked by using the Liquid scintillation analyser 1600TR (Packard). 2 µl of each purified probe was added to 5 ml of scintillation fluid in separate scintillation-counter vials. The ^{32}P-labeled samples were counted and counts were multiplied by a dilution factor of 50. Whole cDNA probes synthesized from total RNA using this procedure had a total activity of 2-5 x 10^6 cpm.

2.2.9.6 Hybridization of atlas arrays with labeled cDNA probes

To 5 ml of prewarmed ExpressHyb solution (68°C) heat-denatured sheared salmon sperm DNA (0.5 mg) was added and kept at 68°C until use. Prewetted atlas arrays were placed into a hybridization tube filled with water. The water was poured off and the membrane

was adhered to the inside wall of the tube without creating air pockets. Then, 5 ml of the prepared hybridization solution was added to each tube and the membranes were prehybridized for 30 min with continuous agitation at 68°C and at 5-7 rpm. During this incubation 5µl Cot-1 DNA (1 mg/ml) was added to the labeled cDNA probe. Subsequently, the probe was incubated at 95°C for 10 min and cooled on ice for 2 min. The prepared cDNA probe mixture was directly added to the prehybridization solution and the filters were hybridized overnight at 68°C. The atlas arrays were washed four times in wash solution 1 (2x SSC, 1% SDS) at 68°C for 30 min and one time in wash solution 2 (0.1x SSC, 0.5% SDS) at 68°C for 30 min. Then, one final 5 min wash in 2x SSC with agitation at RT was performed. The damp membranes were immediately transferred into a plastic wrap and exposed to X-ray film at -70°C or to a phosphorimaging screen at RT. The signals were scanned after a 3 day exposure by using a Molecular Imager FX (Bio-Rad GmbH, Munich) and analysed by using the Quantity one software (Bio-Rad).

2.2.10 Isolation of differentially expressed genes

2.2.10.1 Mouse cancer pathway finder microarray

The Oligo GEArray® mouse cancer pathway finder microarray is designed to rapidly assess the status of six different biological pathways frequently altered during or affected by transformation and tumorigenesis. Deregulation of these biological pathways promotes tumorigenesis by allowing the cells to grow and divide unchecked, to avoid apoptosis (programmed cell death), to respond abnormally to growth factors, to receive blood supply (angiogenesis) and to migrate from one location to another (metastasis and invasiveness). The array includes representative genes from each of these pathways (see the list below) and can help to examine how a cell line has become immortalized or understand the progression of a particular cancer or model system.

Cell cycle control and DNA damage repair:

Atm, Brca1, Brca2, Ccnd1, Ccne1, Cdc25a, Cdk2, Cdk4, Cdkn1a (p21Waf1), Cdknn1b (p27Kip1), Cdkn2a (p16Ink4), Chek2 (Rad53), E2f1, Mdm2, Prkdc, Pten, Rb1, Trp53.

Apoptosis and cell senescence:

Apaf1, Bad, Bak1, Bax, Bcl2, Bcl2l1 (bcl-X), Birc5 (survivin), Casp8, Casp9, Cflar, Gzma, Tert (telomerase), Tnfrsf1a, Tnfrsf6 (Fas), Tnfrsf10b (DR5), Tnfrsf25 (DR3).

Signal transduction molecules and transcription factors:

Akt1, Akt2, Catnb, Erbb2, Ets2, Fos, Grb2, Jun, Map2k1 (MEK), Mapk14 (p38 MAPK), Myc, Nfkb1, Nfkbia (IkBa), Pik3c2a, Pik3cb, Pik3r1, Raf1, Rasa1, Src.

Adhesion:

Cd44, Cdh1, Icam1, Itga2, Itga3, Itga4, Itga5, Itga6, Itgav, Itgb1, Itgb3, Itgb5, Mcam, Mtss1, Ncam1.

Angiogenesis:

Angpt1, Bai1, Col18a1 (endostatin), Egf, Egfr, Fgf1, Fgf2, Fgfr2, Figf, Flt1, Hgf, Ifna1, Ifnb1, Igf1, Pdgfa, Pdgfb, Tek, Tgfb1, Tgfbr1 (ALK-5), Thbs1, Thbs2, Tnf, Vegfa, Vegfb, Vegfc.

Invasion and metastasis:

Kai1, Kiss1, Met, Mmp2, Mmp9, Mta1, Mta2, Muc1, Nme4 (Nm23), Plau (uPA), Plaur (uPAR), S100a4, Serpine1 (PAI1), Serpinb2, Serpinb5 (maspin), Spp1 (osteopntin), Syk, Timp1, Timp3, Twist1.

2.2.10.2 GEArray S series mouse stem cell gene array

The GEArray S series mouse stem cell gene array is designed to profile the expression of genes known to be important for the identification, growth and differentiation of mouse stem cells. It contains 258 known genes that encode markers expressed by stem cells at

various stages of differentiation (91 genes), growth factors and cytokines known to regulate stem cell growth (99 genes), extra cellular matrix molecules expressed at appropriate developmental stages (38 genes), as well as other proteins such as cell cycle regulators that are thought to be involved in stem cell division. Positive controls and housekeeping genes are also included for normalization to generate relative expression profiles. The array is particularly useful in exploring neural stem cell development, but also contains markers for the identification and differentiation of embryonic, mesodermal and hematopoietic stem cells (see the list below).

Molecular markers for stem cells and differentiated cells:

Abcg2, Acta2, Actc1, Actg2, Afp, Anf-ESTs, Cd34, Cd44, Cdh15, Cer1, Cnp1, Col6a2, Drg11, Egfr, Egr2, Erbb2ip, Erbb3, Fabp4, Fabp7, Fgf4, Fgfr4, Foxa1, Fzd9, Gata2, Gata4, Gcg, Gcm2, Gfap, Gja7, Gjb1, Gjb3, Gjb4, Gjb5, Il6st, Ina, Ins1, Isl1, Kdr, Krt1-14, Krt1-15, Krt1-17, Krt1-5, Krt2-8, Lif, Lifr, Mbp, Mtab2, Mtap1b, Myh11, Myhca, Myla, Ncam1, Ncam2, Nes, Nfl, Ngfr, Nkx2-2, Nkx2-5, Ntf3, Numb, Olig1, Olig2, Pax6, Pdgfra, Pdx1, Plp, Pou3f2, Pou3f3, Pou5f1, Pou6f1, Prdc-pending, Prom, Prox1, Ptprc, S100B, Scgn10, Slc1a2, Slc1a6, Slc2a1, Snai1, Snai2, Sox1, Sox10, Sox2, Syn1, Thy1, Tubb3, Utf1, Vim, Zfp42, Zfp110.

Growth factors and cytokines:

Acvr1, Acvr2, Acvrl1, Bdnf, Bmp1, Bmp10, Bmp15, Bmp2, BMP3-ESTs, Bmp4, Bmp5, Bmp6, Bmp7, Bmp8a, Bmp8b, Bmpr1a, Bmpr1b, Bmpr2, Cntf, Cntfr, Dlk1, Egf, Erbb4, Fgf1, Fgf10, Fgf11, Fgf12, Fgf14, Fgf15, Fgf16, Fgf17, Fgf18, Fgf2, Fgf20, Fgf21, Fgf22, Fgf23, Fgf3, Fgf5, Fgf6, Fgf7, Fgf8, Fgf9, Fgfr1, Fgfr2, Fgfr3, Fzd1, Fzd3, Fzd4, Fzd7, Fzd8, Gdf1, Gdf11, Gdf2, Gdf3, Gdf5, Gdf6, Gdf8, Gdf9, Igf1, Igf1r, Igf2, Igf2r, lgfbp3, Il6, Il6ra, Inhba, Inhbb, Insrr, Ngfb, Nodal, Notch1, Notch2, Notch3, Notch4, Nrg1, Nrg3, Nrg4, Ntrk2, Pdgfa, Pdgfb, Pdgfrb, Ptch, Ptch2, Tgfb1, Tgfb2, Tgfb3, Tgfbr1, Tgfbr2, Tgfbr3, Vegfa, Wnt11, Wnt2, Wnt3a, Wnt4, Wnt5b, Wnt6, Wnt7b, Wnt8a.

Extracellular matrix molecules:

Catna1, Catna2, Catnal1, Catnb, Catnd2, Cdh1, Cdh2, Cdh3, Cdh4, Cdh5, Cst3, Icam1, Icam5, Itga2, Itga2b, Itga3, Itga4, Itga5, Itga6, Itga7, Itga8, Itgae, Itgal, Itgam, Itgav , Itgax, Itgb1, Itgb2, Itgb3, Itgb4, Itgb5, Itgb6, Itgb7, Jcam1, Ntrk3, Pecam, Tnc, Vcam1.

Others:

Actb, Ccng2, Cdkn1a, Cdkn1b, Cdkn2d, Dnmt1, Dnmt2, Dnmt3a, Dnmt3b, Dnmt3l, Foxg1, Foxh1, Foxm1, Foxo1, Gapd, Neurod3, Nog, Ppia, Pten, Rpl13a, Shh, Sox13, Sox15, Sox17, Sox18, Sox3, Sox4, Sox5, Sox6, Sox9, Tebp-pending, Tep1, Terf1, Tert.

2.2.10.3 Overview of the GEArray™ Q and S series procedure

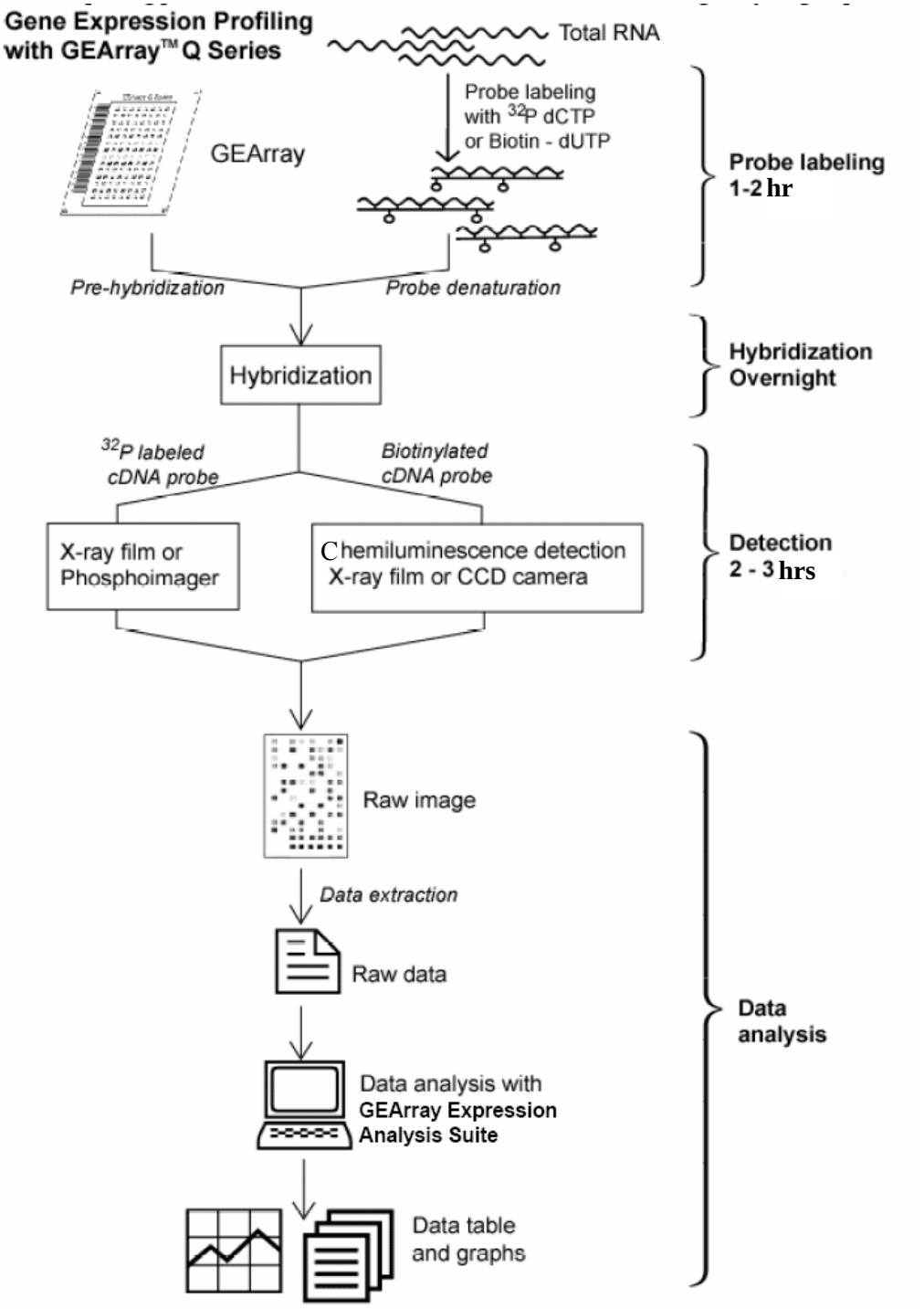

Figure 2.2: Protocol overview for performing gene expression profiling experiments with the GEArray products. A full experiment lasts 2 days, requires 1-2 hrs hands-on time in 1st day and 2-3 hrs in 2nd day. In day 1, a radioactive or biotin labeled cDNA probe is first generated through a reverse transcription reaction. At the same time, the GEArray membrane must undergo a prehybridization treatment. The labeled cDNA probed is then added to pre-hybridized array membrane and incubated in a hybridization oven overnight. In day 2, the membranes are subjected to multiple washes to remove the free probe. For radioactive detection, the array image is then recorded with X-ray film or a phosphoscreen. For chemiluminescent detection the washed membrane is blocked and then incubated with streptavidin-AP conjugate. After final washes, the array image is developed with CDP-Star chemiluminescent substrate and recorded with X-ray film or a CCD camera imaging system.

2.2.10.4 RNA preparation and quality control

High quality sample RNA is essential for obtaining good microarray results. The most important prerequisite for any gene expression analysis experiment is consistent, high-quality RNA from every experimental sample before starting the labeling process. Therefore, the sample handling and RNA isolation procedures are critical to the success of the experiment. Residual traces of proteins, salts or other contaminants will either degrade the RNA or decrease the efficiency of the enzyme activities necessary to produce amplified and labeled cRNA of consistent quality for microarray analysis. For best results from this kit, all RNA samples should be suspended in RNase-free water (not DEPC-treated water) or RNase-free 10 mM Tris buffer, pH 8.0.

GEArray Express, combined with its companion labeling method, TrueLabeling-AMP 2.0, may be used at maximum speed and convenience when at least 1.0 µg of total RNA is available at a concentration greater than 0.2 mg/ml for every sample. Under these conditions, the labeling method produces enough labeled cRNA target in 3 hrs for the GEArray Express analysis (approximately 2.0 µg).

2.2.10.5 cDNA probe synthesis

For each total RNA sample, combine the following in a sterile PCR tube:

Total RNA 2.5-5.0 µg (For mRNA, use 0.25-0.5 µg.)
Buffer A (CLEAR tube) 3 µl
RNase-free H_2O to 10 µl final volume.

The content was mixed gently with a pipettor followed by brief centrifugation. The mixture was placed in a pre-heated heat block or thermal cycler at 70°C for 3 min, cooled down to 42°C and kept at that temperature for 2 min. This mixture can be prepared while the Annealing Mixture is incubating at 70°C.

RT cocktail	Buffer B	8 µl
	[α-^{32}P]-dCTP	6 µl
	RNase-free H_2O	2 µl
	RNase inhibito (RI)	2 µl
	Reverse transcriptase (AE)	2 µl

The RT cocktail was heated at 42°C for 1 min before proceeding to the next step. Two arrays were transferred each 10 µl of the pre-warmed RT cocktail into the 10 µl annealing mixture. The mixtures were mixed well but gently with a pipettor and incubated at 42°C for 90 min. The cDNA probe was heated at 94°C for 5min and quickly chilled on ice.

2.2.11 Protein methods

2.2.11.1 Isolation of total protein

Proteins were extracted from fresh or frozen mouse tissues by homogenization in protein lysis buffer (150 mM NaCl, 10 mM EDTA, 50 mM Tris/HCl, pH 7.6, 1% Triton X-100 and 1% sodium deoxycholate) containing protease inhibitors (1µg/µl leupeptin, 3µg/µl aprotinin, 1µg/µl pepstatin). Lysates were sonicated on ice (about 20 impulses) and

centrifuged at 1200 x g for 10 min at 4°C. Supernatant, containing membrane, organelles and cytosol proteins was collected and stored at -80°C, or used immediately for Western blot.

2.2.11.2 Determination of protein concentration

(Bradford, 1976)

To determine the protein concentration, Bio-Rad protein assay was employed which is a dye-binding assay based on the differential colour change of a dye in response to various concentrations of protein. The assay is based on the observation that the absorbance maximum for an acidic solution of Coomasie Blue G-250 shifts from 494 to 595 nm when the binding to protein occurs. The bovine serum albumin (BSA) stock solution of 1 mg/ml was diluted in order to obtain standard dilutions in range of 10 µg/ml to 100 µg/ml. The Bio-Rad's color reagent was diluted 1:5 with H_2O and filtered through 0.45 µm filters. In a 96-well microtiter plate, 20 µl of each standard dilution and the samples to be measured were pipetted with 280 µl of the colour reagent. The absorption of the colour reaction was measured at 595 nm in a microplate reader (Microplate Reader 450, Bio-Rad).

2.2.12 "Random Prime" method for generation of ^{32}P labelled DNA

(Feinberg and Vogelstein, 1983)

Rediprime™II Random Prime Labeling System (Amersham Pharmacia) was used for labelling of DNA probes. The method depends on the random priming principle developed by Feinberg and Vogelstein (1983). The reaction mix contained dATP, dGTP, dTTP, dCTP, Klenow fragment (4-8 U) and random oligodeoxyribonucleotides. Firstly, 10-25 ng of DNA were denatured in a total volume of 46 µl at boiling water for 10 min and quickly chilled on ice for 5min. After pipetting, the denatured probe to Rediprime™ II Random Prime Labeling System cup and 4 µl of [α-^{32}P] dCTP (3000 Ci/mmol) were added to the reaction mixture. The labelling reaction was carried out at 37°C for 0.5-1 hr. The labelled

probe was purified from nonincorporated [α-^{32}P] dCTP by using microspin columns (Amersham Pharmacia).

2.2.13 Hybridization of nucleic acids

(Denhardt, 1966)

The membrane to be hybridized was equilibrated in 2x SSC and transferred to a hybridization tube. After adding 8 ml of hybridization solution and 150 µl of sheared salmon DNA, the membrane was incubated for 2 hrs in the hybridization oven at an appropriate temperature, which was usually 65°C. Then, the labelled probe was denatured at 95°C for 10 min, quickly chilled on ice and added to the hybridization solution, together with 150 µl of sheared salmon DNA. The hybridization was carried out overnight in the oven. Next day, the filter was washed for 10 min with 2x SSC at RT. Finally it was washed with 0.2x SSC containing 0.1% SDS and then with 0.02x SSC at the hybridization temperature. After drying the filter, it was sealed in plastic foil and exposed to autoradiography overnight to few days (depending on the value of radioactive signal) at -80°C. The film was developed in X-ray automatic processor Curix 60. If the membrane has to be used again, it was stripped in 0.2x SSC at 80°C, until radioactive signal was no longer detectable.

2.2.14 Non-radioactive dye terminator cycle sequencing

Non-radioactive sequencing was performed with the Dye Terminator Cycle Sequencing-Kit (Applied Biosystem). The reaction products were analysed with automatic sequencer (Mega Base 1000).

For the sequencing reaction, four different dye labelled dideoxy nucleotides were used (Sanger et al., 1977), which, when exposed to an argon laser, emit fluorescent light which can be detected and interpreted. The reaction was carried out in a total volume of 10 µl containing 1 µg plasmid DNA or 100-200 ng purified PCR products, 10 pmol primer and 4 µl reaction mix (contains dNTPs, dideoxy dye terminators and *Taq* DNA polymerase). Elongation and chain termination take place during the following program in a thermocycler: 4 min denaturation followed by 25 cycles at 95°C, 30 sec, denaturation; 55°C, 15 sec, annealing; 60°C, 4 min, elongation. After the sequencing reaction, the DNA was precipitated with 1/10 volume 3 M sodium acetate and 2.5 volume 100% ethanol and washed in 70% ethanol. The pellet was dissolved in 4 µl of loading buffer, denatured at 95°C for 3 min and finally loaded into the sequence gel.

2.2.15 Generation of polyclonal antibody

2.2.15.1 Peptide analysis

Different computational tools supported by Eurogentec Company were applied to select potential antigenic peptides. Before synthesis of the peptide, a hydrophilicity/ hydrophobicity profile analysis was carried out and for further confirmation antigenicity prediction was performed. In next step, predictions of secondary structure such as ß- turns and α-helices in combination with the surface probability of the protein region were the parameters, which enabled us to select the best peptides. In the last step, we compared primary sequence of our protein with international data bank to select unique sequence for antibody generation. Two peptides for the generation of antibody against Piwil2 were selected and synthesised. The sequences of peptides were as follows:

Peptide EP034147: H_2N- DPV RPL FRG PTP VHP C -$COONH_2$

Peptide EP034148: H_2N- GLT ARD PPR LPQ PPA C -$COONH_2$

2.2.15.2 Immunisation of rabbit

Eurogentec Company did immunisation under DOUBLE X program. Two peptides were selected and synthesised. Using modern algorithms for peptide selection, the success rate for peptide immunization can be as high as 75%. This still means a 25% chance of failure. Under DOUBLE X program the success rate is increased to 1-25% = 93.75%. Two rabbits were immunised with 100 µg of antigen mixed with Freund's complete adjuvant in 1:1 ratio. Before injection, pre- immune sera were collected from the animals. After 14 days, first booster immunisation was performed with 1:1 ratio of antigen with Freund's incomplete adjuvant. Second booster was given after 28 days and a third booster after 56 days after first immunisation. Final bleeding was done after 86 days after first immunisation. The antiserum was aliquoted and stored at -80°C.

2.2.15.3 Affinity purification of polyclonal antibody against peptide

For antibody purification SulfoLink® Coupling Gel (Pierce) was used. The gel consists of immobilized iodoacetyl on a crosslinked agarose support. SulfoLink® supports binding specifically to sulfhydryls. The 12-atom spacer arm deduces steric and makes binding more efficient. This longer arm is designed for conjugating small peptides to the support.

2.2.15.3.1 Immobilization

Sample preparation buffer:	0.1 M sodium phosphate 5 mM EDTA-Na, pH6.0
Coupling buffer:	50 mM Tris 5 mM EDTA-Na, pH 8.5

The peptide (10mg) was dissolved in 1 ml of sample preparation buffer. The solution was added to vial containing 6 mg of reductant: 2-mercaptoethylamine HCl (2-MEA) and incubated at 37°C for 1.5 hrs. The mixture was cooled to RT and applied to the 5 ml

desalting column (equilibrated with 20 ml of coupling buffer) to remove excess 2-MEA from the reduced sample. Reduced peptide was eluted from the column by applying 3 ml of coupling buffer.

2.2.15.3.2 Coupling to gel and blocking non-specific binding sites on gel

Reduced protein mixture (3 ml) was added to SulfoLink® Coupling Gel column after equilibrating with 8 ml of coupling buffer. The column was mixed at RT for 15 min and then incubated for 30 min without mixing. After that, the column was washed with 6 ml of coupling buffer. 2 ml of 0.05 M cysteine in coupling buffer was applied to the column to block non-specific sites. The column was mixed for 15 min at RT and then incubated for 30 min without mixing.

2.2.15.3.3 Washing and deactivation

Wash solution: 1.0 M NaCl
0.05% NaN_3

Column was washed with at least 12 ml of wash solution and then with 4 ml of 0.05% sodium azide in PBS. Finally, after replacing of bottom cap, 2 ml of 0.05% sodium azide in PBS was added. Column was stored at 4°C.

2.2.15.3.4 Purification

The column was equilibrated with 6 ml of PBS. The antiserum (1.5 ml sample) was applied onto the column. The column was incubated at room temperature for 1 hr. This procedure, using always 1.5 ml sample, was repeated, until whole antiserum (about 12 ml) was used. The column was washed with 12 ml of PBS. Elution was done with 8 ml of ImmunoPure®IgG Elution Buffer (Pierce). Fractions of 1 ml were collected and monitored by A280. Fractions of interest were pooled and exchanged into PBS containing 0.05%

sodium azide by dialysis. Purified antiserum was stored at -20°C and the column was re-equilibrated with 10 ml of PBS containing 0.05% sodium azide.

2.2.16 Generation of fusion gene constructs

2.2.16.1 NIH3T3-pcDNA and NIH3T3-pcDNA-*Piwil2* construct

Plasmid pcDNA-*Piwil2* was constructed using a complete *Piwil2* cDNA obtained by PCR from a testis cDNA. The complete cDNA was amplified using the primers containing the restriction sites *EcoRI* given in section RT-PCR analysis. PCR product was digested with the restriction endonuclease and subcloned in a pcDNA plasmid (BCCM/LMBP Plasmid collection, Gent, Belgium) which was digested with the same enzyme. The pcDNA plasmid is composed of human cytomegalovirus immediate early promoter (CMV-IE), enhancer phage T7 gene 10 promoter (T7g10), phage SP6 promoter, simian virus 40 early promoter (SV40 early), ampicillin (amp) and neomycin (neo; G418).
Sequence analysis was performed to ensure that the cDNA was in-frame and that no mutations were added to the *Piwil2* sequence by the amplification process.

2.2.16.2 GFP fusion constructs using human *PIWIL2* promoter

The green fluorescent protein (GFP) is a very useful tool to perform sub-cellular localisation of proteins and to observe their expression, due to the green fluorescent light that emits at 507 nm after being excited at 488 nm. A fusion protein with the enhanced green fluorescent protein (EGFP) was produced by cloning in frame the entire or truncated coding regions of the protein of interest in C-terminal position with respect to the EGFP sequence. For h*PIWIL2-EGFP* construct, 2 kb of flanking region of human *PIWIL2* gene was amplified and cloned into a plasmid vector containing the coding region of *EGFP* gene and the SV40 polyadenylation signals. Plasmid contains neomycine resistance gene under

control of SV40 early enhancer and promoter elements for positive selection. The final construct was sequenced completely.

The ligation reaction was transformed in DH5α competent cells. Then, a positive clone was selected and a single colony was cultured to obtain enough quantity of DNA. After checking the sequence subcloned in the expression vector by restriction analysis and sequencing, the DNA was used for transfection.

2.2.17 Cell culture conditions and transfections

Mouse NIH3T3 fibroblasts were maintained in DMEM supplemented with 10% fetal calf serum (FCS), 1% glutamine (200 mM) and 1% penicillin/streptomycin. GC-1 was purchased from America Tissue Cell Collection (Rockville, USA) and maintained in DMEM, containing 15 mM HEPES and supplemented with 0.45% glucose (w/w), 10% FCS and 2% penicillin (50units/ml)/ streptomycin (50µg/ml). The human breast cancer cell line MDA-MB-231 was obtained from the American Type Culture Collection and maintained in DMEM supplemented with sodium pyruvate (1 mM), 10% FCS, 2% penicillin/streptomycin. HeLa cells were cultured in Dulbecco's modified Eagle's medium (DMEM) containing 10% heat-inactivated fetal bovine serum, 2 mM L-glutamine, 100 U/ml penicillin and 100 µg/ml streptomycin. Cells were cultured at 37°C in a humidified atmosphere of 5% CO_2. Cells were plated at a density of 10^6 cells/ml in 25 cm^2 culture flask and the monolayer was transfected with a freshly prepared liposome solution (55°C), containing HEPES-NaCl and 1 µg/µL Clonfectin. For the transfection, 4 µg of each construct DNA was mixed with 100 µl serum-free medium and 8 µg of Clonfectin and incubated for 30 min at RT. Cells were incubated in this solution for 4 hrs in a 5% CO_2 incubator. After washing in PBS (37°C), expansion medium was added and cells were further cultivated for 3 days. Hela cells were observed under a fluorescence microscope (Olympus BX60) after 48 hrs. Stable NIH3T3 transfectants were selected by cultivating in medium containing 1 mg/ml of G-418 for 4 weeks. This cell line was designated as

NIH3T3-pcDNA-*Piwil2*. As control, NIH3T3 cells were transfected with pcDNA plasmid and the stable cell line was designated as NIH3T3-pcDNA.

2.2.18 Cell proliferation assay

2.2.18.1 Proliferation assay kit

Stratagene's Quantos™ cell proliferation assay kit is a system for accurately quantitating the number of cells in a culture. The cell proliferation assay produces accurate counts of either adherent or free-floating cells for a wide range of cell concentrations and experimental conditions. The Quantos assay kit can also be used to measure the amount of double-stranded DNA in a sample of plasmid, lambda or genomic DNA. The cell proliferation assay is performed by lysing the cells in a sample and incubating the cell lysate with a dye that fluorescence when bound to DNA. The intensity of the fluorescence from the DNA-dye complex is then measured with a standard fluorometer. The number of cells in the sample is determined by comparing the fluorescence intensity of the sample to a previously generated standard curve. The standard curve relates the number of cells in a sample of the specific cell type of interest to the intensity of the fluorescence from the DNA-dye complex. The Quantos cell proliferation assay kit is useful as a high-throughputscreening method because a large number of samples can be analysed quickly in the 96-well format. The Quantos kit is ideal for quantitating cell proliferation during the course of an experiment because samples collected at many time points during an experiment can be analysed quickly.

2.2.18.2 Generation of a standard curve

The standard curve is a graph of the mathematical relationship between the number of cells in a sample and the intensity of the fluorescence from the DNA-dye complex. The relationship between the fluorescence intensity and the number of cells is linear for up to

10^5 cells/well or greater, depending on the cell type (in 100 µl suspensions). The absolute fluorescence intensity of the DNA-dye complex differs for different cell types. Therefore, a standard curve must be generated for the specific cell type of interest. A standard curve is generated by measuring the fluorescence intensity of the DNA-dye complex of several standards that contain different numbers of lysed cells. The fluorescence intensity vs. the number of cells for each standard is plotted and a regression line through the data points is determined using linear regression analysis.

Prepared suspensions of cells (1×10^6 cells) were counted by using a hemacytometer, transferred to a centrifuge tube, which was spun for 5 min at 200 x g to pellet the cells. Carefully removed, the supernatant was frozen at -70°C (or below) for 15 min and thawed at room temperature.

1 ml of the 1×dye reagent was added to the cells and cells were resuspended using a vortex mixer. The cell concentration should now be 1000 cells/µl. The cell suspension was added to the wells of a 96-well microtiter plate in aliquots of 1, 5, 10, 20, 30, 40, 50, 60 and 70 µl/well (a range of 1000-70000 cells/well). The reverse-pipetting technique to minimize formation of air bubbles increase the final volume in each well to 100 µl with 1x dye reagent (i.e., add 99, 95, 90, 80, 70, 60, 50, 40 and 30 µl/well, respectively). The microtiter plate was incubated for 1 hr at RT and was read by using a microtiter plate-reading fluorometer with filters appropriate for 355 nm excitation and 460 nm emission. The fluorescence intensity was plotted vs. the number of cells for each standard and the regression line through the data points was determined.

2.2.18.3 Observation of increased cell proliferation

NIH3T3-pcDNA and NIH3T3-pcDNA-*Piwil2* cells were seeded at 2000, 6500 and 9500 cells/well in 96-well plates, respectively. Cells were cultivated in microtiter plates for 2 hrs and 10 hrs. Quantification of cell proliferation was performed using Quantos cell proliferation assay kit. Fluorescence of a DNA-dye complex from lysed cells was determined using a microtiter plate-reading fluorometer with filters appropriate for 355 nm excitation and 460 nm emission.

2.2.19 Soft agar colony assay

NIH3T3-pcDNA, NIH3T3-pcDNA-*Piwil2* and GC-1 cells were mixed with cell culture medium containing 0.8% agarose. This cell suspension of 2000 cells/well was immediately plated in six-well plates coated with 0.3% agar in cell culture medium (2 ml per well) and cultured at 37°C with 5% CO_2. After 2 weeks, the top layer of the culture was stained with 0.001% Crystal violet for 1 hr. The culture was analysed in triplicate and colonies larger than 100 μm in diameter were counted.

2.2.20 Apoptosis Assay

2.2.20.1 Introduction to apoptosis assay

Apoptosis, or programmed cell death, plays a fundamental role in many normal biological processes, as well as in several disease states. Apoptotic cells undergo many distinct morphological and biochemical changes, including fragmentation of nuclear DNA. During apoptosis, cellular endonucleases cleave nuclear DNA between nucleosomes, producing a mixture of DNA fragments whose lengths vary in multiples of 180 to 200 bp. The BD ApoAlert™ DNA Fragmentation Assay Kit detects apoptosis-induced nuclear DNA fragmentation via a fluorescence assay. The assay is based on terminal deoxynucleotidyl transferase (TdT)-mediated dUTP nick-end-labeling. TdT catalyzes incorporation of fluorescein-dUTP at the free 3'-hydroxyl ends of fragmented DNA. Fluorescein-labeled DNA can be detected via fluorescence microscopy or flow cytometry. This kit uses a direct labeling procedure for detecting DNA fragmentation at the single-cell level. With a fluorescence microscope equipped with FITC filters, areas of apoptotic cells in situ in tissue sections can be visualized. The kit can be used with adherent cells and cells in suspension.

2.2.20.2 Sample preparation for microscopic detection

Most steps are performed in Coplin jars (Section III). The cells were grown in Lab-Tek Chamber Slides and washed by dipping twice in a Coplin jar containing PBS.

To fix the cells, the slides were immersed in a Coplin jar containing fresh 4% formaldehyde /PBS at 4°C for 25 min, immersed in a Coplin jar containing fresh PBS for 5 min at RT and repeated with PBS washing. The cells were permeabilized by immersing the slides in a Coplin jar containing prechilled 0.2% Triton X-100/PBS and then incubated for 5 min on ice. The cells were washed with fresh PBS for 5 min at RT, tapped gently to remove excess liquid, covered in 100 µl of equilibration buffer and then equilibrated at room temperature for 10 min. The cells were thawed Nucleotide Mix on ice was prepared by TdT incubation buffer for all experimental samples, positive controls and biological negative controls.

Equilibration Buffer	45 µl
Nucleotide Mix	5 µl
TdT Enzyme	1 µl

For TdT-minus negative control, TdT-minus control incubation buffer was prepared by replacing the TdT Enzyme with deionized H_2O. After removing the plastic coverslip, the slides were gently tapped to remove excess liquid with forceps, gently placed 50 µl of TdT incubation buffer and gently placed a piece of plastic coverslip on top of the cells to evenly spread the liquid with forceps. To perform the tailing reaction, the slides were placed in a dark, humidified 37°C incubator for 60 min. Then the plastic coverslips were removed with forceps. The tailing reaction was terminated by immersing the slides in a Coplin jar containing 2x SSC for 15 min and then washed with PBS. The cells were stained with propidium iodide (PI) by incubating the slides in a Coplin jar containing 40 ml of fresh PI/PBS at RT for 5-10 min, washed by transferring the slides to a fresh Coplin jar filled with deionized H_2O and then incubated at RT for 5 min.

Apoptotic cells will exhibit strong nuclear green fluorescence using a standard fluorescein filter set (520±20 nm). All cells stained with PI exhibit strong red cytoplasmic fluorescence

when viewed at >620 nm.

2.2.20.3 Detection by flow cytometry

3-5x 10^6 cells were collected by centrifugation at 300 x g for 10 min at 4°C. 5 ml of PBS were added to the cells, gently resuspended and collected by centrifugation at 300 x g for 10 min at 4°C. The cells were prechilled with 1% formaldehyde/PBS, incubated at 4°C for 20 min and collected by centrifugation at 300 x g for 10 min at 4°C. The cells were gently resuspended in 0.5 ml of PBS, permeabilized by adding 5 ml of 70% ice-cold ethanol and incubated at -20°C for at least 4 hrs. The cells can be stored at -20°C for up to 1 week. After centrifugation, the supernatant was carefully aspirated, gently resuspended in 80 µl of Equilibration Buffer and incubated at RT for 5 min. The Nucleotide Mix was thawed on ice. The TdT incubation buffer was prepared for all experimental samples, positive controls and biological negative controls.

Equilibration Buffer	45 µl
Nucleotide Mix	5 µl
TdT Enzyme	1 µl

For TdT-minus negative control, TdT-minus control incubation buffer was prepared by replacing the TdT enzyme with deionized H_2O. The cells were resuspended in 50 µl of TdT incubation buffer, incubated at 37°C in a water bath for 60 min and added 1 ml of 20 mM EDTA to terminate the reaction. The cells were collected by centrifugation at 300 x g for 10 min at 4°C, resuspended in 1 ml of 0.1% Triton X-100/BSA/PBS, collected by centrifugation at 300 x g for 10 min at 4°C, carefully aspirated, stained with propidium iodide (PI) by gently resuspending them in 0.5 ml of PI/RNase/PBS and incubated at RT in the dark for 15-30 min. Apoptotic cells can be collected based on green fluorescence at 520 ± 20 nm. All cells can be sorted based on red fluorescence at >620 nm.

2.2.21 Gene silencing by RNA interference

The term RNA interference (RNAi) describes the use of double-stranded RNA to target specific mRNAs for degradation, thereby silencing their expression. RNAi is one manifestation of a broad class of RNA silencing phenomena that are found in plants, animals and fungi (Cogoni and Macino, 2000). The discovery of RNAi has changed the understanding of how cells guard their genomes, led to the development of new strategies for blocking gene function and may yet yield RNA-based drugs to treat human diseases.

2.2.21.1 Overview of the RNAi mechanism

In the initiation step, input dsRNA is digested into 21-23 nucleotide small interfering RNAs (siRNAs), which have also been named "guide RNAs" (Elbashir et al., 2001). The siRNAs are produced when the enzyme Dicer, a member of the RNaseIII family of dsRNA-specific ribonucleases, processively cleaves dsRNA (introduced directly or via a transgene or virus) in an ATP-dependent. Successive cleavage events degrade the RNA to 19-21 bp duplexes (siRNAs), each with 2-nucleotide 3' overhangs (Hutvagner et al., 2002). In the effector step, the siRNA duplexes bind to a nuclease complex to form what is known as the RNA-induced silencing complex, or RISC. An ATP-depending unwinding of the siRNA duplex is required for activation of the RISC. The active RISC then targets the homologous transcript by base pairing interactions and cleaves the mRNA ~12 nucleotides from the 3' terminus of the siRNA (Elbashir et al., 2001). Consensus RNase III active site in the second RNase III domain inactivates the central catalytic sites, resulting in cleavage at 22-nucleotide intervals.

2.2.21.2 siRNA experiments for transient transfections

GC-1 and MDA-MB-231 cells were used for siRNA transfections. Cells were plated at $2.0x10^5$cells per well in a 6-well tissue culture plate. Following 24 hrs in culture, cells were transfected with 80 nM *Piwil2* siRNA (Invitrogen siRNA).

Piwil2 siRNA (mouse)
Sense: 5'-ACACAGCAUUC CGGCCUCCUUCAAA-3'
Antisense: 5'-UUUGAAGGAGGCCGGA AUGCUGUGU-3'

Piwil2 siRNA (human)
Sense: 5'-GGAUCUAUUCUCUAUCUGCCUGUUA-3'
Antisense: 5'-UAACAGGCAGAUAGAGAAUAGAUCC-3'

Luciferase double-stranded RNA (Eurogentec, Belgium) was used as a control RNAi treatment.
luc sense: 5'- CGUACGCGGAAUACUUCGAdTdT -3'
luc antisense: 5'- UCGAAGUAUUCCGCGUACGdTdT -3'

For transfections, GC-1 and MDA-MB-231 cells were cultured in 6 well plates up to 10-20% and 40-50% confluency, respectively. 3 µl of duplex RNA (1.4 µg/µl), 6 µl of sense and 6 µl of antisense single strand RNA (0.7 µg/µl) were added to 400 µl OPTI-MEM I (Invitrogen) in three separate 1.5 ml tubes. Next, 10 µl of Lipofectamine 2000 was added to 234 µl of OPTI-MEM I in an 1.5 ml tube, mixed by pipetting and incubated 10 min at RT. After this incubation step, Lipofectamine 2000 solution was added to each RNA sample and the tubes were incubated for 20 min at RT. During this time, the cells were washed with PBS and 2 ml OPTI-MEM I medium was added to each flask. After the 20 min incubation step, transfection mixtures (RNA/Lipofectamine 2000 in OPTI-MEM) were added to the cells and the cells were incubated at 37°C in a humidified incubator with 5% CO_2 for 8 hrs. After this time 4 ml of normal medium was added to each flask and the cells were cultured at the same conditions. At different time points after transfections (0, 24, 48 and 72 hrs), both living cells attached to the bottom and cells floating in the medium were collected and used for total RNA and protein isolation, followed by RT-PCR and Western blot analysis to verify silencing of gene expression and for determination of cell death and apoptosis. All experiments were carried out in triplicate.

2.2.22 Immunofluorescence staining of cells

NIH3T3-pcDNA cells, NIH3T3-pcDNA-*Piwil2* cells, MDA-MB-231 cells and GC-1 cells transfected with *Piwil2* siRNA were seeded on culture slides to 50 to 60% confluence. Cells were fixed in 4% paraformaldehyde solution and washed 3 times in PBS. These cells were incubated with a 1:100 anti-rabbit Piwil2 peptide Ab, Itga6 anti-goat polyclonal Ab (Santa Cruz Biotechnology), Stra8 anti-mouse peptide Ab (Eurogentec, Belgium), CD9 anti-mouse monoclonal Ab (Santa Cruz Biotechnology) and Hsp90a anti-goat polyclonal Ab (Santa Cruz Biotechnology), respectively, or together as primary antibodies in a humidifying chamber at 4°C overnight. After the coverslips were washed five times, for subcellular studies they were incubated with a 1:500 fluorescein isothiocyanate-conjugated goat anti-rabbit-IgG (Sigma-Aldrich), fluorescein isothiocyanate-conjugated goat anti-mouse-IgG (Sigma-Aldrich), Cy3-conjugated anti-mouse-IgG secondary antibody (Sigma-Aldrich), Cy3-conjugated anti-rabbit-IgG secondary antibody (Sigma-Aldrich), or Cy3-conjugated anti-goat-IgG secondary antibody (Sigma-Aldrich). Slides were washed with PBS (3 times). The cells were observed under a fluorescence microscope (Olympus BX60). The morphology of NIH3T3-pcDNA and NIH3T3-pcDNA-*Piwil2* cells were observed by using OLYMPUS IX81 Inverted Microscope.

2.2.22.1 DAPI staining of eukaryotic cells

Cells undergoing apoptosis display typical features, namely cell shrinkage, chromatin condensation and nuclear fragmentation. Dramatic changes occur within the nucleus during apoptotic death. Later, the nucleolus disintegrates, nuclear membrane develops deep invaginations and ultimately, the nucleus fragments into dense granular particles (apoptotic bodies). Chromatin condensation, nuclear shrinkage and formation of apoptotic bodies can easily be observed by fluorescence microscopy after appropriate staining of nuclei with DNA-specific fluorochromes (DAPI) (Collins et al., 1997).

For DAPI staining, cells were cytocentrifuged on glass slides, dried overnight and fixed for 10 min in 100% acetone. Thereafter, cells were incubated with Vectashield Mounting Medium with DAPI (Vector Laboratories Ltd., Peterborough, England). Stained cells were

analysed and counted under a fluorescent microscope BX60 (Olympus Optical Co. LTD, Japan).

2.2.23 Histological techniques

2.2.23.1 Tissue preparation for paraffin-embedding

The freshly prepared tissues were fixed in Bouin's solution for 24-72 hrs to prevent alterations in the cellular structure. The tissue to be embedded in paraffin should be free of water. The dehydration process was accomplished by passing the tissue through a series of increasing alcohol concentrations. For this purpose, the tissue was let in 70%, 80%, 90%, 96% and 100% ethanol for at least 1 hr at RT. Later, the ethanol was removed from the tissue by incubating it in isopropanol overnight. Tissue was then incubated in different mixtures of isopropanol/xylol (histoclear) in ratios 3:1, 1:1 and 1:3 for 30 min-1 hr at RT. Then tissue was incubated in 100% xylol overnight. Further, tissue was incubated in paraplast at 60°C overnight. Before embedding, paraplast was changed at least three times. Finally, the tissue was placed in embedding mould and melted paraffin was poured into the mould to form a block. The block was allowed to cool and was then ready for sectioning or stored at 4°C.

2.2.23.2 Sections of the paraffin block

The paraffin blocks were pre-cut to the optimal size and clamped into the microtom (Hn 40 Ing., Nut hole, Germany). The cut-thickness of the paraffin embedded was for 3-7 µm. The sections were floated on 40°C water to allow actual spread and subsequently put onto Superfrost slides. A fine brush was used to transfer the sections to slides. Slides were then dried at 40°C and incubated in 80°C for about 15 min to get rid off excess of paraffin. Slides were then stored at RT for further analysis.

2.2.23.3 Tissue preparation for electron microscopy

Freshly isolated testes were treated with fixation solution for 8-12 hrs at 4°C. Tissues were then washed in washing buffer for 1-2 hrs and used for electron microscopical analysis.

Fixation solution:	1% paraformaldehyde
	3% glutaraldehyde
	In 0.1 M Cacodylat buffer, pH 7.4
Washing solution	3.4% Saccharose
	In 0.1 M Cacodylat buffer, pH 7.4

2.2.23.4 Hematoxylin-eosin staining of the histological sections

The stored slides with the paraffin sections were first incubated three times in histoclear (Xylol) for 3 min, followed by incubation in 100%, 96%, 80%, 70% and 50% ethanol for 2 min in each. Slides were then washed 1 min in H_2O and stained for 15 min in hematoxylin. Staining was followed by washing in running tap water for 10 min. Thereafter slides were stained with eosin (0.1%+2% acetic acid) for 1 min, then in dH_2O for 1 min and incubated in 50%, 70%, 80%, 90%, 96% and 100% ethanol for 2 min in each. Finally they were incubated two times in histoclear (Xylol) for 3 min and closed with cover slides.

2.2.23.5 Tissue preparation for electron microscopy

For conventional electron microscopy, mouse testis was fixed with 1% paraformaldehyde and 3.5% glutaraldehyde in 0.1 M cacodylate buffer (pH 7.4) for 8-12 hr. Fixed testes were cut into small pieces and thoroughly washed over 3-4 days at 4 °C in 0.1 M cacodylate buffer containing 0.1 M saccharose. Tissue fragments were then treated with 1% OsO_4 in cacodylate buffer for 2 hrs, washed three times, dehydrated and embedded in epoxy resin. Ultrathin sections were contrasted using uranyl acetate and lead citrate and examined with a Leo 906 electron microscope.

2.2.24 Indirect immunohistochemistry

Fixation and subsequent treatment of mouse testis was performed as described in 2.2.16. Tissue cross sections (5-7 µm) were deparaffinized with roticlear solution (Roth) and rehydrated by descending ethanol concentrations. For immunostaining, sections were washed 3 times in PBS and were then incubated with a blocking solution (60 µl of horse serum, 150 µl of 10%Triton X-100 and 2790 µl o PBS) for 1 hr at RT. Testis sections were incubated with primary antibody (1:50-1:100) overnight at 4°C. Sections were then rinsed three times in PBS and subsequently incubated with secondary antibody (e.g. FITC-conjugated IgG or Cy3-conjugated IgG 1:500; Sigma) for 1 hr at RT. After incubation with secondary antibody, sections were washed again in PBS and the nuclei were counterstained with DAPI (Vector). Immunostaining of the sections was examined using a fluorescence-equipped microscope (BX60; Olympus).

2.2.25 Generation of transgenic mice

Generation of transgenic mice was performed by "Transgenic Service" of Max Planck Institute for Experimental Medicine in Göttingen by pronuclear microinjection of DNA. Method for transgenic animal production was based on Hogan et al. 1986.

2.2.25.1 Preparation of DNA for pronuclear microinjection

Transgenic constructs were released from cloning vector by restriction digestion. Digested fragments were separated by agarose gel electrophoresis (without EtBr) in the way that 25 µg of digested plasmid was loaded to many slots of the gel. After separation, outer lanes were cut out and stained with EtBr. After staining, gel was reconstructed and appropriate gel slices were cut out from the rest of the gel under UV light. DNA was then eluted from gel with QIAquick extraction kit and filtered through 0.45 µm microfilter (Milipore). Concentration of DNA was estimated by EtBr electrophoresis of DNA aliquot in

comparison with Smart ladder marker (defined DNA amounts in each band). For microinjection, DNA was diluted to 4 ng/µl in microinjection buffer (10 mM Tris, pH 7.5, 0.1 mM EDTA, pH 8.0).

2.2.26 Determination of sperm parameters

2.2.26.1 Sperm count in epididymis, uterus and oviducts

Epididymes of mice were dissected under aseptic conditions and put into 0.5 ml of in vitro fertilization (IVF) medium. Spermatozoa were allowed to swim out of the epididymis for 1 hr at 37°C, 5 % CO_2. Sperm suspension was diluted 10-40 times with PBS before counting, when necessary. 5 µl of this suspension was put into Neubauer counting chamber and sperms were counted in 8 independent fields (each having an area of 0.0025 mm^2) under the microscope (Olympus BX60) with 20x magnification. Total sperm numbers were calculated by following formula:

Total Sperm = average No. of sperm x 10 x 500 x B (B is the dilution)

For determination of sperm number in the uterus and the oviduct *Piwil2*-overexpressing males were mated with wild type females. The uteri and oviducts of those mice which were positive for vaginal plug were dissected in IVF medium and the sperm were flushed out.

2.2.26.2 Determination of sperm abnormalities

For the determination of sperm abnormalities, sperm suspensions were spread onto Superfrost slides, air-dried and fixed in 4% PFA for 10 min at RT. Slides were then washed 1 min in H_2O and then stained 15 min in haematoxylin. Next, they were washed in running tap water for approximately 10 min and finally stained with eosin (0.1%+2% acetic acid) for 1 min and washed in H_2O for 1 min. 200 sperms were counted and designed as normal

or abnormal (normal or unusual sperm head shape). Percentage of abnormal sperm was determined.

2.2.26.3 Sperm motility

10 µl of sperm suspension was put on a dual sided sperm analysis chamber. Sperm motility was quantified using the computer assisted semen analysis (CASA) system (CEROS version 10, Hamilton Thorne Research). 5000-10000 spermatozoa from 3 mice of mutant line and 2 of wild type were analysed using the following parameters: path velocity (VAP), progressive velocity (VSL), track speed (VCL), lateral displacement (ALH), beat cross frequency (BCF) and straightness (STR). Frequencies of these six sperm motility parameters were examined by probability plots categorised by mouse type (wild type/mutant) and by time of observation (1.5, 3.5 and 5.5 hrs after preparation) for statistical analysis.

2.2.27 Computer analysis

For the analysis of the nucleotide sequences, programs like BLAST, BLAST2, MEGABLAST and other programs from National Center for Biotechnology Information (NCBI) were used (www.ncbi.nlm.nih.gov). For restriction analysis of DNA NEBcutter V2.0 program was used (http://tools.neb.com/NEBcutter2/index.php). Information about mouse alleles, phenotypes and strains were used from Jackson Laboratory (www.informatics.jax.org). For proteins studies ExPASy tools (www.expasy.ch) were used. Mouse genome sequence and other analysis on mouse genes, transcript and putative proteins were downloaded from Celera discovery system (www.celera.com). For statistical analysis Statistic program (Statsoft ®, http://www.statsoftinc.com) was used.

2.2.28 Analysis of spermatogenesis

Prof. Dirk G. de Rooij (Utrecht, Netherlands) analysed the spermatogenesis in *Piwil2* transgenic mice.

3. RESULTS

3.1 Introduction to result section

Piwil2 cDNA was first cloned from the genital ridges of developing embryos and adult testis (Kuramochi-Miyagawa et al., 2001). By comparison of cDNA and mouse genomic sequences available in electronic databases (NCBI, Celera) we were able to determine exon-intron structure of the gene. *Piwil2* is composed of 23 exons, is localized on mouse chromosome 14 and codes for 4913 bp of mRNA, 971 amino acids (Fig. 3.1). Genomic structure of human orthologue gene *PIWIL2* has 24 exons, 3250 bp of transcript length and codes for 973 amino acids (NCBI). The human gene is localized on chromosome 8p21.3. *Piwil2* gene belongs to *piwi* gene family. The *piwi* family genes encode basic proteins that contain a highly conserved PAZ domain of 110 amino acid residues in the middle region of the proteins and a 300 amino acid Piwi domain in the C-terminal region (NCBI) (Fig. 3.1 and 3.2).

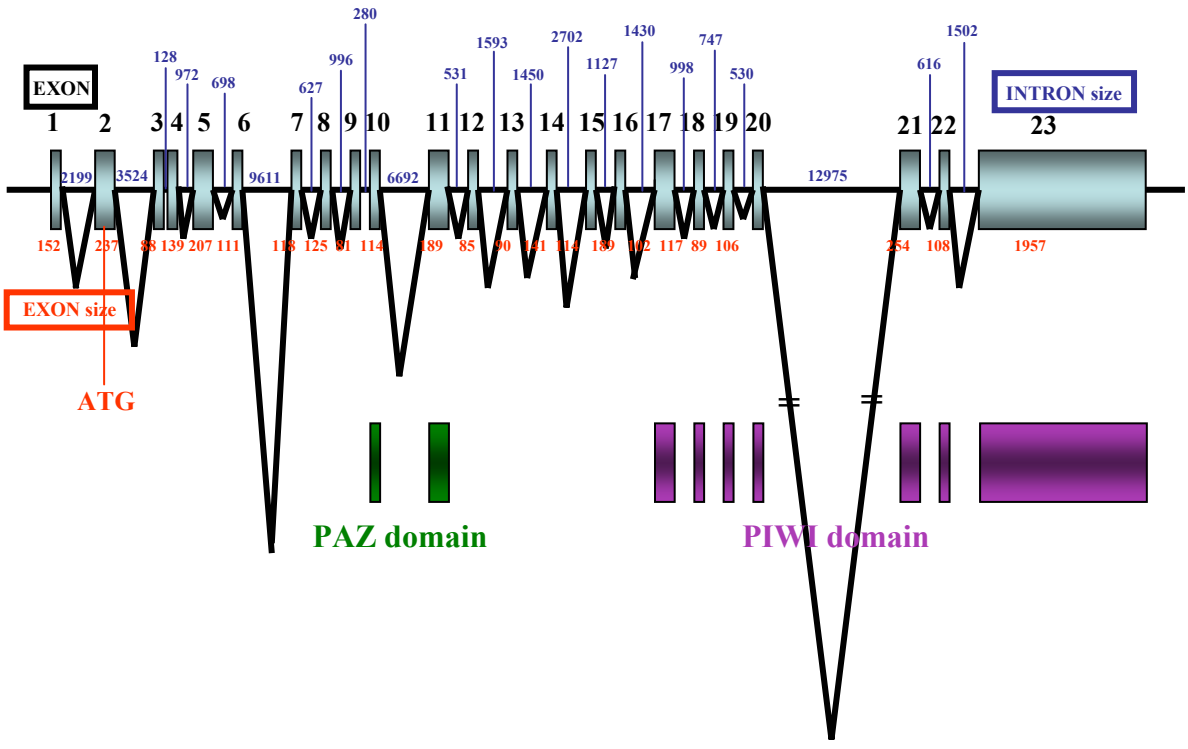

Figure 3.1: Schematic representation of the exon-intron structure of mouse *Piwil2*. Boxes indicate the positions of exons. Red numbers indicate the size of exons and blue numbers indicate the size of introns. Green boxes indicate PAZ domains and violet boxes indicate PIWI domains. The position of ATG is in second exon.

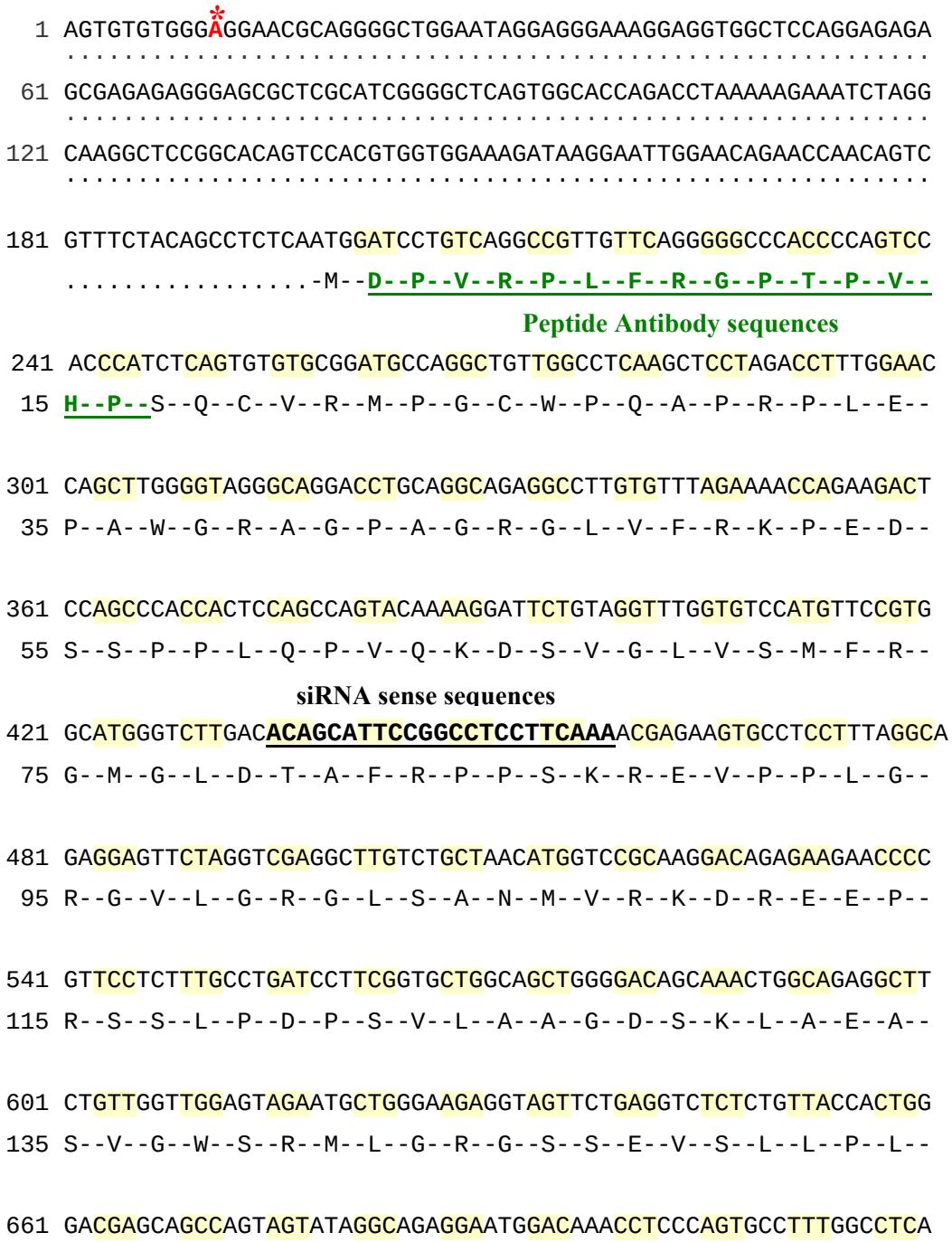

```
 155 G--R--A--A--S--S--I--G--R--G--M--D--K--P--P--S--A--F--G--L--

 721 CAGCTCGGGATCCCCCACGGCTGCCACAGCCTCCAGCTCTGTCTCCAACTTCACTGCACT
 175 T--A--R--D--P--P--R--L--P--Q--P--P--A--L--S--P--T--S--L--H--

 781 CTGCCGATCCCCCTCCGGTCCTGACTATGGAACGAAAGGAAAAAGAGCTTTTGGTCAAGC
 195 S--A--D--P--P--P--V--L--T--M--E--R--K--E--K--E--L--L--V--K--

 841 AAGGATCAAAAGGAACTCCTCAGTCTTTGGGACTGAACCTCATCAAAATCCAGTGTCATA
 215 Q--G--S--K--G--T--P--Q--S--L--G--L--N--L--I--K--I--Q--C--H--

 901 ACGAAGCAGTTTATCAGTACCATGTGACTTTCAGCCCCAGTGTGGAATGCAAAAGCATGA
 235 N--E--A--V--Y--Q--Y--H--V--T--F--S--P--S--V--E--C--K--S--M--

 961 GGTTTGGCATGTTGAAGGACCACCAGTCTGTCACTGGAAACGTCACTGCTTTTGATGGCT
 255 R--F--G--M--L--K--D--H--Q--S--V--T--G--N--V--T--A--F--D--G--

1021 CTATTCTTTATCTTCCTGTTAAGCTTCAACAAGTTGTTGAGTTAAAAAGTCAGAGGAAAA
 275 S--I--L--Y--L--P--V--K--L--Q--Q--V--V--E--L--K--S--Q--R--K--

1081 CTGACGATGCCGAGATCAGTATCAAGATTCAGCTGACAAAGATCCTGGAGCCGTGTTCTG
 295 T--D--D--A--E--I--S--I--K--I--Q--L--T--K--I--L--E--P--C--S--

1141 ACCTGTGCATCCCCTTCTACAATGTTGTCTTCCGGCGGGTAATGAAACTTCTGGATATGA
 315 D--L--C--I--P--F--Y--N--V--V--F--R--R--V--M--K--L--L--D--M--

1201 AGCTTGTGGGGAGAAACTTCTATGACCCTACAAGTGCCATGGTACTGCAGCAACACAGAT
 335 K--L--V--G--R--N--F--Y--D--P--T--S--A--M--V--L--Q--Q--H--R--

1261 TGCAGATCTGGCCTGGCTATGCGGCTAGTATCCGGAGGACAGACGGGGGTCTCTTCCTGC
 355 L--Q--I--W--P--G--Y--A--A--S--I--R--R--T--D--G--G--L--F--L--

1321 TCGCTGATGTCTCTCATAAGGTCATTCGGAACGACTCTGTGCTGGATGTCATGCATGCTA
 375 L--A--D--V--S--H--K--V--I--R--N--D--S--V--L--D--V--M--H--A--

1381 TCTACCAGCAGAACAAGGAGCACTTCCAGGACGAGTGCAGCAAGCTTCTGGTTGGCAGCA
 395 I--Y--Q--Q--N--K--E--H--F--Q--D--E--C--S--K--L--L--V--G--S--
```

```
1441 TTGTCATCACGCGCTACAACAATCGTACCTACCGAATCGATGATGTGGACTGGAACAAGA
 415 I--V--I--T--R--Y--N--N--R--T--Y--R--I--D--D--V--D--W--N--K--

1501 CCCCTAAAGACAGCTTTGTCATGTCGGACGGGAAGGAAATCACATTCCTGGAATACTACA
 435 T--P--K--D--S--F--V--M--S--D--G--K--E--I--T--F--L--E--Y--Y--

1561 GCAAAAACTATGGGATCACAGTCAAGGAAGATGACCAGCCGCTGCTGATCCACCGGCCCA
 455 S--K--N--Y--G--I--T--V--K--E--D--D--Q--P--L--L--I--H--R--P--

1621 GTGAGAGACAGAATAACCATGGCATGTTGCTGAAGGGCGAGATCCTGCTGCTGCCCGAGC
 475 S--E--R--Q--N--N--H--G--M--L--L--K--G--E--I--L--L--L--P--E--

1681 TCTCCTTCATGACGGGGATCCCTGAGAAGATGAAGAAGGACTTCAGGGCCATGAAGGACT
 495 L--S--F--M--T--G--I--P--E--K--M--K--K--D--F--R--A--M--K--D--

1741 TGACTCAGCAGATTAACCTGAGCCCCAAGCAGCACCACGGTGCTTTGGAATGCCTGCTGC
 515 L--T--Q--Q--I--N--L--S--P--K--Q--H--H--G--A--L--E--C--L--L--

1801 AGAGAATTTCACAAAACGAGACAGCCAGCAATGAGCTGACCCGCTGGGGGCTCAGTCTGC
 535 Q--R--I--S--Q--N--E--T--A--S--N--E--L--T--R--W--G--L--S--L--

1861 ATAAAGATGTCCACAAGATTGAAGGTCGGCTTCTGCCAATGGAGAGGATCAACTTAAGGA
 555 H--K--D--V--H--K--I--E--G--R--L--L--P--M--E--R--I--N--L--R--

1921 ACACTTCATTTGTCACATCGGAGGACCTGAACTGGGTTAAGGAAGTGACCAGAGATGCTT
 575 N--T--S--F--V--T--S--E--D--L--N--W--V--K--E--V--T--R--D--A--

1981 CCATTCTAACTATTCCCATGCATTTCTGGGCACTCTTTTATCCAAAGAGAGCAATGGACC
 595 S--I--L--T--I--P--M--H--F--W--A--L--F--Y--P--K--R--A--M--D--

2041 AAGCCAGAGAACTGGTTAACATGTTGGAAAAGATTGCCGGGCCCATTGGCATGCGCATAA
 615 Q--A--R--E--L--V--N--M--L--E--K--I--A--G--P--I--G--M--R--I--

2101 GCCCCCCAGCCTGGGTTGAGCTGAAGGATGACCGAATAGAGACCTATATCAGGACCATTC
 635 S--P--P--A--W--V--E--L--K--D--D--R--I--E--T--Y--I--R--T--I--

2161 AGTCCTTACTGGGAGTTGAGGGGAAGATACAAATGGTCGTTTGCATCATCATGGGCACAC
 655 Q--S--L--L--G--V--E--G--K--I--Q--M--V--V--C--I--I--M--G--T--
```

```
2221 GTGATGATCTCTATGGAGCCATCAAGAAGCTGTGCTGCGTGCAGTCCCCAGTGCCCTCAC
 675 R--D--D--L--Y--G--A--I--K--K--L--C--C--V--Q--S--P--V--P--S--

2281 AGGTCATCAATGTCCGAACCATTGGTCAGCCCACCAGGCTTCGGAGCGTGGCTCAGAAAA
 695 Q--V--I--N--V--R--T--I--G--Q--P--T--R--L--R--S--V--A--Q--K--

2341 TTTTACTTCAGATGAACTGTAAACTGGGTGGTGAGCTCTGGGGAGTGGATATTCCGCTGA
 715 I--L--L--Q--M--N--C--K--L--G--G--E--L--W--G--V--D--I--P--L--

2401 AACAACTAATGGTGATTGGAATGGATGTGTACCATGACCCCAGCAGAGGCATGCGCTCTG
 735 K--Q--L--M--V--I--G--M--D--V--Y--H--D--P--S--R--G--M--R--S--

2461 TGGTCGGCTTCGTGGCCAGCATAAATCTCACACTCACCAAATGGTACTCGAGGGTGGTGT
 755 V--V--G--F--V--A--S--I--N--L--T--L--T--K--W--Y--S--R--V--V--

2521 TCCAGATGCCACATCAGGAGATTGTGGACAGCCTGAAGCTCTGCCTGGTGGGTTCCTTGA
 775 F--Q--M--P--H--Q--E--I--V--D--S--L--K--L--C--L--V--G--S--L--

2581 AAAAGTATTATGAGGTGAACCATTGTCTCCCAGAGAAAATTGTGGTGTACCGAGATGGAG
 795 K--K--Y--Y--E--V--N--H--C--L--P--E--K--I--V--V--Y--R--D--G--

2641 TGTCTGATGGCCAGCTAAAGACAGTTGCCAACTACGAGATCCCTCAGCTGCAGAAGTGTT
 815 V--S--D--G--Q--L--K--T--V--A--N--Y--E--I--P--Q--L--Q--K--C--

2701 TTGAAGCCTTTGATAACTACCACCCCAAGATGGTGGTGTTTGTAGTTCAGAAGAAAATCA
 835 F--E--A--F--D--N--Y--H--P--K--M--V--V--F--V--V--Q--K--K--I--

2761 GCACCAATCTGTACCTTGCTGCTCCTGATCACTTCGTAACCCCCTCCCCCGGGACTGTGG
 855 S--T--N--L--Y--L--A--A--P--D--H--F--V--T--P--S--P--G--T--V--

2821 TTGATCATACCATAACCAGCTGTGAGTGGGTGGATTTCTACCTTCTTGCCCATCATGTGC
 875 V--D--H--T--I--T--S--C--E--W--V--D--F--Y--L--L--A--H--H--V--

2881 GACAGGGCTGTGGCATACCTACACACTACATCTGTGTTCTGAACACTGCAAATCTGAGCC
 895 R--Q--G--C--G--I--P--T--H--Y--I--C--V--L--N--T--A--N--L--S--

2941 CTGATCACATGCAGAGGTTGACTTTCAAACTATGCCACATGTACTGGAATTGGCCTGGTA
```

```
 915 P--D--H--M--Q--R--L--T--F--K--L--C--H--M--Y--W--N--W--P--G--

3001 CCATCCGAGTTCCAGCTCCTTGCAAGTATGCCCACAAGCTAGCTTTCCTGTCCGGACAGA
 935 T--I--R--V--P--A--P--C--K--Y--A--H--K--L--A--F--L--S--G--Q--

3061 TTTTGCATCATGAGCCAGCCATCCAGCTGTGTGGGAACCTGTTCTTCCTGTAACTGGGAA
 955 I--L--H--H--E--P--A--I--Q--L--C--G--N--L--F--F--L--*-.......

3121 CTTGGACACCGGCTGCAAGGAGCAACTGGACTCAGCTCAGCTCCTCCTTACAGAATCAAC
     ............................................................

3181 AGAAATGGCAGTGGAATTTTATGTTTGCATTTTCTCTTTCTCCATCCTTGTAGAATTAGA
     ............................................................

3241 TTTCTGTTCTTCTTTTAACCCTGATATCATAGTAGGGTGTTGTGGTGCATGCCTTTTATC
     ............................................................

3301 CCAGCACTTGGGAGACTGAAGCAGGAGTATCTTTAGTTCAAGGCCAGCCTAGACTACATG
     ............................................................

3361 GTGAGTTCTAGGCTAGCCAAGATTACAGAGTGAGACCCTGTCTCAAAAAACAAAAACAAA
     ............................................................

3421 CCACTGTCCCCTCAAAGCCCACAACAAAACCAAAGCCTGGGGTCAAGGAAGCAAGTTTGT
     ............................................................

3481 AGGTAGCCGCTGGCTGCCCGCTGCCTTCATGGAGTGTGTGCCGTCAGCGCTGCTTCTCCT
     ............................................................

3541 CAGCCGAGCGTGGAGCTTCGGACAGGGCAGTGATGACATGTTCTTAGCATGTCAAATCCC
     ............................................................

3601 CCTACCAAATAAGTCAAGCAAGGAAAAAATAGCCCCCAAGGCAGCCTGAGCATCAGTTCC
     ............................................................

3661 TAGAGGTTATGCCTACAGAACCATCCTATTTCTGGTGGCAGAAGTGACATGAAGTCATTG
     ............................................................

3721 CAGACATCTTAAAGGAGAGTTACTGTGCAGCTGTCTACATGTGTGAAAGACATGTAGAAA
     ............................................................

3781 AACCAGCGTAGGGTACAGTCGGGCGTATGTGCCCACCTGACCCAGGGCTGTGAGTCTGAC
     ............................................................

3841 TTCCCGAGAGTCTGGCTAGAGCTGCTTTTCTGGTCCTTTTGGTTATTTGCAACCATCATC
     ............................................................

3901 AGATTGCTTTCCTGCAGCCCGACTGATACACGCATGTGCGCACGCACACACTTTTGTTCT
     ............................................................

3961 TTGTGACTAATCTTGAATAAATTCAATTAGAACACATGGAAAGGATTCAGCAGACCTAGG
     ............................................................

4021 AACATTTGGGGTGGAGTGTAGTTTTTCTGCAAAAGTCTGTAAATGAGATTACGCAAGAGT
     ............................................................

4081 CTCTTCCAGCTGTGGGCTGGTGTTGCTTGGAAAATTTCAAAATCCCAAAGTTTCAGGCTT
     ............................................................

4141 CCCAAAGTTGGCTTGGAAAAATGTGATAGTCTCACCTGAGTCTAGACATGTAGGAAATTT
     ............................................................

4201 TCCTAGGGCCTCTGGGCTTCAGTATTTGGGGGAAGCACTGGTTTTCTGTGTTATTTTTTT
     ............................................................

4261 CCTTCTGTTTCAGAATCTTCAAGTTTCTTCAGGCTTCAGTGGGCCATCCCTTTACTGGGC
     ............................................................
```

```
4321 TCTAAAAGCTAATTTTACTTAACCTTTTCAAATGTGTATGTATCTATTTATGTTTTGGTG
     ............................................................
4381 TGGTGGATGGATGGTAGGGGACTGAGCAGAAATAGTCATTTTAAATAACAGTGTGCTAGG
     ............................................................
4441 AGAGCCTCAGTGTGAAGTCCTGAGGAGCAGCGGGGGCTGTGGGAGTCAGTGTCAGCCCTC
     ............................................................
4501 ACTCAGACAGGCCAAGCCTGGGCTCGAAGACAACATTGTCCAGGGAAGCCTTTAGTTTGC
     ............................................................
4561 TATAGCACCCAGAGGTTGGCGAGGAATAAGGGTTAGGGTCCTCAAATACACCCATGGCTT
     ............................................................
4621 TTGGAGTCTATGACCAAGGCCAGGCTGAGACCTGAAATGTAAAAGCCATAGAATTAAACA
     ............................................................
4681 GAACAGACTGAAAAACGAGTCTTAAGTTCCACTTTCTGGATTTCTCTGGAAGTCTTTTGA
     ............................................................
4741 ATTTGTCTGTAGAAGTTGCTGTTCCTAGCACTCCTTTTCTCTTTAGGTAGAACAGATACT
     ............................................................
4801 TGACCATAATGCCAGAATGTACTTTCTCTGCCTTGGTTTTTCTATGCCTTGTTTTTCAGT
     ............................................................
4861 TTCAGGGCCAAACAATTGGGCCCTGTGGTGTAAAATAAAAACAATGTATGTGT
     ...................................................
```

Figure 3.2: Nucleotide sequence of *Piwil2* cDNA and deduced amino acid sequence. Numbering of nucleotide and amino acid sequence is given on the left, transcription start site is indicated by red asterisk and end of an exon sequence is marked with violet underline. The amino acid sequences of peptides used for generation of polyclonal antibodies are shown in green underline. Black underline indicates siRNA sense sequences. The PAZ domain (blue underline) binds the 2nt 3'-overhang of the siRNA duplex and facilitates anchoring of this guide RNA into the effector complex. The *Piwi* domain which mediates the interaction of PPD (PAZ and Piwi domains) proteins with Dicer is marked with red underline.

3.2 Expression analysis of *Piwil2*

3.2.1 Expression pattern of *Piwil2* in mouse and human by using RT-PCR

The expression of mouse and human *Piwil2* genes in different organs was analysed using RT-PCR and primers specific for mouse and human *Piwil2* gene. A 660 bp fragment of mouse *Piwil2* and a 630 bp fragment of human *Piwil2* gene were amplified. RT-PCR fragments were purified from the gel, cloned in pGEMT easy vector and sequenced to ensure that PCR products are specific for *Piwil2*. *Piwil2* expression was obtained only in testes of mouse and human (Fig. 3.3 A and B). To avoid detection of contaminating DNA in mRNA samples, primers were designed from different exons whose positions are from exon 1 to exon 6 in human *PIWIL2* and from exon 1 to exon 5 in mouse *Piwil2*.

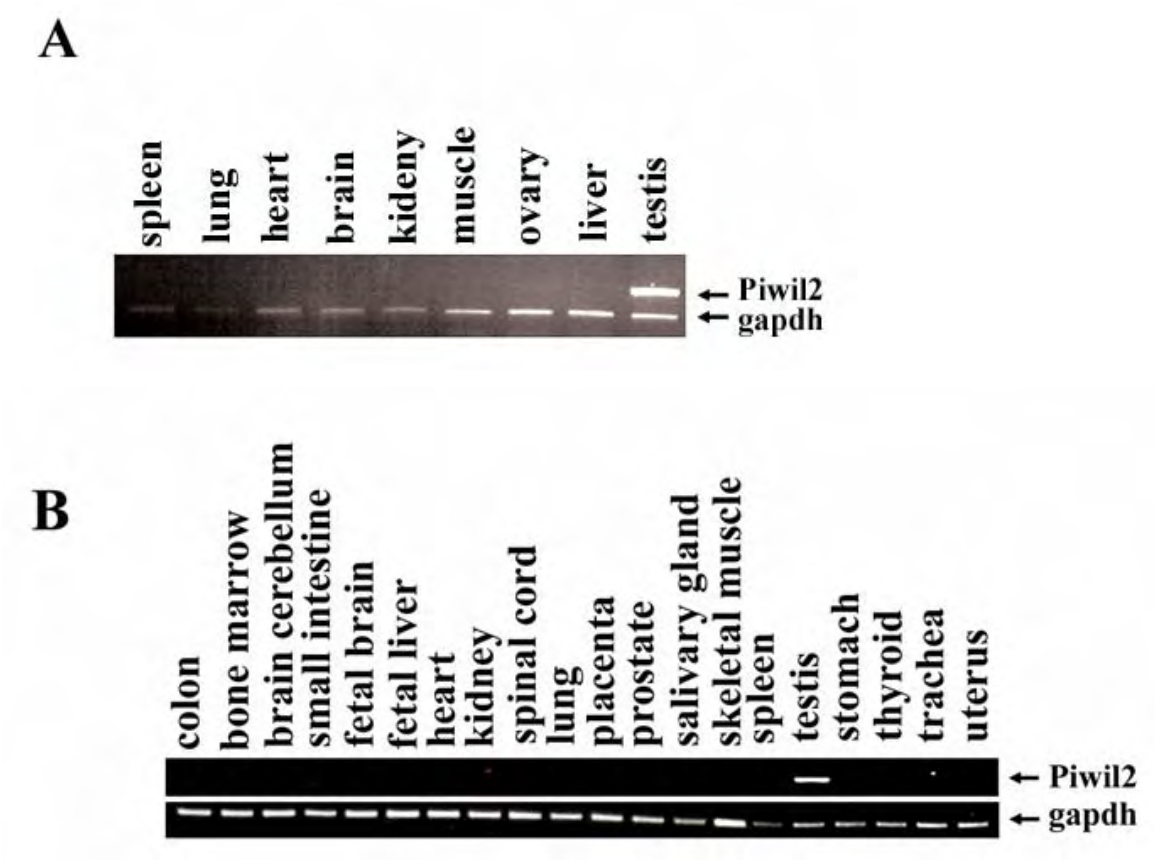

Figure 3.3: Expression analysis of *Piwil2* in different organs from mouse and human. (A) A testis-specific expression was observed using RT-PCR analysis in mouse (spleen, lung, heart, brain, kidney, skeletal muscle, ovary, liver, testis) and (B) human (colon, bone marrow, brain, small intestine, fetal brain, fetal liver, heart, kidney, spinal cord, lung, placenta, prostate, salivary gland, skeletal muscle, spleen, testis, stomach, thyroid, trachea and uterus). Mouse and human *gapdh* was used as positive control.

3.2.2 Expression pattern of *Piwil2* in mouse and human by using immunohistochemistry

Paraffin embedded adult mouse and human testes were cross-sectioned to a thickness of 7-10 µm. These testes sections were then immunostained with Piwil2 antibody. After an initial blocking step with goat serum in PBS, the slides were incubated with affinity-purified antibody against Piwil2 in a dilution of 1:100. Specific immunostaining (arising from binding of FITC and alkaline phosphatase conjugated secondary antibody) was observed only in spermatogonia and spermatocytes of mouse (Fig. 3.4 A) and human (Fig. 3.4 B). The Piwil2 immunostaining was superimposed with DAPI staining (which stains only the nucleus of the cell). Piwil2 is a cytoplasmic protein in mouse and human. However, Piwil2 expression was observed also in nucleus of some spermatogonia (Fig. 3.4 A). No staining was observed in Sertoli cells or in Leydig cells (Fig. 3.4). These data indicate that *Piwil2* gene is specifically expressed in spermatogonia and spermatocytes of testis and confirm the observations obtained by other groups (Kuramochi-Miyagawa et al., 2001; Sasaki et al., 2003).

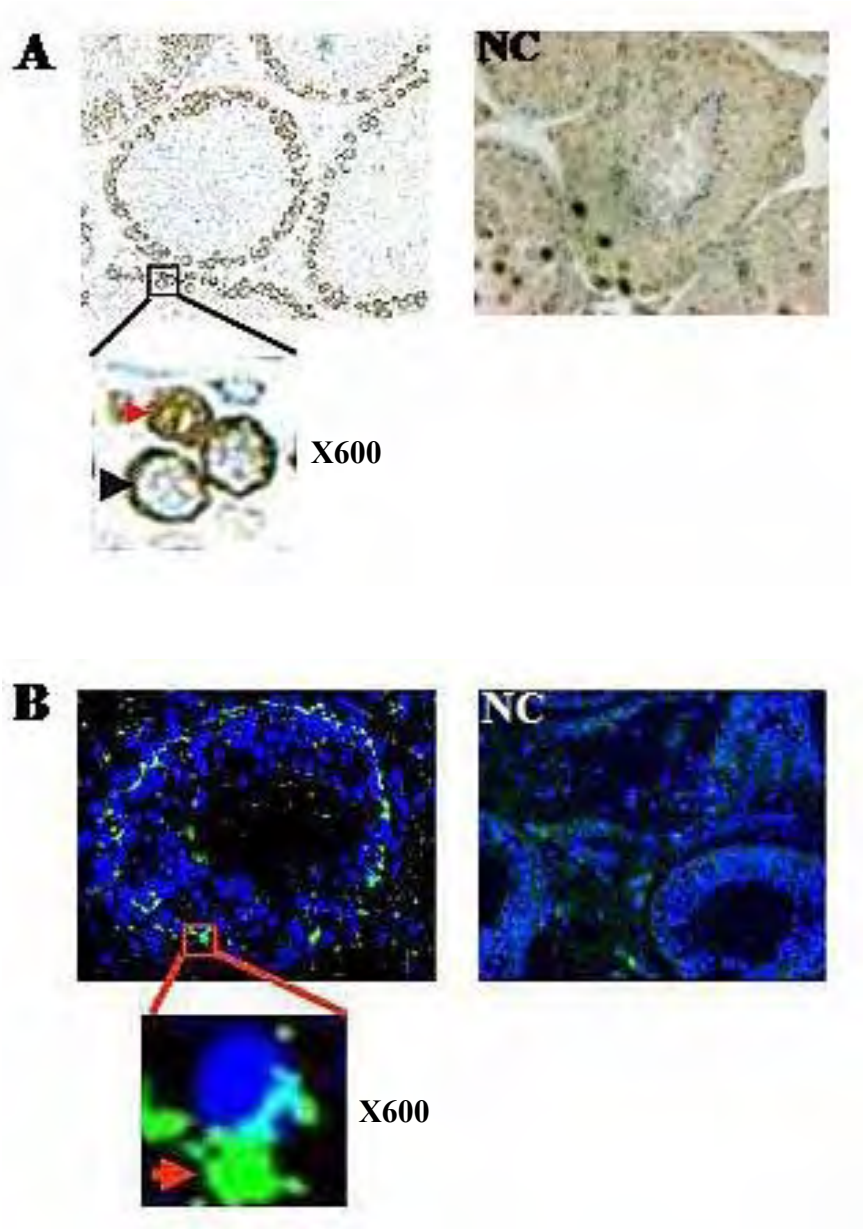

Figure 3.4: Expression analysis of Piwil2 in testis using immunohistochemical analysis. (A) In mouse, expression is restricted to nuclei of spermatogonia (red arrow) and cytoplasm of spermatocytes (black arrow) (magnification X200). No staining was observed after blocking using Piwil2 peptide (NC, negative control) (magnification X200). (B) In human testis, staining is also restricted to premeiotic germ cells (red arrow) (magnification X200). No staining was observed after blocking using Piwil2 peptide (NC, negative control) (magnification X200).

3.2.3 Expression pattern of *Piwil2* during germ cell development

To analyse the expression pattern of *Piwil2* during mouse germ cell development, total testicular RNA from different postnatal developmental stages was prepared, namely from stages 5, 11, 16, 20, 25, 30 and 36 days. *Piwil2* expression could be detected in all postnatal stages (Fig. 3.5 A). RT-PCR was done as well with RNAs from testes of different mutants with spermatogenesis defects: W/W^V, *Tfm/y*, *Leyl-/-*, *olt/olt* and *qk/qk*. W/W^V mice are characterized by lack of any germ cell, in *Tfm/y* and *Leyl-/-* mutants spermatogenesis is arrested at spermatocyte stage, while in *olt/olt* the arrest is at round spermatid stage and in *qk/qk* at elongated spermatid stage. The *Piwil2* transcript was detectable in all of these mutants, except W/W^V, which is lacking spermatogenesis capacity as a result of mutations in the *c-kit* gene (Loveland and Schlatt, 1997). The lack of the *Piwil2* transcript in W/W^V mutant demonstrates that expression of the gene is restricted to germ cells (Fig. 3.5 B).

Figure 3.5: Expression analysis of *Piwil2* gene by RT-PCR. (A) Total RNA was isolated from different developmental stages of mouse testis and (B) from testes of different mutants. Expression was detected in all mutants except W/W^V mice (5 months old), indicating germ cell specific expression of the gene. W: W/W^V, o: *olt/olt*, q: *qk/qk*, l: *Leyl-/-* and t: *Tfm/y*.

For analysis of Piwil2 expression on protein level, total testicular protein extracts from the different mutant mice were prepared and Western blot was performed (Fig. 3.6 A). Polyclonal antibodies against Piwil2 peptides were generated as described in Methods section 2.2.15. The positions and sequences of the peptides are shown in figure 3.2. In order to determine the specificity and affinity of antiserum, immunoblotting analysis was performed. Total protein extracts from testis and from kidney as control were separated on SDS-PAGE and transferred onto a PVDF membrane. The protein band of 107 kDa is in agreement with the predicted molecular weight of Piwil2 major protein (Fig. 3.6 B). As shown in figures 3.5 and 3.6, Piwil2 is not detectable in the testis of W/W^{V} mice by RT-PCR and Western blot analysis. Thus, Piwil2 expression appears to be restricted to germ cell lineage in mouse adult testis.

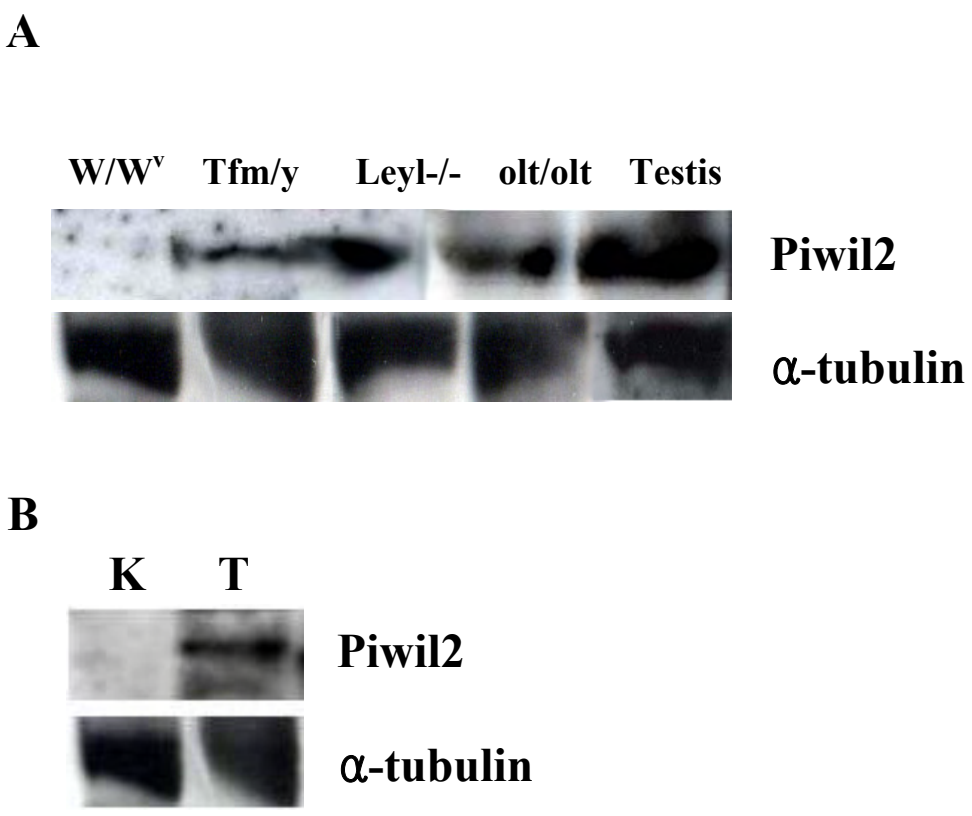

Figure 3.6: Expression analysis of Piwil2 by using Western blotting. (A) Western blot analysis using Piwil2 peptide antibody (1:50) on total testicular protein from different mouse mutants and (B) kidney (K) and testis (T) of wild type. Piwil2 antibody detects a strong band corresponding to size of 107 kDa in testis protein extract but not in total kidney protein. 50 µg of protein was loaded in each lane of the gel. α-tubulin served as positive control.

3.2.4 *Piwil2* expression in different mouse and human tumor cell lines

It was reported that in *Drosophila*, *piwi* activity modulates the number of germline stem cells and the rate of their division; overexpression of *piwi* leads to a significant increase in the number of germline stem cells and their rate of division (Cox et al., 2000). In this organism, piwi functions both as a component of a somatic signaling pathway that controls the self-renewal of germline stem cells and as a cell-autonomous factor that promotes stem cell division (Cox et al., 1998, 2000). Therefore, we performed expression of mouse and human *Piwil2* genes using RT-PCR in various tumor cell lines of mouse and human. A specific RT-PCR product was observed in most examined tumor cell lines (in 7 of 10 murine tumor cell lines). The *Piwil2* gene is strongly expressed in transformed germ cells as compared with transformed Leydig cell line (MA-10), teratocarcinoma cell line (F9), pituitary gland tumor cell lines (PCT), breast tumor (BT cell line) and neuroblastoma (NS 20Y) (Fig. 3.7 A). In 8 of 10 human tumor cell lines *PIWIL2* gene was found to be expressed. *PIWIL2* expression was slightly detected in prostate cancer (DU-145) and in embryonic carcinoma (H12.1) and a weak expression of *PIWIL2* was found in breast adenocarcinoma (MCF-7) and Burkitt's lymphoma (Daudi) (Fig. 3.7 B). No expression was detected in NIH-3T3 cells and in Sertoli cell (15P-1) (Fig. 3.7 A). These data indicate that *Piwil2* is expressed specifically in tumor cells of mouse and human.

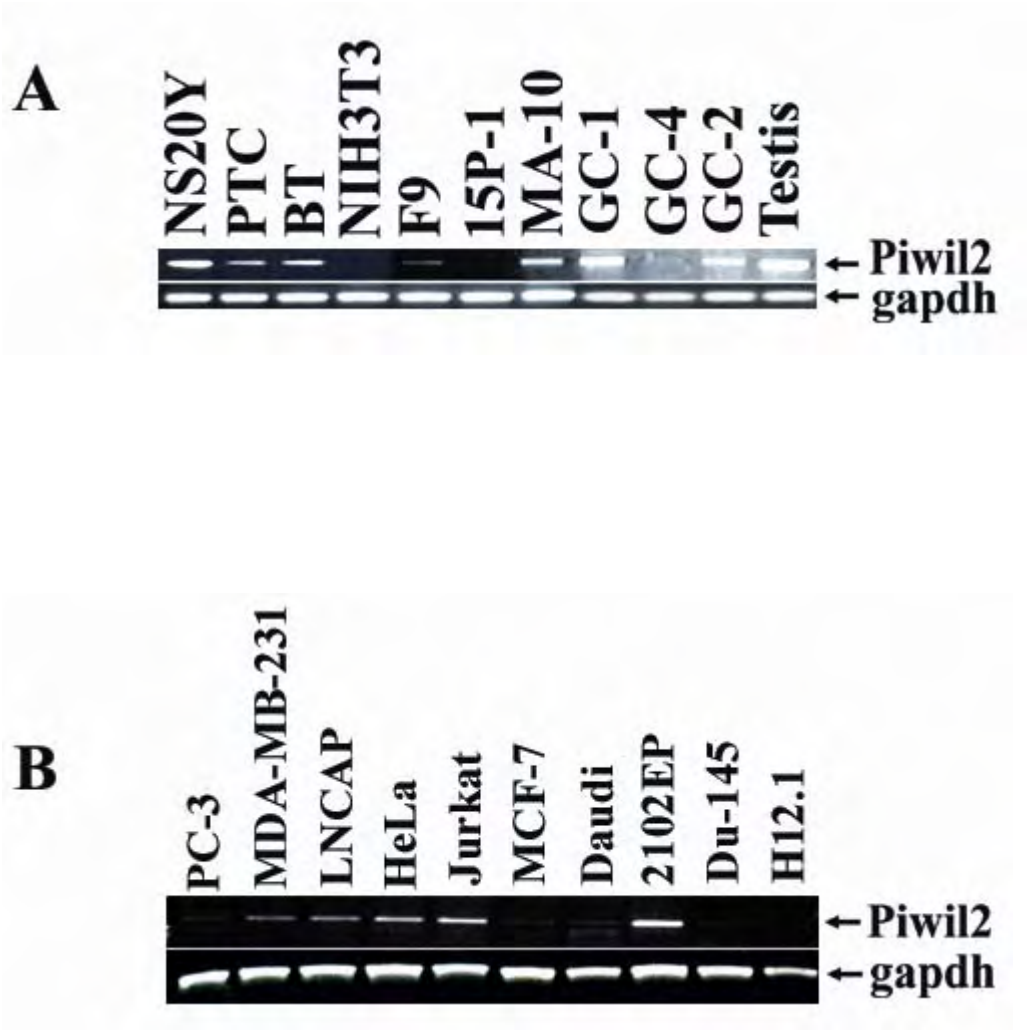

Figure 3.7: Expression of *Piwil2* in different cancer cell lines using RT-PCR. (A) In mouse, expression was obtained in transformed germ cells (GC-1 and GC-2), in transformed Leydig cell line (MA-10), and in teratocarcinoma cell line F9, breast tumor cell line (BT), in neuroblastoma cell line (NS20Y), in pituitary tumor cell line (PTC), but not in non-transformed spermatocyte (GC-4), Sertoli cell (15P-1) and NIH3T3 cell lines. Testicular RNA served as positive control. (B) In human, expression of Piwil2 was obtained in prostate cancer cell lines (PC-3, LNCAP and DU-145), breast cancer cell lines (MDA-MB-231, MCF-7), cervical cancer (HeLa), T cell leukaemia (Jurkat), Burkitt's lymphoma (Daudi) and embryonal carcinoma (2102EP). A very weak expression was detected in H12.1 cell.

3.2.5 *Piwil2* expression in different mouse and human tumor tissues

To examine expression of *Piwil2* in tumor tissues, RNAs were isolated from different mouse and human solid tumors and were subjected to RT-PCR analysis. In mouse, three types of tumors with their corresponding normal tissues were examined. Whereas in breast tumor, rhabdomyosarcoma and medulloblastoma expression of *Piwil2* was detected, no expression was observed in normal breast, muscle and cerebellum (Fig. 3.8 A). In different human tumor types, expression of *PIWIL2* was detectable using RT-PCR (Fig. 3.8 B). In 3 of 4 different ovarian tumors, in 4 of 4 different prostate carcinomas, in 4 tumors of lymphatic gland, and in 7 of 7 breast tumors expression of *PIWIL2* was detected (Fig. 3.8 B). These data suggest that *Piwil2* expression is correlated to a proliferation state.

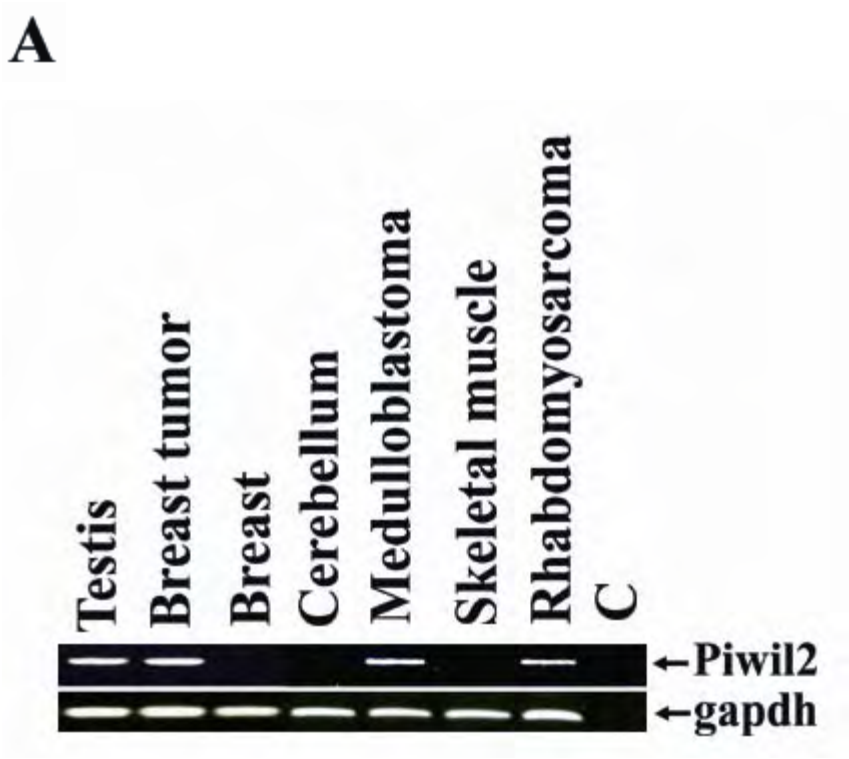

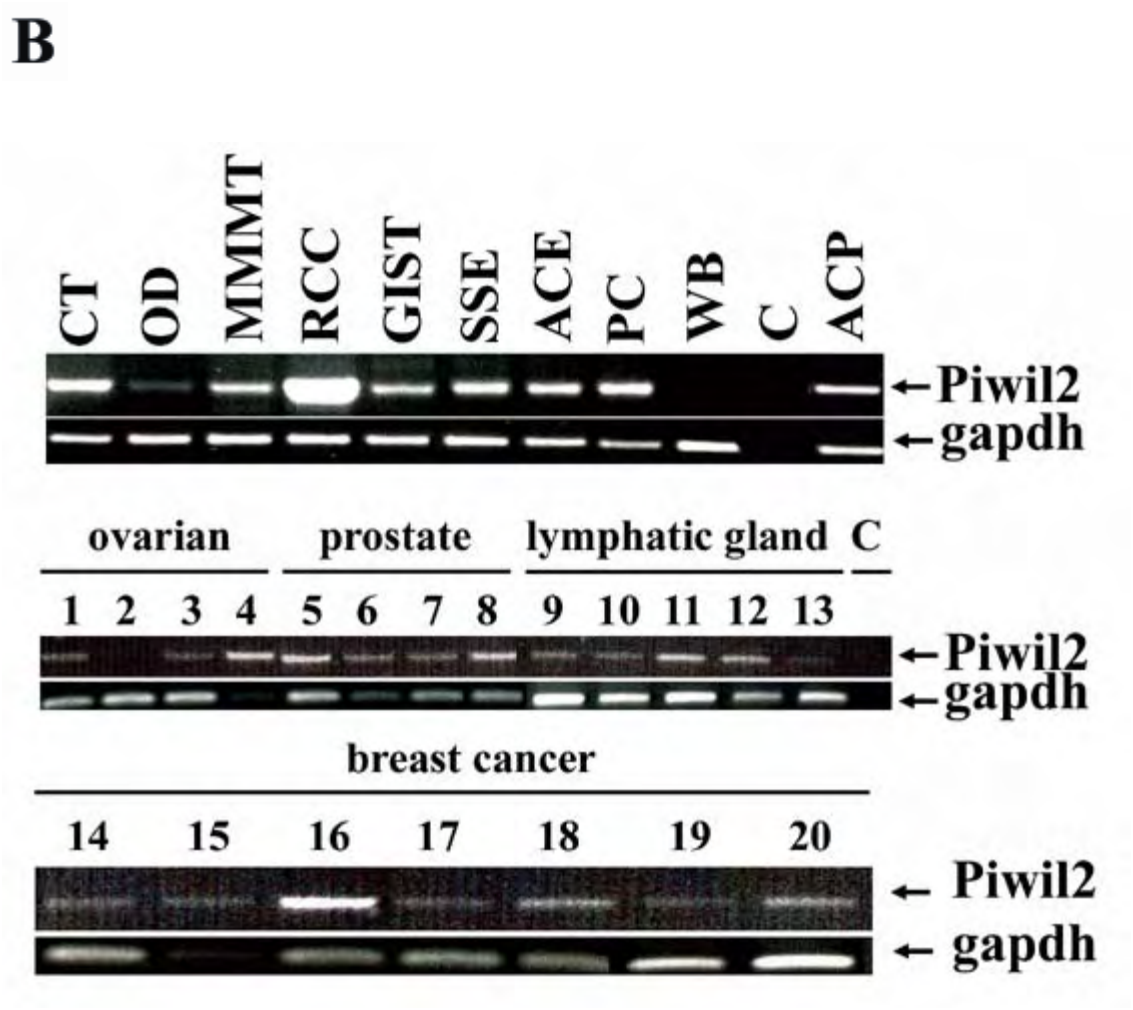

Figure 3.8: Expression of *Piwil2* in different cancer tissues using RT-PCR. (A) In mouse, three types of tumors with corresponding normal tissues were examined. Expression was detected in breast tumor, in medulloblastoma and in rhabdomyosarcoma, whereas no expression was detected in normal breast, cerebellum and skeletal muscle tissues, no-template control (C). (B) In human, in most tumors, expression of *Piwil2* was observed: colon tumor (CT), ovarian dysgerminoma (OD), malignant mixed mullerian tumor of the endometrium (MMMT), clear cell renal cell carcinoma (RCC), gastrointestinal stromal tumor (GIST), stromal sarcoma of endometrium (SSE), adenocarcinoma of endometrium (ACE), squamous cell carcinoma of pancreas (PC), normal woman blood (WB), adenocarcinoma of pancreas (ACP). For some types of tumors, tumor tissues from different patients were examined: ovarian cancer (1-4), prostate carcinoma (5-8), lymphatic gland tumors (9-13) and breast tumors (14-20). Expression of *Piwil2* was detected in nearly all tumors. C, no-template control; *gapdh* served as positive control.

To examine expression of Piwil2 on protein level, immunostaining was performed using antibody against Piwil2 peptide. GC-1 cells were seeded on culture slides (FALCON, Le Pont De Claix, France) to 50 to 60% confluence and then incubated with an anti-Piwil2 antibody. The cells were observed under a fluorescence microscope (Olympus BX60). In mouse, expression of Piwil2 was detected in transformed testicular germ cell line GC-1. Expression was observed in proliferating cells (Fig. 3.9 A). Expression of Piwil2 was not detected in normal skeletal muscle and cerebellar tissues (Fig. 3.9 B), Piwil2 was detectable in corresponding tumor tissues, rhabdomyosarcoma and medulloblastoma (Fig. 3.9 B).

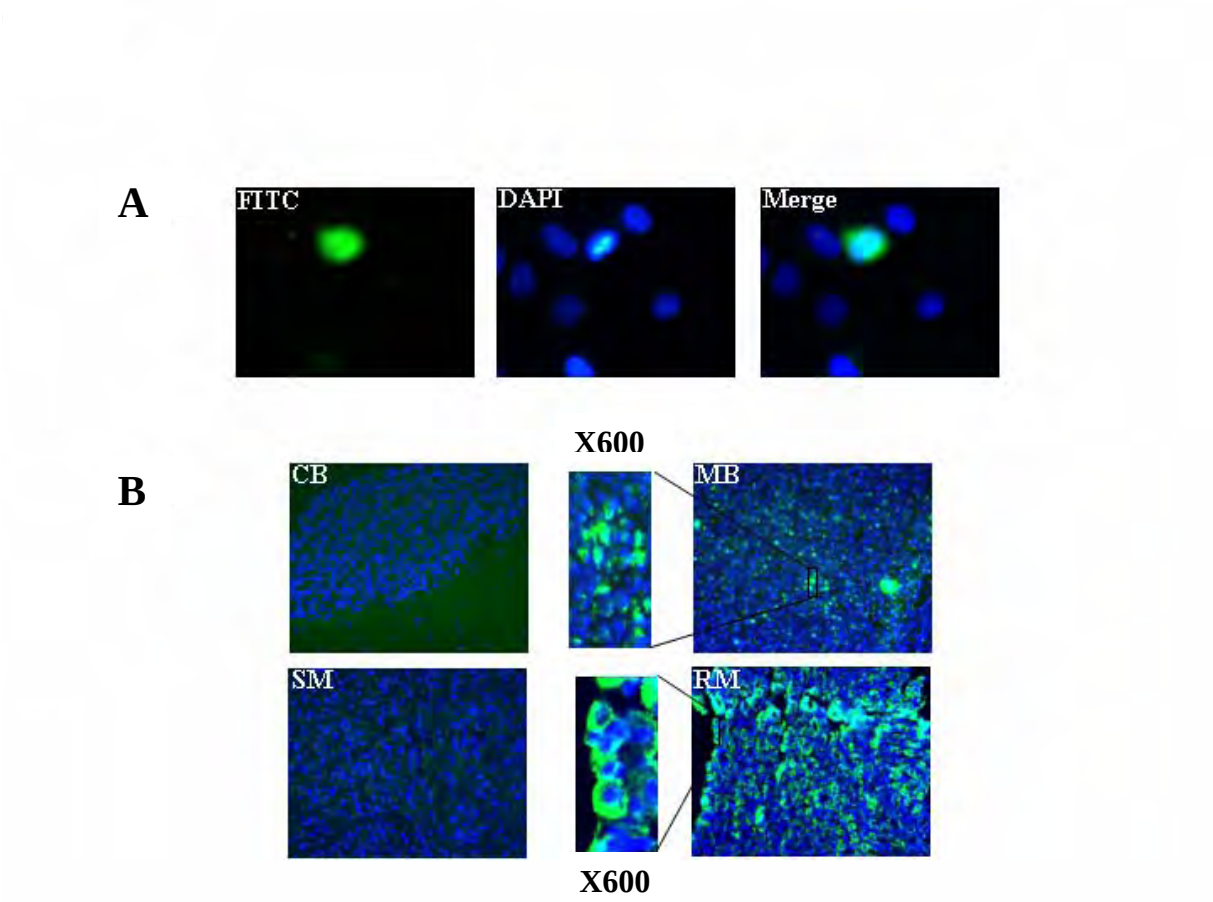

Figure 3.9: Expression analysis of Piwil2 in transformed germ cell line GC-1 and mouse tumor tissues using immunohistochemical analysis. (A) Expression of Piwil2 was detected in cytoplasm of proliferating GC-1 cell (FITC, green signal), nuclei are shown in blue (DAPI staining) (magnification X200). (B) No signal was observed in cerebellum (CB) and skeletal muscle (SM), but Piwil2 was highly expressed in medulloblastoma (MB) and in rhabdomyosarcoma (RM), the magnifications show a cytoplasmic localization of Piwil2 in medulloblastoma and rhabdomyosarcoma (magnification X200).

In human, PIWIL2 was found in cytoplasm of breast tumor cell line MDA-MB-231 (Fig. 3.10 A). In breast tumor tissues from 4 different patients, expression of PIWIL2 was observed (Fig. 3.10 B-E). No expression was detectable in normal breast tissue (Fig. 3.10 F). Furthermore, immunohistochemical analysis in other tumors resulted either in dispersed (Fig. 3.10 K, L, P, Q, R, S) or in clonal form (Fig. 3.10 G, I, J, M, N, O, T). These results indicate that Piwil2 is specifically expressed in spermatogonia of testis and ectopically in most tumor cell lines and tumor tissues.

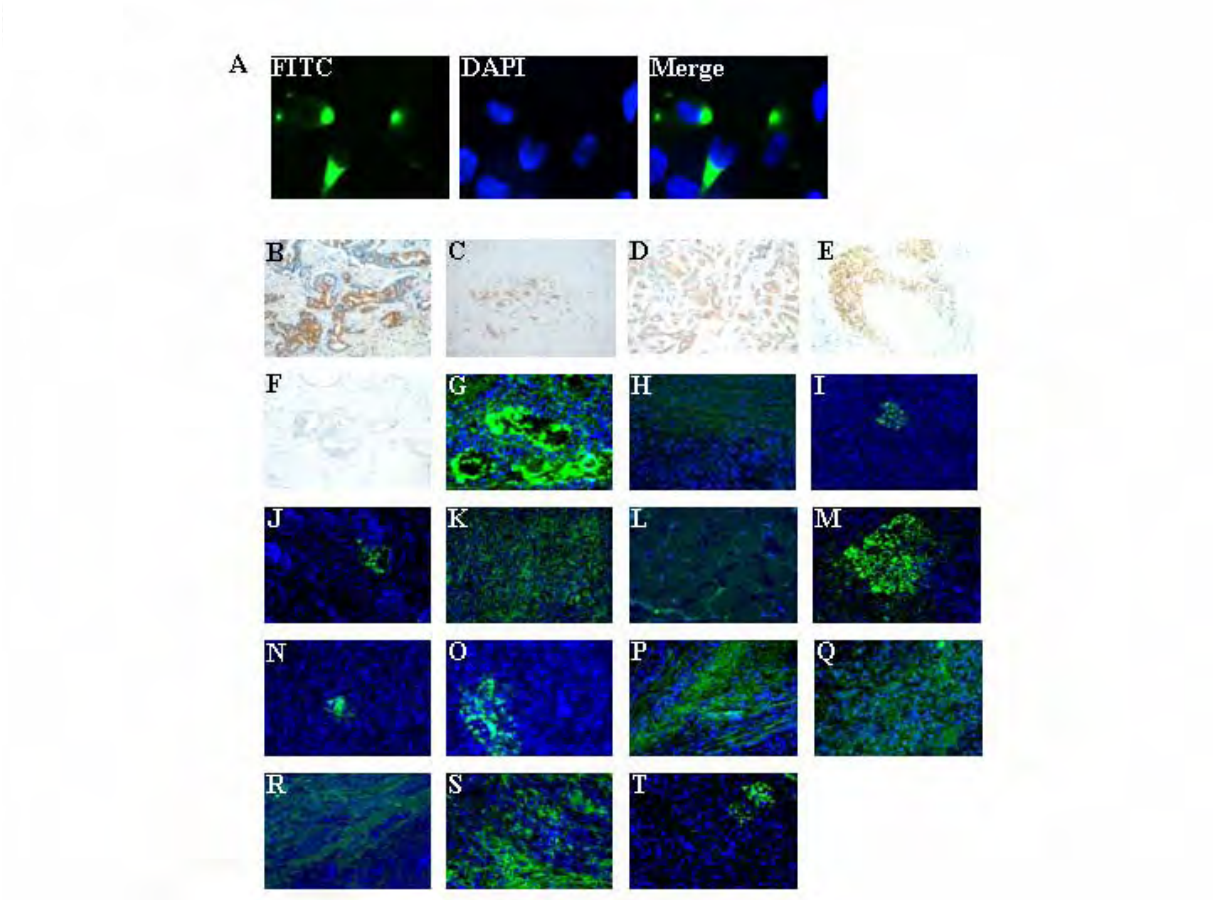

Figure 3.10: Immunostaining of MDA-MB-231 cells and of different human tumors shows positive immunoreactions for Piwil2. (A) The Piwil2 expression was observed in cytoplasm of human breast tumor cell line MDA-MB-231 (FITC), DAPI nuclear staining (blue signal). (B-E) Immunostaining with anti-Piwil2 antibody was shown in three different breast tumors (B, C, D) and in ductal carcinoma in situ (E) using secondary alkaline phospatase-conjugated antibody. No staining was observed in normal breast tissue (F). (G) Testicular germ cell tumor, (H) negative control of same section in (G) using only secondary FITC-conjugated antibody, (I) testicular germ cell tumor, (J) coccyx teratoma, (K) ovarian dysgerminoma, (L) ovarian teratoma, (M) adenocarcinoma of colon, (N, O and P) gastrointestinal stromal tumors, (Q) clear cell renal cell carcinoma, (R) MMMT of endometrium, (S) stromal sarcoma of endometrium, (T) adenocarcinoma of endometrium. Magnification X200.

3.3 *Piwil2* is overexpressed in testicular germ cell tumors

To examine expression of *PIWIL2* in human testicular germ cell tumors, a human testicular cancer profiling array with RNAs from seminomas, nonseminoma tumors and surrounding normal testicular tissue was hybridized with a *PIWIL2* specific probe as described in Materials and Methods section 2.2.17. The signals were scanned after a 1-day exposure by using a Microplate-Reader (Model 450) from BioRad. As shown in figures 3.11 A and 3.11 B, an overexpression of *PIWIL2* was observed in seminomas (9 of 10). No enhanced expression of *PIWIL2* was detected in testicular nonseminoma tumors (Fig. 3.11 B). In contrast, no enhanced expression was detected in 10 nonseminoma testicular tumors that originate from the same precursor cells as seminomas yet have lost their germ cell characteristics. Interestingly, seminomas showed *PIWIL2* expression levels that are about twice higher than the average level of *PIWIL2* expression in normal testicular tissue. In contrast to seminomas, no elevated expression was found in any of the nonseminomas. These results suggest that an enhanced *PIWIL2* expression level is likely restricted to seminomas and a possible synergistic effect of *piwi* genes is correlated with initiation and progression of testicular germ cell tumors.

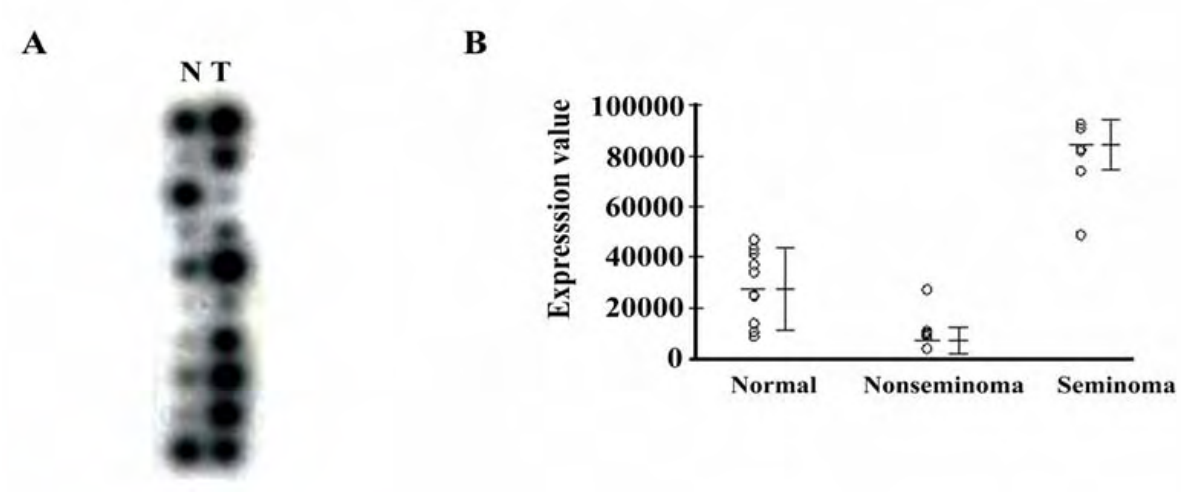

Figure 3.11: Expression of *PIWIL2* in human testicular germ cell tumors. (A) Overexpression of *PIWIL2* was observed in 9 of 10 testicular seminomas (T) compared to normal testicular tissues (N). (B) Quantification of *PIWIL2* expression in seminomas and nonseminoma tumors as compared to normal testicular control tissues. Significant overexpression of *PIWIL2* was detected in seminomas (P<0.01) but not in testicular nonseminoma tumors.

3.4 Identification of downstream targets for *Piwil2*

The identification and characterization of *Piwil2* downstream targets is crucial for understanding its function in stem cell self-renewal and differentiation. To identify *Piwil2* regulated genes, stably transfected NIH3T3 cells expressing Piwil2 were generated.

3.4.1 Establishment of a stable cell line with *Piwil2* expression

To search for potential molecular downstream targets of *Piwil2*, we established NIH-3T3 cell lines stably expressing *Piwil2* using a fusion gene harbouring coding region of *Piwil2* under control of CMV promoter (Fig. 3.12). Next, we performed molecular profiling of *Piwil2*-transfected and only pcDNA vector transfected NIH3T3 cell line, respectively. Finally, the stable cell lines NIH3T3-pcDNA-*Piwil2* and NIH3T3-pcDNA were established. Expression of *Piwil2* in the stable transfected cell line NIH3T3-pcDNA-*Piwil2* was examined on RNA level (Fig. 3.13 A) by RT-PCR and Northern blot analysis (Fig. 3.13 B). On protein level, expression was examined by immunostaining (Fig. 3.14 A and B) using mouse anti-Piwil2 antibody. It was demonstrated that *Piwil2* is transcribed and translated properly in NIH3T3-pcDNA-*Piwil2* cell line but not in NIH3T3-pcDNA cell line.

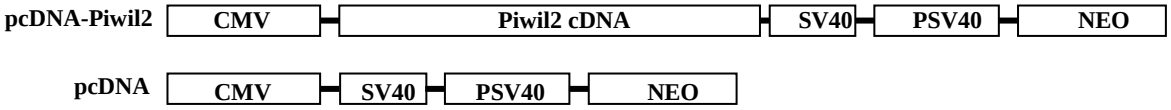

Figure 3.12: Schematic representation of fusion constructs used for transfection of NIH3T3 cells. The pcDNA-*Piwil2* construct contains the coding region of *Piwil2* gene (cDNA) under control of cytomegalovirus (CMV) promoter, SV40 polyadenylation signal (SV40) and neomycin resistance gene (NEO) under control of SV40 promoter (PSV40). The control plasmid contains all DNA sequences except Piwil2 cDNA (pcDNA). Two stable cell lines NIH3T3-pcDNA and NIH3T3-pcDNA-*Piwil2* were established.

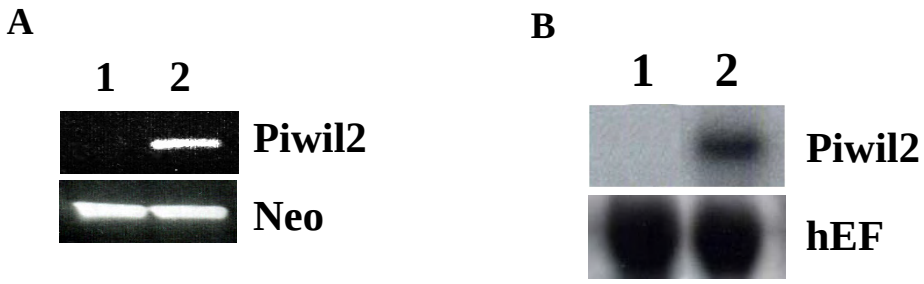

Figure 3.13: (A) RT-PCR analysis using RNA isolated from NIH-3T3-pcDNA (1) and NIH3T3-pcDNA-*Piwil2* (2) cell lines. (B) Northern blotting analysis using RNA isolated from NIH3T3-pcDNA (1) and NIH3T3-pcDNA-*Piwil2* (2) cell lines. Controls: RT-PCR for glyceraldehyde-3-phosphate dehydrogenase (*GAPDH*) and for Northern blot human elongation factor 2 (*hEF*) probes were used.

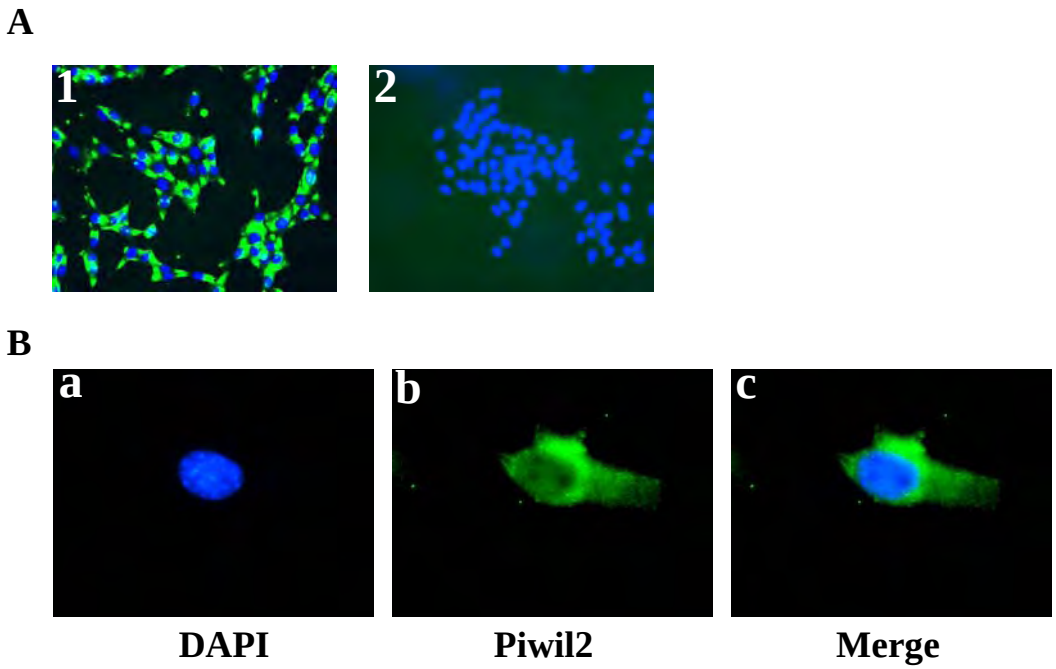

Figure 3.14: (A) By immunohistochemical analysis with the antibody against Piwil2, signals were detected only in NIH3T3-pcDNA-*Piwil2* cells (2) and not in NIH3T3-pcDNA cells (1) (magnification X100). (B) Magnification of NIH3T3-pcDNA-*Piwil2* cell line with an antibody against Piwil2 protein. (a) Fluorescence DAPI (4', 6'-diamidino-2-phenylindole) staining (blue), (b) Piwil2 is localized in the cytoplasm (green), (c) merge of (a) and (b) (magnification X600).

3.4.2 Isolation and identification of differentially expressed genes

Mouse cancer pathway finder microarray was designed to rapidly assess the status of six different biological pathways frequently altered during or affected by transformation and tumorigenesis. To identify genes which are differentially expressed between NIH3T3 cell line and *Piwil2* expressing cell line, expression profiles of NIH3T3 cells expressing stably *Piwil2* were compared with control cell line NIH3T3-pcDNA (Fig. 3.15) using a cancer pathway finder array. Total RNA prepared from these cell lines was used to synthesize ^{32}P-labeled whole cDNAs by reverse transcription, followed by hybridization to two identical cancer arrays from superarray as described in Materials and Methods (2.2.10). The signals were scanned after a 1-day exposure by using a Molecular Imager FX, as shown in figure 3.15. The results are summarized in table 1. This analysis revealed activation of genes related to cell growth, adhesion and apoptosis (Table 1 and Fig. 3.15). Obviously, an activation of *Bcl-*X_L was found to occur in cells expressing *Piwil2* (Fig. 3.15).

Symbol	Gene name	Expression level in NIH3T3-pcDNA-Piwil2 Cells
1. Agpt	angiopoietin1	▼
2. Bcl2l	Bcl-X_L	▲
3. Cflar	Casper (CASP8 and FADD-like apoptosis regulator)	▲
4. Catnb	Catenin beta	▲
5. Ccnd1	Cyclin D1	▲
6. Cd44	CD44 antigen	▲
7. Grb2	Grb2	▲
8. Itga6	Integrin alpha 6	▲
9. Itgb1	Integrin beta1 (fibronectin receptor beta):CD29	▲
10. Mmp2	Matrix metalloproteinase2:Gelatinase A	▲
11. Thbs1	thrombospondin1	▼

Table 1: Differential gene expression in NIH3T3 cells expressing *Piwil2* as compared to NIH3T3 control cells. Overexpression of apoptosis, growth and adhesion related genes was obtained. Arrows indicate upregulated gene expression (▲) and downregulated gene expression (▼) in NIH3T3-pcDNA-*Piwil2* cells.

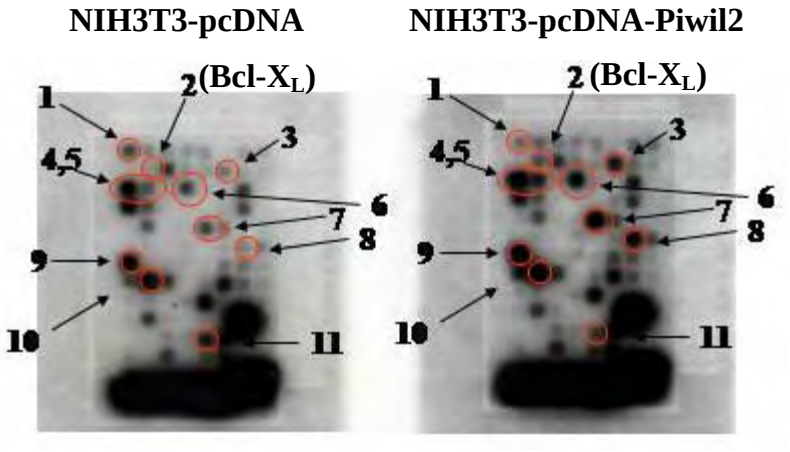

Figure 3.15: Identification of downstream target genes of *Piwil2*. Mouse cancer pathway finder array using RNA samples isolated from NIH3T3-pcDNA cells and from NIH3T3-pcDNA-*Piwil2* cells was used to identify genes putatively activated or modulated by *Piwil2*. Activation of *Bcl-X_L* expression was obtained specifically in NIH3T3-pcDNA-*Piwil2* cell line. 1: *angiopoietin1*, 2: *Bcl-X_L*, 3: *Casper*, 4: *Catenin beta*, 5: *Cyclin D1*, 6: *CD44 antigen*, 7: *Grb2*, 8: *Integrin alpha 6*, 9: *Integrin beta1*, 10: *Matrix metalloproteinase2*, 11: *thrombospondin1*.

3.4.3 Characterization of target genes for *Piwil2*

To further examine whether expression of *Bcl-X_L* is regulated directly *by Piwil2* or indirectly by upstream regulatory factors of *Bcl-X*, expression of the signal transducers and activators of transcription 3 (*Stat3*) and serine/threonine kinase *Akt*, two upstream

regulatory factors of *Bcl-X* (Zamzami et al., 1998; Jost et al., 2001) were examined. Whereas a slight increase (about 2 fold) was observed in expression level of *Akt*, a clear activation of *Stat3* was obtained in cells stably expressing *Piwil2* (Fig. 3.16). As shown in figure 3.16, expression pattern of *Cyclin D1* (about 2 fold) was similar to the result of cancer array (Fig. 3.16). At this time, we wondered whether *Piwil2* can regulate via other signal transduction pathway, either in addition to or exclusive of the *Stat3/Bcl-x* pathway. *Stat2* was overexpressed about 2 fold and a reduction of expression of *RelA* and *NF-Kappa B* was observed in NIH3T3-pcDNA-*Piwil2* cell lines (Fig. 3.16). No change was detected in expression of *Ets2*. To analyse further the association between *Piwil2* expression and expression of *Stat3*, *Akt*, *Bcl-*X_L and *Cyclin D1*, expression of these genes was examined in human testicular germ cell tumor cell line Tera-1 and mouse breast tumor tissues. In human and mouse, association between *Piwil2* overexpression and overexpression of *Stat3*, *Akt* and *Cyclin D1* was demonstrated (Fig. 3.17).

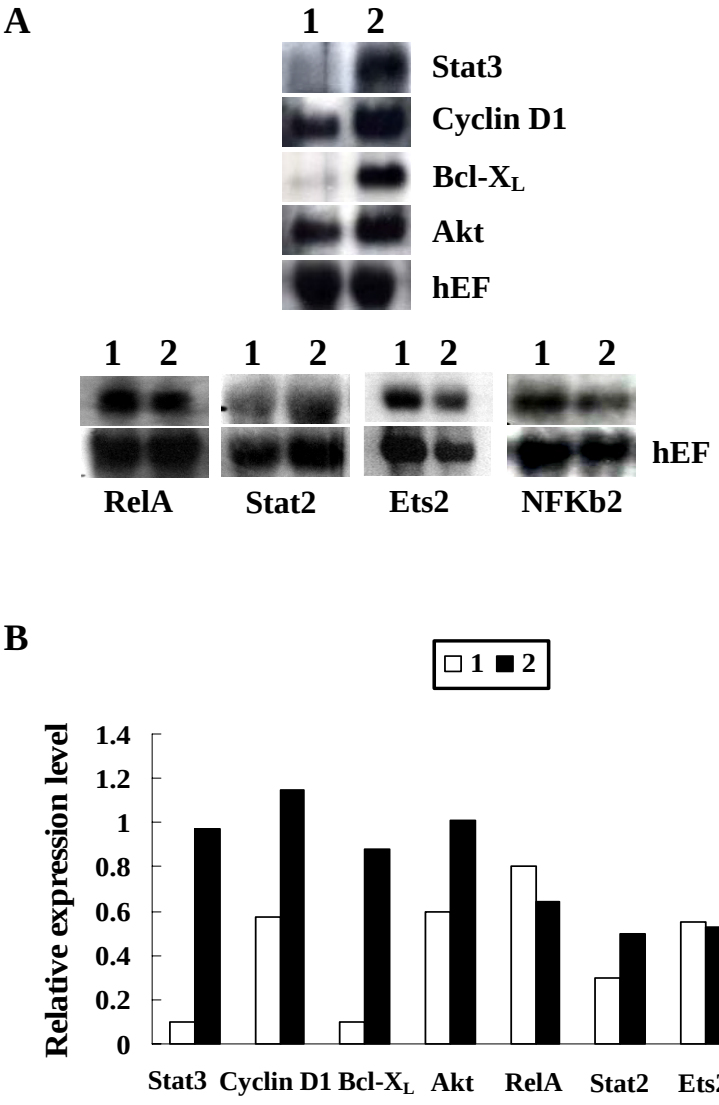

Figure 3.16: (A) Northern blot analysis of RNA isolated from control NIH3T3-pcDNA cells (1) and from NIH3T3 cell line stably expressing *Piwil2*, NIH3T3-pcDNA-*Piwil2* (2), using probes specific for *Stat3*, *Cyclin D*, *Bcl-X$_L$*, *Akt*, *RelA*, *Stat2*, *Ets2* and *NFkB2*. An activation of *Stat3* and *Bcl-X$_L$*, an enhancement of *Cyclin D1* expression and slight increase of *Stat2* were observed. Expression of *Ets2* and *NFkB2* is slightly reduced. *hEF*: human elongation factor cDNA probe as control for RNA integrity. (B) Quantification of expression of differentially expressed genes shown in (A), relative expression level in NIH3T3-pcDNA cells (1) as compared to expression level in NIH3T3-pcDNA-*Piwil2* cells (2).

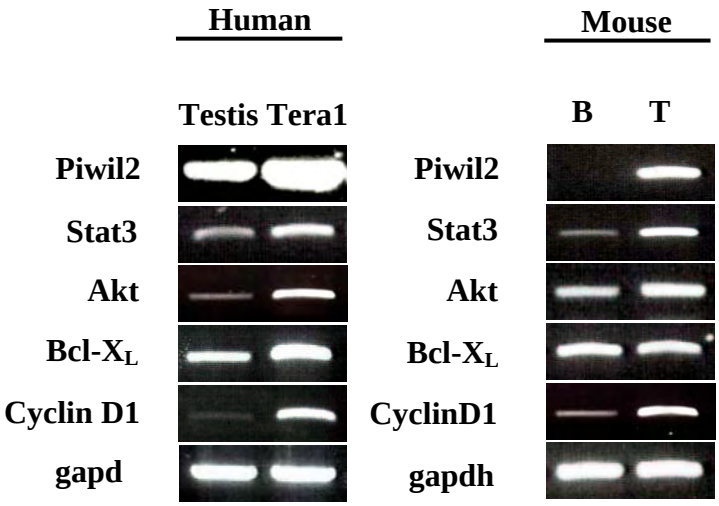

Figure 3.17: Correlation between *Piwil2* expression and expression of *Stat3, Akt, Bcl-X_L* and *Cyclin D1* in human teratocarcinoma cell line (Tera 1) compared with normal testis and in mouse breast tumor tissue (T) compared with normal mouse breast (B). *Gapdh* was used as control. In human, a correlation between elevated expression of *Piwil2* and *Stat3, Akt, Bcl-X_L* and *Cyclin D1* was observed. In mouse, this correlation was detected only for *Stat3, Akt* and *Cyclin D1*.

3.5 Expression of Piwil2 and Stat3 in NIH3T3-pcDNA-*Piwil2* cells

In order to find a correlation between Piwil2 and Stat3 expression, we examined coexpression of Piwil2 and Stat3 in NIH3T3-pcDNA-*Piwil2* cell line (Fig. 3.18 A and D). On protein level, co-immunostaining with anti-Piwil2 and anti-Stat3 antibodies showed presence of cytoplasmic (Fig. 3.18 B) and nuclear (Fig. 3.18 C) forms of Stat3 protein in Piwil2 expressing cells. Furthermore, activation of Stat3 expression was demonstrated by Western blot analysis using anti-Stat3 antibody in Piwil2 expressing NIH3T3 cells (Fig. 3.19).

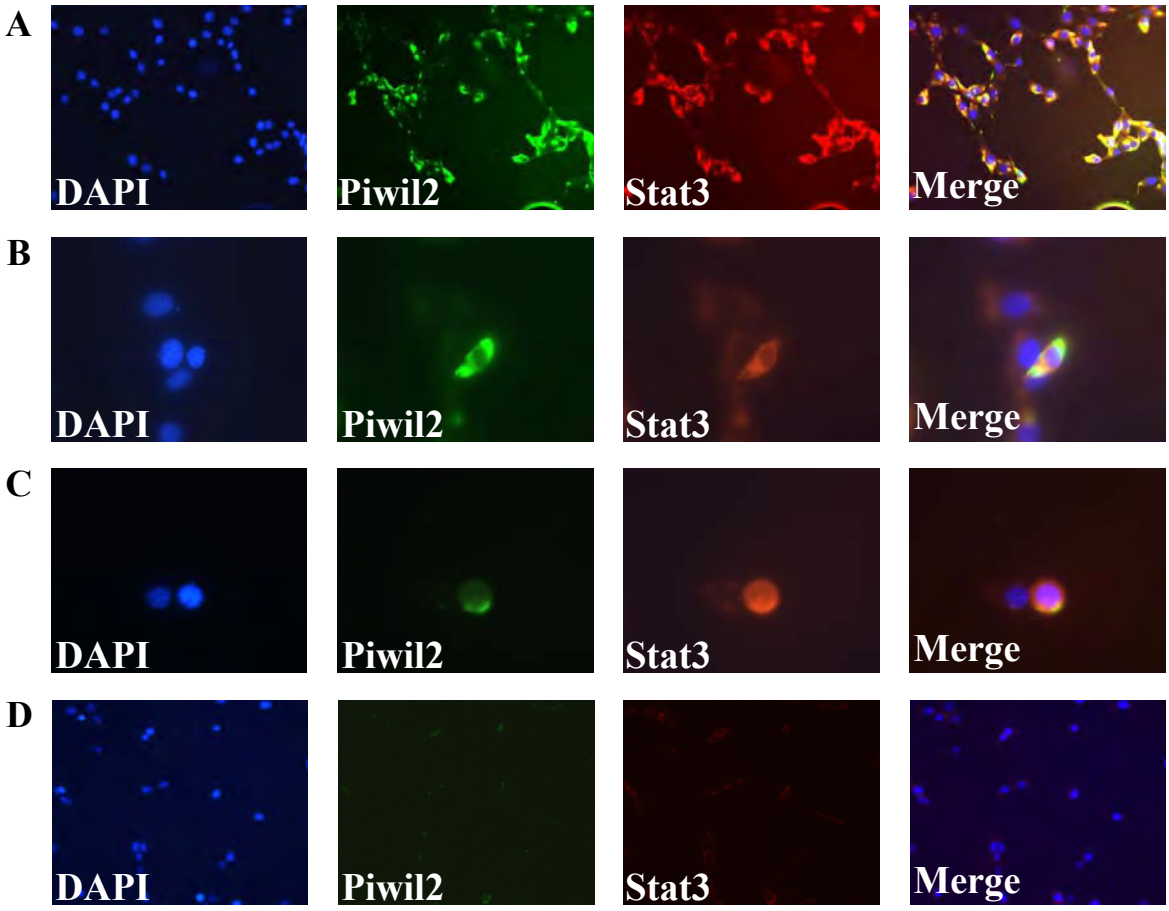

Figure 3.18: Activation of Stat3 expression in Piwil2 expressing cell line NIH3T3-pcDNA-*Piwil2* is shown by double immunostaining using anti-Piwil2 (green) and anti-Stat3 (red) antibodies and FITC- and Cy3-conjugated secondary antibodies, respectively. DAPI nuclear staining (DAPI); co-expression of Piwil2 and Stat3 was detected (merge). Localization of Stat3 was found in cytoplasm (B) as well as in nucleus (C) (magnification X600). (A) and (D) co-localization of Piwil2 and Stat3 and negative control (only 2nd antibody) to ensure whether each signal is specific or not (magnification X100).

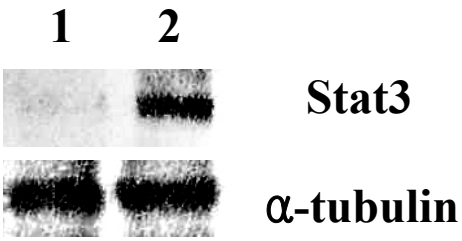

Figure 3.19: Western blot analysis of proteins isolated from control NIH3T3-pcDNA cells (1), and from NIH3T3 cell line stably expressing Piwil2 (2) using anti-Stat3 antibody. An activation of Stat3 expression was induced by Piwil2 expression; α-tubulin was used as positive control.

3.6 *Piwil2* gene silencing in GC-1 and MDA-MB-231 cell line

We have found that *Piwil2* induces the expression of anti-apoptotic genes (*Stat3* and *Bcl-X_L*).Therefore, we performed *Piwil2* gene silencing via siRNA experiment to analyse whether *Piwil2* expression regulates expression of *Stat3*, *Akt*, *Bcl-X_L* and *Cyclin D1* in GC-1 and MDA-MB-231 cell lines. Cells were transfected with Piwil2 siRNA. Cells were plated at 2.0 x 10^5cells per well in a 6-well tissue culture plate. Following 24 hrs in culture, cells were transfected with 80nM *Piwil2* siRNA of mouse (Sense: 5'-ACACAGCAUUCC GGCCUCCUUCAAA-3', Antisense: 5'-UUUGAAGGAGGCCGGAAUGCUG U GU-3') and human (Sense: 5'-GGAUCUAUUCUCUAUCUGCCUGUUA-3', Antisense: 5'-UAA CAGGCAGAUAGAGAAUAGAUCC-3'), respectively (Invitrogen siRNA). We examined the effect of down-regulation of *Piwil2* on expression level of *Stat3*, *Akt*, *Bcl-X_L* and *Cyclin D1* in GC-1 cells and in MDA-MB-231 cells. *Piwil2* level was not changed in GC-1 cells and MDA-MB-231 cells transfected with control siRNA (See section 2.2.21.2) (Fig. 3.20). Clearly, there was an obvious decrease in expression of *Piwil2* following transfection with the *Piwil2* siRNA after 24 hrs (Fig. 3.20). Suppression in *Piwil2* expression resulted in down-regulation of *Stat3*, *Bcl-X_L* and *Cyclin D1* (Fig. 3.20), but not in expression of Akt. These results suggest the role of *Piwil2* as a regulatory factor of *Stat3*/*Bcl-X_L*/*Cyclin D1*

pathway. Luciferase was used to prove that silencing of *Piwil2* gene results from the effect of *Piwil2* siRNA as control.

A

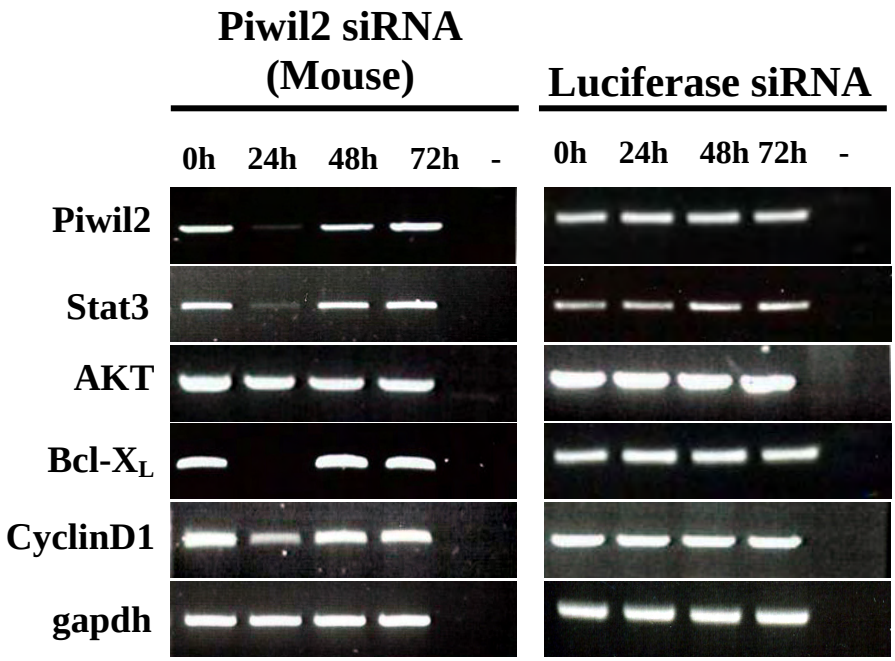

B

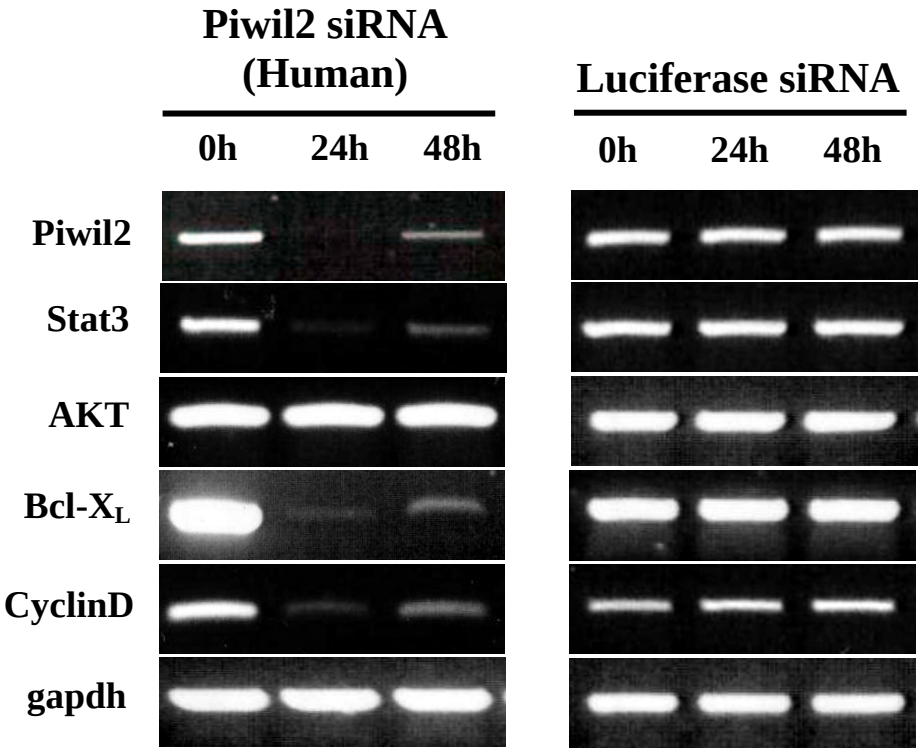

Figure 3.20: Silencing of Piwil2 expression with *Piwil2* siRNA in GC-1 cells and in MDA-MB-231 cells (A and B). After siRNA treatment for 0, 24, 48, 72 hrs, mRNA expression levels of *Piwil2*, *Stat3*, *Akt*, *Bcl-X_L* and *Cyclin D1* of mouse and human were determined by semiquantative RT-PCR in GC-1 cells (A) and in MDA-MB-231 cells (B) transfected with *Piwil2* siRNA. While a correlation of *Piwil2* downregulation and reduced expression of *Stat3*, *Bcl-X_L* and *Cyclin D1* was demonstrated, only a slight decrease in expression of *Akt* was detected. The integrity of RNA in RT-PCR was checked by using a gapdh primer. *Luciferase* siRNA oligos were used as control.

3.7 Cellular effects mediated by Piwil2

3.7.1 Inhibition of apoptosis by Piwil2

To study the effect of Piwil2 expression on cellular phenotype, NIH3T3 cells stably expressing Piwil2 (NIH3T3-pcDNA-*Piwil2*) were compared to control NIH3T3-pcDNA cells concerning apoptosis. Using two different techniques, microscopically and cytometrically, a significant decrease of apoptosis was observed in NIH3T3 cells expressing Piwil2 (Fig. 3.21). Interestingly, the rate of apoptosis was decreased from 25% to 12.8% in NIH3T3-pcDNA cell line using microscopy analysis (Fig.3.21 A) and a decrease of apoptosis from 29% to 16% was observed in NIH3T3-pcDNA-*Piwil2* cell line by flow cytometry (Fig. 3.21 B). At this time, to explore the correlation between Piwil2 and apoptosis, a combined apoptosis assay and Piwil2 immunostaining was carried out. It was demonstrated that apoptotic cells do not express Piwil2 (Fig. 3.22) and cells expressing Piwil2 are not apoptotic (Fig. 3.22).

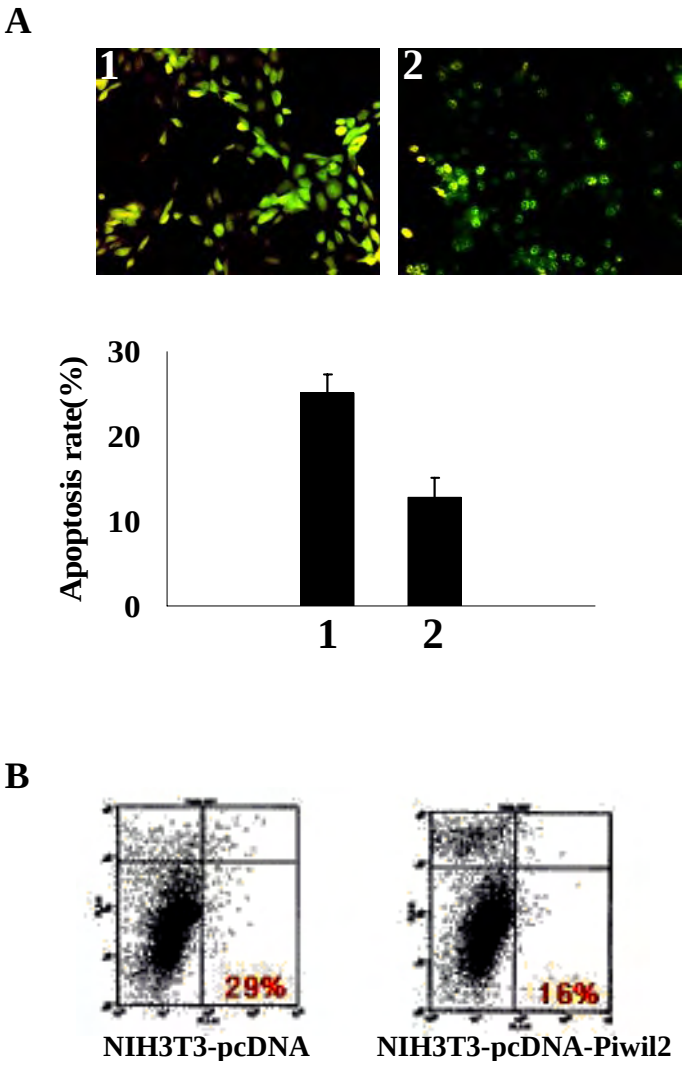

Figure 3.21: Inhibition of apoptosis by Piwil2. (A) Apoptosis of control NIH3T3-pcDNA cell line (1) was compared with apoptosis of NIH3T3 cell lines stably expressing Piwil2, NIH-3T3-pcDNA-Piwil2 (2). Apoptotic cells were counted (n>300) and presented as percentage of total cell counts (magnification X100). A significant decrease of apoptosis was found in Piwil2 expressing cells ($p<0.01$). (B) These results could be confirmed by apoptosis assay using FACS analysis. A decrease of apoptosis from 29% to 16% was observed by flow cytometry.

Figure 3.22: Combined apoptosis assay and immunohistochemical analysis using antibody against Piwil2. These results demonstrate that apoptotic cells (green) do not express Piwil2 (red) (magnification X200).

3.7.2 Silencing of Piwil2 expression induces apoptosis in GC-1 cells and MDA-MB-231 cells

To investigate whether Piwil2 induces the apoptosis in GC-1 cells and MDA-MB-231 cells, which express Piwil2 endogenously, expression of Piwil2 was downregulated by siRNA and resulted in apoptosis of these cells (Fig. 3.23 A and C).

Here, it was demonstrated that GC-1 and MDA-MB-231 cells with a suppression of Piwil2 expression undergo apoptosis (Fig. 3.23 A and C). Analysis of apoptosis by TUNEL assay revealed that apoptotic cells (34.7%) in GC-1 and apoptotic cells (20.6%) in MDA-MB-231 cells transfected with *Piwil2* siRNA were detected. Whereas, not much apoptotic cells (10%) in untransfected GC-1 cells and (2.5%) in untransfected MDA-MB-231 cells were observed (Fig. 3.23 B and D). These results suggest that reducing Piwil2 induces apoptosis rate in GC-1 cells.

A

GC-1 cells

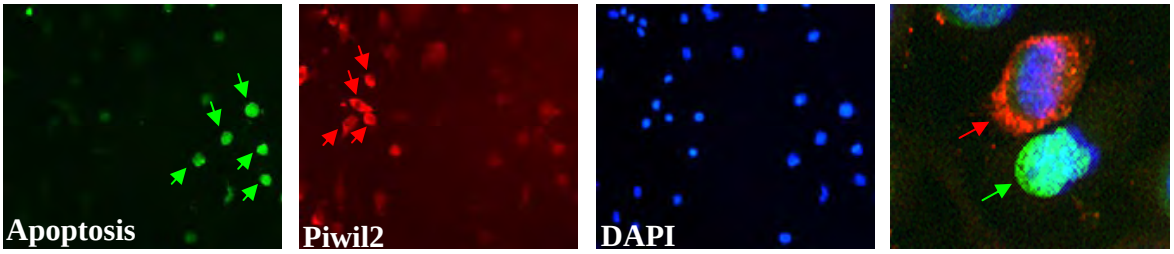

B

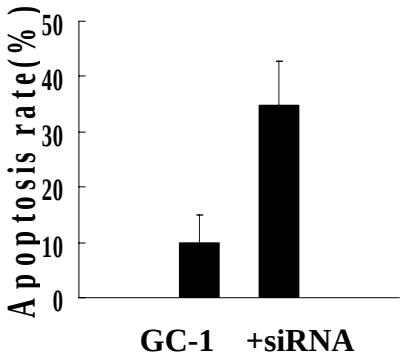

C

MDA-MB-231 cells

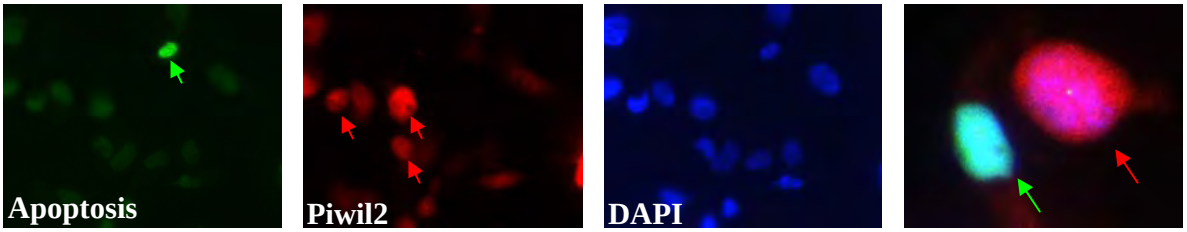

D

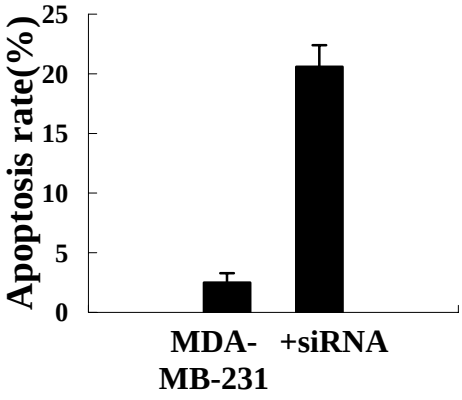

Figure 3.23: (A) (C) Silencing of Piwil2 expression induces the apoptosis in GC-1 cells and MDA-MB-231 cells. Cells with downregulation of Piwil2 expression (red arrows) undergo apoptosis (green arrows), DAPI staining (blue signal). (B) (D) Apoptotic cells were counted (n>500) and presented as percentage of total cell counts. A significant increase of apoptotic cells was detected after *Piwil2* siRNA treatment. (A) Magnification X100 and (C) X200. All experiments were carried out in triplicate.

3.7.3 Downregulation of Stat3 expression induces apoptosis via silencing of Piwil2 in GC-1 cells and MDA-MB-231 cells

To examine whether increased apoptosis and Piwil2 downregulation are mediated by Stat3, we performed a combination of immunostaining against Stat3 antibody and apoptosis assay. Cells were plated at 2.0 x 10^5cells per well in a 6-well tissue culture plate. After 24 hrs in culture, the cells were transfected with 80nM *Piwil2* siRNA of mouse (GC-1) and human (MDA-MB-231), respectively. We examined the effect of direct down-regulation of Piwil2 using its siRNA on expression level of Stat3 in GC-1 cells and MDA-MB231 cells (Fig. 3.24). After transfection with the *Piwil2* siRNA, a decrease of Stat3 expression was observed in GC-1 cells and MDA-MB-231 cells. Suppression in Piwil2 expression resulted in down-regulation of Stat3. Stat3 was not expressed in the apoptotic cells and anti-apoptotic cells did express Stat3, which is downstream of Piwil2. These results suggest that silencing of Piwil2 expression induces downregulation of Stat3 and apoptosis in GC-1 cells and MDA-MB-231 cells.

A

GC-1 cells

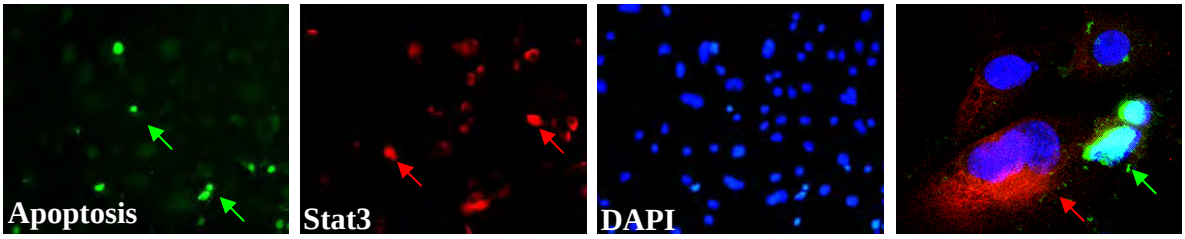

B

MDA-MB-231 cells

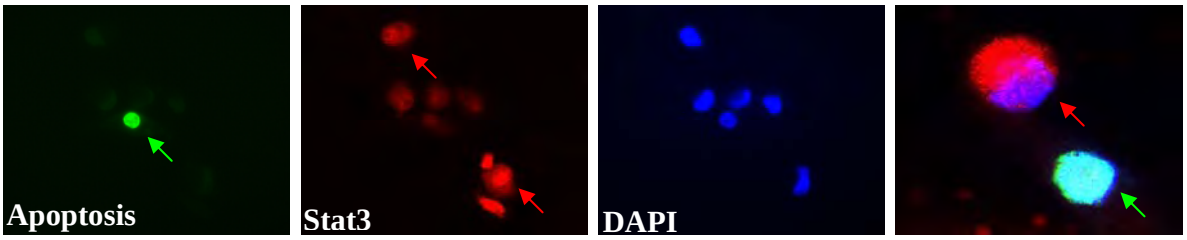

Figure 3.24: (A) Reduction of Stat3 expression in GC-1 cells (magnification X100) and (B) in MDA-MB-231 cells transfected with siRNA for *Piwil2*. Apoptotic cells (green arrows) did not express Stat3 (red arrows) (magnification X200). Stat3 expression was not detected in apoptotic cells in GC-1 and MDA-MB-231-transfected with siRNA for Piwil2.

3.8 Effect of Piwil2 on cell proliferation and transformation

3.8.1 *Piwil2* gene expression leads to increased cell proliferation

To further investigate the effect of *Piwil2* expression on NIH3T3-pcDNA-*Piwil2* cell, an increased proliferative activity of NIH3T3 cells expressing *Piwil2* was obtained using proliferation assay (Fig. 3.25). NIH3T3-pcDNA cells and NIH3T3-pcDNA-*Piwil2* cells were seeded at 2000, 6500, and 9500 cells/well in 96-well plates, respectively. Cells were cultivated in microtiter plates for 2 hrs and 10 hrs. Quantification of cell proliferation was performed using Quantos cell proliferation assay kit (Stratagene, La Jolla, CA) as described in Materials and Methods section 2.2.18. Fluorescence of a DNA-dye complex from lysed cells was determined using a microtiter plate-reading fluorometer with filters appropriate for 355-nm excitation and 460-nm emission. Increased proliferation was observed when the number of starting cells was higher than 9000 ($p<0.01$) and not detectable if the starting cell number was low (for example 2000 and 6500 starting cells in Fig. 3.25).

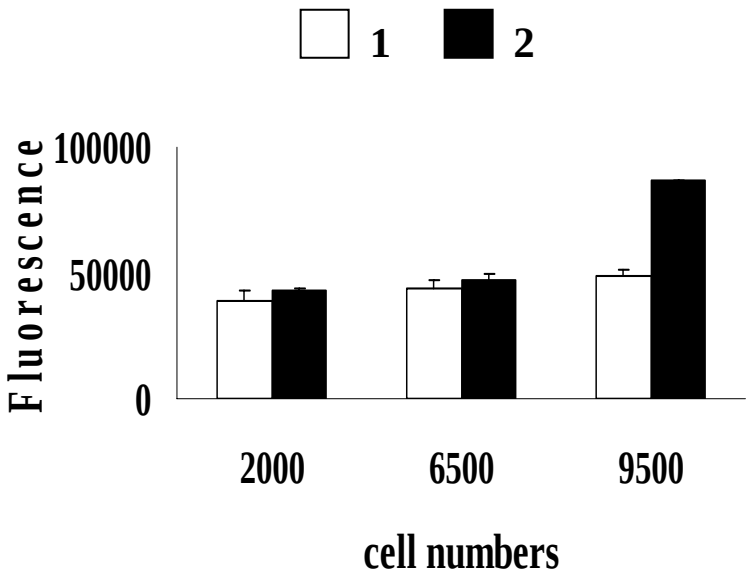

Figure 3.25: *Piwil2* induces proliferation. In proliferation assay, an increased cell proliferation was observed depending on the starting cell number of NIH3T3 cells expressing *Piwil2* (2) as compared to NIH3T3-pcDNA control cell (1).

3.8.2 Growth characteristics of NIH3T3-pcDNA-*Piwil2* cells using soft agar assay

To examine whether expression of *Piwil2* induces cell transformation, soft agar assay was performed with NIH3T3-pcDNA-*Piwil2* cells. NIH3T3-pcDNA cells, NIH3T3-pcDNA-*Piwil2* cells and GC-1 cells were cultured in medium containing 0.8% agar. 2000 cells/well were immediately plated on six-well plates coated with 0.3% agar in cell culture medium (2 ml per well) and cultured at 37°C with 5% CO_2. After 2 weeks the top layer of the culture was stained with 0.001% Crystal violet (Sigma-Aldrich) for 1 hr. The culture was analysed in triplicate, and colonies larger than 100 μm in diameter were counted. The average of colony number was 59.1 in NIH3T3-pcDNA cells, 105.8 in NIH3T3-pcDNA-*Piwil2* cells and 158.75 in GC-1 cell lines. It was demonstrated that NIH3T3-pcDNA-*Piwil2* cells with constitutive expression of *Piwil2* are more rounded than NIH3T3-pcDNA cells (data shown in result section 3.10) and formed significantly more colonies in soft agar (Fig. 3.26).

A

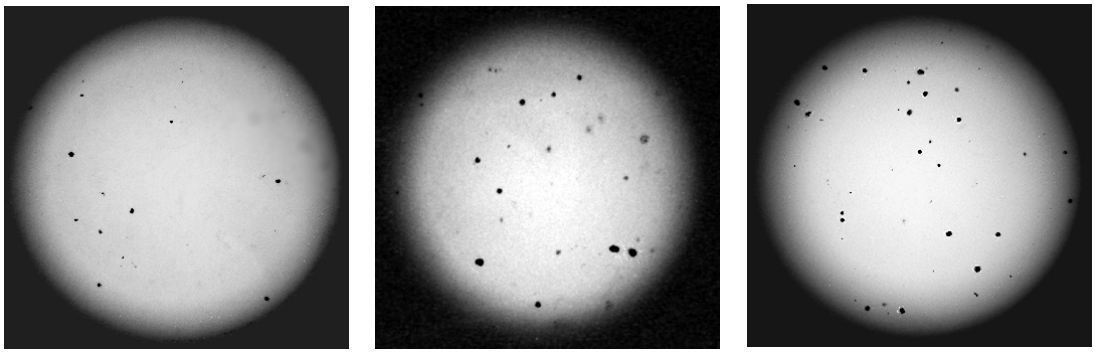

NIH3T3-pcDNA **NIH3T3-pcDNA-Piwil2** **GC-1**

B

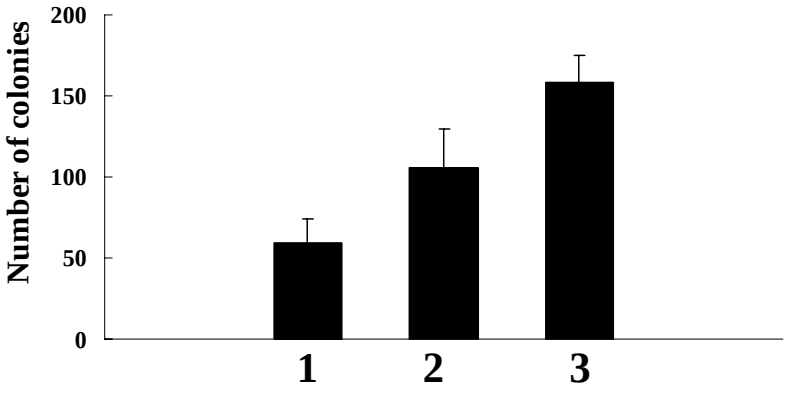

Figure 3.26: Soft agar assay. (A) Numbers of formed colonies were compared among different cell lines, 1, NIH3T3-pcDNA cells; 2, NIH3T3-pcDNA-*Piwil2* cells and 3, GC-1 cells as control. (B) Numbers represent average of total colonies; average colony numbers 1: 59.1, 2: 105.8, 3: 158.75. An increased number of colonies was observed in cells expressing *Piwil2* ($p<0.05$). Magnification X40.

3.8.3 Human PIWIL2 expression in Hela cell

To examine the correlation between *PIWIL2* expression and cell cycle, 2 kb of flanking region of human *PIWIL2* gene was amplified and cloned into a plasmid vector containing coding region of EGFP gene and SV40 polyadenylation signal. Additionally, this hpiwil2-EGFP construct contained a neomycin resistance gene under control of SV40 early enhancer and promoter elements for positive selection. The final construct (hpiwil2-EGFP) was sequenced completely. This fusion construct was transfected into HeLa cells and expression of EGFP was observed after 48 hrs. Expression of EGFP was always observed in proliferating cells with condensed metaphase chromosomes (Fig. 3.27).

A

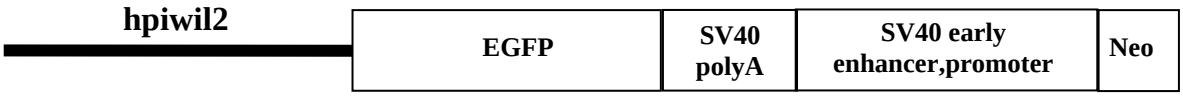

B

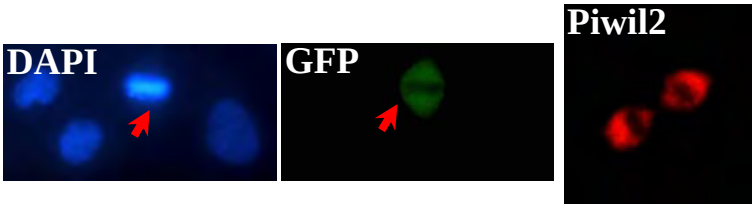

Figure 3.27: Fusion gene harbouring promoter of human *PIWIL2* gene (hpiwil2) and coding region of EGFP (A) in HeLa cells demonstrates that *PIWIL2* is active in mitotic cells with condensed chromosomes (B) (EGFP) (red arrow) (magnification X600).

3.9 Generation of transgenic mice with *Piwil2* overexpression in testis

As reported, Piwil2 induces proliferation and reduces apoptosis in vitro. Furthermore, we found an elevated expression of Piwil2 in germ cell tumors.

Therefore, it was possible that overexpression of Piwil2 leads to dysregulation in stem cell renewal and results in tumorigenesis. To check this hypothesis, we generated transgenic mice with overexpression of Piwil2 in premeiotic germ cell.

3.9.1 Generation of the fusion gene construct

To overexpress *Piwil2* specifically in testis, we used the promoter of the *human elongation factor-1α* (*hEF-1α*) gene. The *hEF-1α* promoter is specifically expressed in germ cell.

A 1.2 kb *Hind III-EcoR I* fragment containing *human EF-1α* promoter was derived from pEF-BOS (BCCM/LMBP Plasmid collection, Belgium) (Fig.3.28 A). Mouse *Piwil2* cDNA amplified from mouse testis RNA with specific primers containing *Sal I* and *Not I* enzyme sites were cloned into the pEGFP-1 vector without EGFP gene. For monitoring of transgene expression, native pEGFP-1 vector (Clontech, Palo Alto) (Fig.3.28 B) under the *hEF-1α* promoter was designed as a screening marker in mouse testis. Due to green signal, transgenic mice can be easily analysed and *Piwil2* expression under *hEF-1α* promoter can be monitored (Fig. 3.28 C).

A

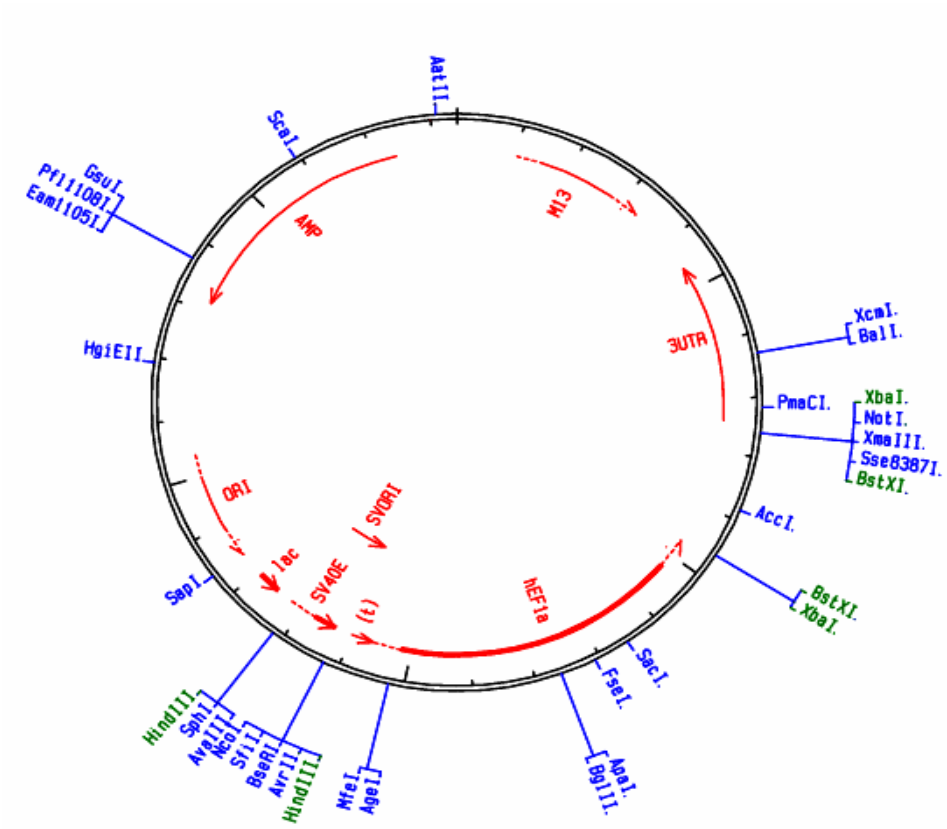

B

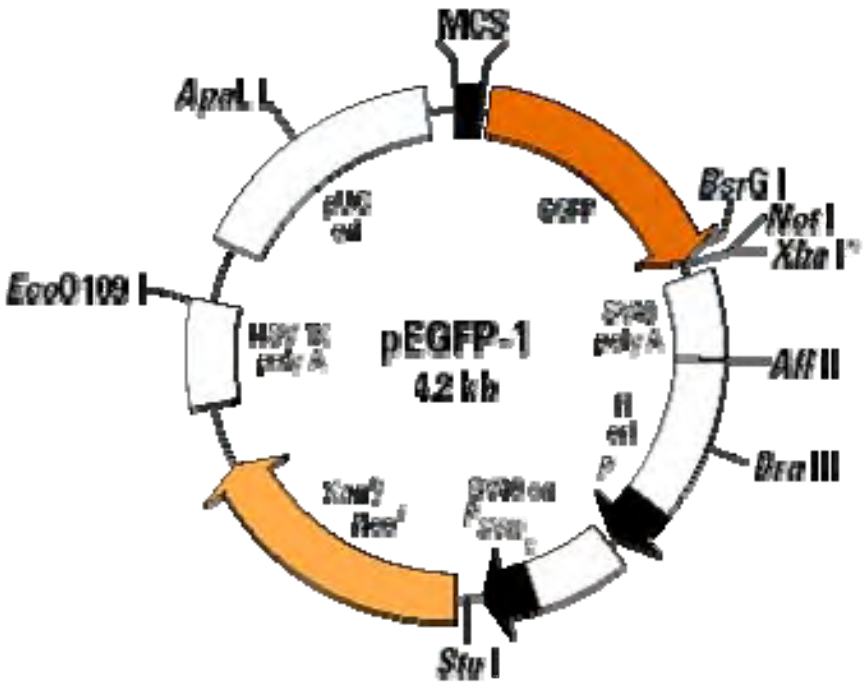
MCS
ApaL I
BstG I
Not I
Xba I
Eco0109 I
pEGFP-1
4.2 kb
Aff II
Bsa III
Stu I

C

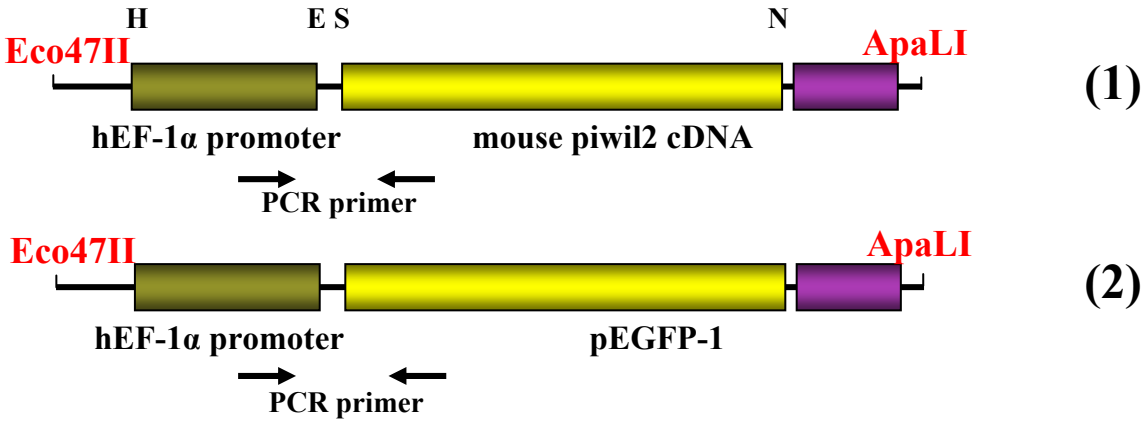
H
E S
N
Eco47II
ApaLI
hEF-1α promoter
mouse piwil2 cDNA
PCR primer
(1)
Eco47II
ApaLI
hEF-1α promoter
pEGFP-1
PCR primer
(2)

Figure 3.28: *Piwil2* transgene construct used to generate transgenic mice. (A) A map of pEF-BOS vector. (B) A map of pEGFP-1 vector. (C) The construct contains the human elongation factor-1α promoter (1.2 kb) fused to the mouse *Piwil2* cDNA (2.9 kb) and SV40 polyadenylation signal (1). Original pEGFP-1 vector under the *hEF-1 α* (2).

3.9.2 Generation of transgenic mice with Piwil2 overexpression in testis

The *hEF-1α-EGFP/hEF-1α-Piwil2* transgenic mouse lines were generated by double co-injection of *Piwil2-GFP* and *hEF-1α-Piwil2* fragments (released from vector sequences by digestion with *Eco47 II* and *ApaL I* and purified after gel electrophoresis) into the pronuclei of fertilized 1-cell mouse embryos. The injected embryos were transferred into FVB pseudopregnant hosts. Transgenic mice harbouring *hEF-1α-EGFP/hEF-1α-Piwil2* construct were identified by Genomic PCR and Southern blot, using *hEF-1 α/Piwil2* and *hEF-1α/EGFP* as a primer pair, respectively (Fig. 3.29). Three male founders and one female founder were obtained, designated as #20, #21, #22 and #23 (Fig. 3.29 A). In order to establish transgenic mouse lines, positive founder animals were bred with wild type FVB mice and heterozygous transgenic males were identified by PCR. Their transgenic progeny was crossed to produce homozygous animals. To examine expression of *Piwil2* in transgenic mice, RNA from different organs like testis, kidney and brain were isolated and subjected to Northern blot hybridization. *Piwil2* cDNAs and *EGFP* were used as probes (Fig. 3.29 B and C). Simultaneous expression of Piwil2 and EGFP could be detected in one transgenic line (Line #22, Fig. 3.29).

A

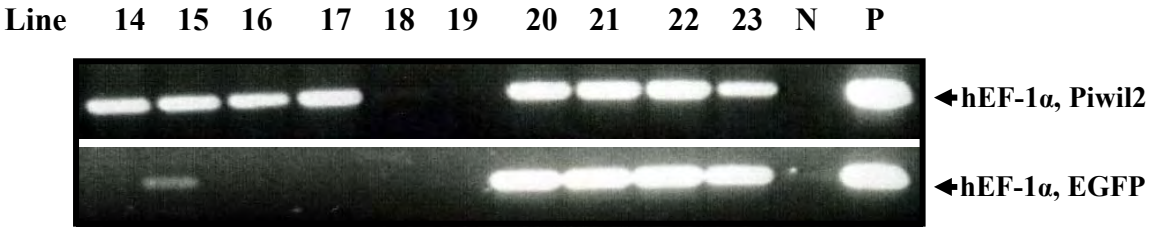
Line 14 15 16 17 18 19 20 21 22 23 N P
hEF-1α, Piwil2
hEF-1α, EGFP

B

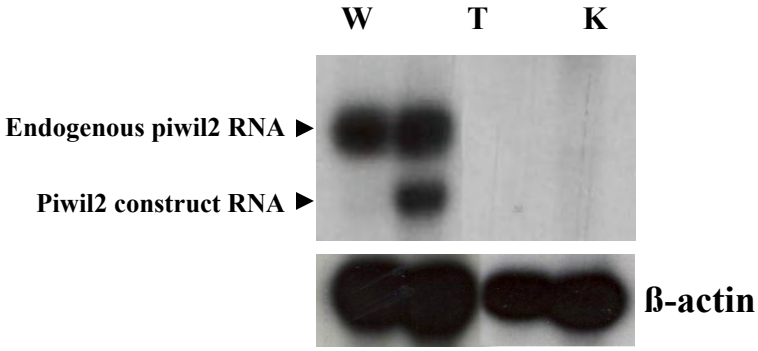
W T K
Endogenous piwil2 RNA
Piwil2 construct RNA
ß-actin

C

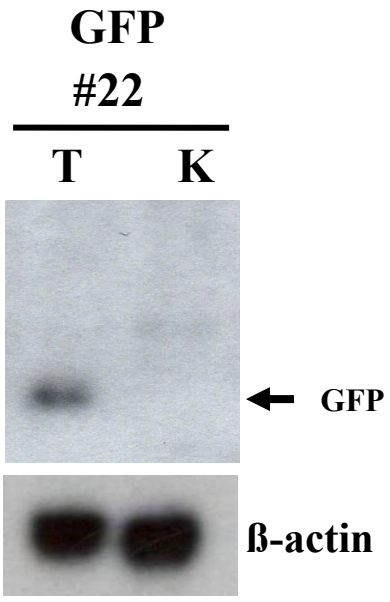
GFP
#22
T K
GFP
ß-actin

Figure 3.29: Generation of transgenic mice and expression analysis. (A) Genomic PCR screening of mice in order to obtain positive transgenic founders. N: negative control, H_2O, P: positive control, *Piwil2* transgene construct. (B) Northern blotting analysis of different tissues of transgenic mice expressing specifically in testis using *Piwil2* cDNA probe. W: wild type testis, T: testis of transgenic mouse, K: kidney of transgenic mouse, B: brain of transgenic mouse. The upper band indicates endogenous expression of *Piwil2* and the lower band indicates *Piwil2-EGFP* transgene RNA. (C) Northern blotting of testis and kidney of *Piwil2* transgenic mouse using *EGFP* cDNA probe. *ß-actin* was used as a positive control.

We further analysed the expression of the *Piwil2* transgene by immunohistological technique. In the testes of #22 transgenic mice (infertile), Piwil2 protein expression was stronger than in those of wild type (Fig. 3.30 A, white arrows). The specificity of *EGFP* expression was observed in testis of transgenic mice under the UV light but not in testis of wild type. Testes of *Piwil2* transgenic mice appeared smaller in size than wild type mice (Fig. 3.30 A). Ectopic *Piwil2* expression was detected in basally located cells, many of which are spermatogonia and some are spermatocytes (Fig. 3.30 E-J). The heterozygous transgenic mice for *Piwil2* were phenotypically normal and fertile. To investigate the effects of *Piwil2* overexpression in transgenic mice on fertility, each male (6 months old) was placed for 50 days in a cage with one female and the female was checked daily for the presence of vaginal plug. 7 males were used in this experiment and performed twice to check infertility. In fact, transgenic males mated and produced vaginal plugs in females, but these matings did not result in pregnancies. Three male mice out of seven male mice were observed as infertile transgenic mice through sperm analysis (See results section 3.10). Gross anatomical analysis of reproductive organs from *Piwil2* transgenic mice, including brain, heart, liver and kidney (data not shown), did not reveal abnormalities. The testes were slightly smaller than those in nontransgenic mice (Fig.3.30 A). As shown in figures 3.30 B, C, D, the size of the seminiferous tubules was reduced although the number of tubules per testis appeared normal. The interstitial Leydig cells surrounding the tubules appeared to be increased in number, probably because of the decrease in the number of germ cells (Nakai et al., 2000).

A

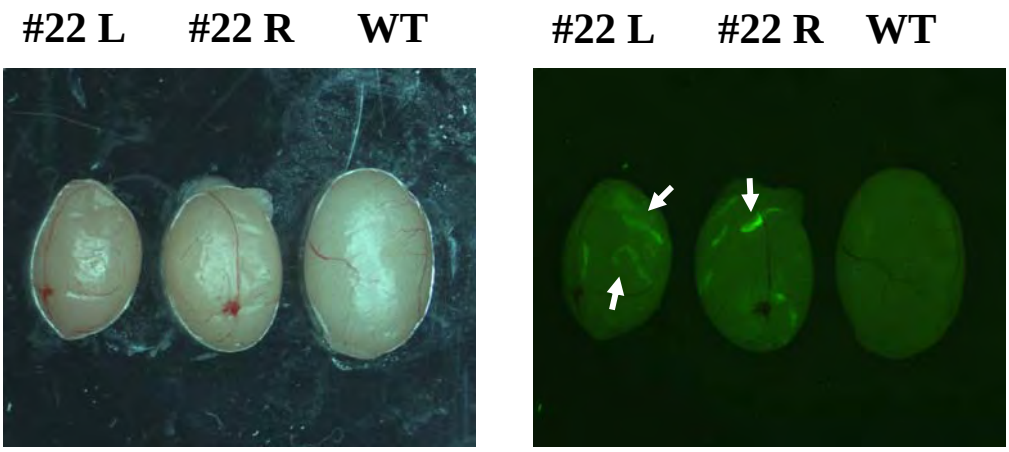
#22 L
#22 R
WT
#22 L
#22 R
WT

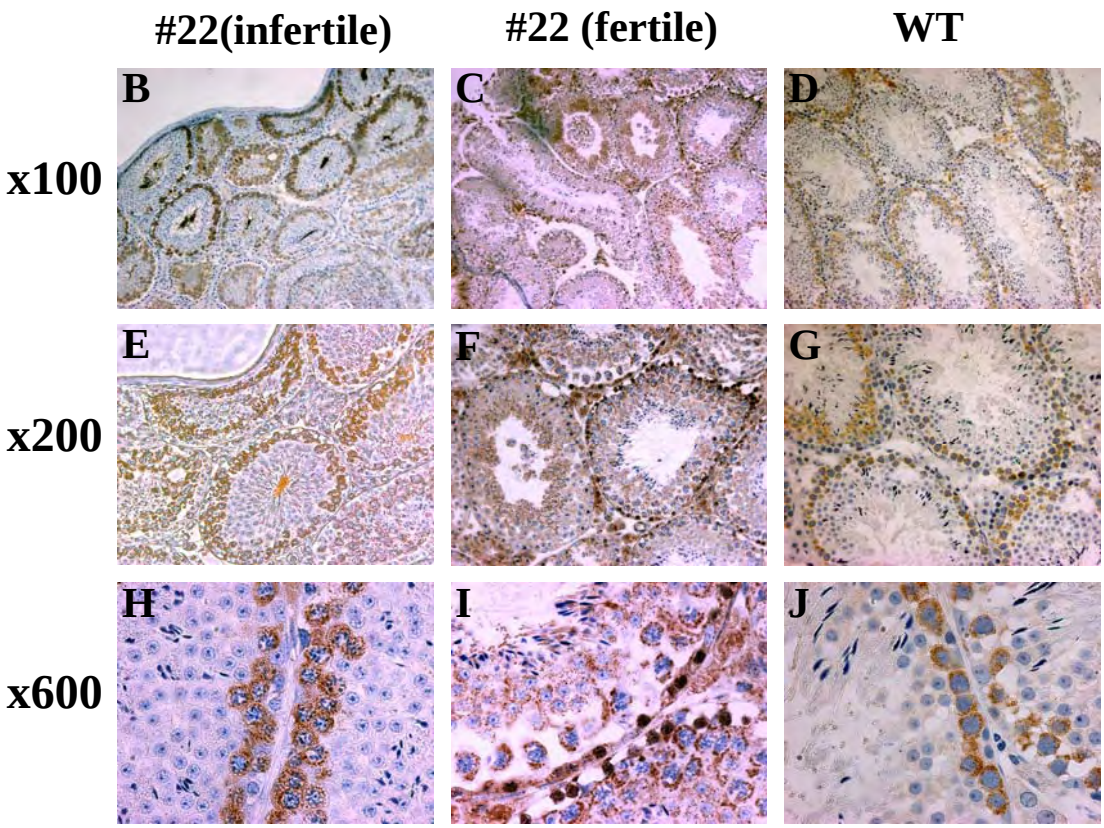
#22(infertile)
#22 (fertile)
WT
x100
x200
x600
B
C
D
E
F
G
H
I
J

Figure 3.30: (A) Expression of GFP in testis of a mouse transgenic for an *EGFP* reporter gene controlled by the *human elongation factor-1alpha* promoter. The fertile transgenic mouse of line #22 and the control mouse were 3 months old. The testis of the transgenic mouse is smaller as compared to that of the wild type and expresses GFP (white arrows, right). (B-J) Expression of the transgenic Piwil2 protein in the testis of transgenic (infertile, fertile of #22) and wild type mice from 6 months old by using immunohistochemistry with Piwil2 antibody (1:100). (B, E, H) Piwil2 protein is ectopically overexpressed in the testis of #22 infertile mice. (C, F, I) Testis of fertile mouse and (D, G, J) wild type. Piwil2 protein was immunodetected by anti-Piwil2 and visualized as brownish. Sections were counter stained by hematoxylin.

3.10 Sperm analysis of transgenic mice

To analyse male infertility, sperms were prepared from wild type, infertile and fertile mice of #22 transgenic mice as described in Materials and Methods section 2.2.26. For each testis of wild type, fertile and infertile mice, testes of three mice were weighted and the mean weight was taken. The weight datum shows a reduced testis weight of #22 infertile mice (0.087±0.07) as compared with wild type (0.108±0.05) and #22 fertile mice (0.097±0.03). We determined the total sperm count in the cauda epididymes of transgenic and wild type mice. A significant reduction of the number of spermatozoa in comparison to the wild type was observed ($P<0.001$). Morphological analysis of sperm from #22 infertile mice (10.2±1.13) showed a slightly increased abnormality of morphology, when compared with wild type (3.7±0.41) and fertile mice (8.7±0.83).

There is no significant difference between wild type and fertile transgenic mice. To analyse sperm motility, a computer assisted sperm analyser was used and the following parameters were evaluated: progressive velocity (which represents the straight line progressive movement of the sperm between the beginning and the end of the measurement divided by the time elapsed), straightness (straight line progressive movement of the sperm between the beginning and the end of the measurement). After 3.5 hrs of incubation time, sperm motility of *Piwil2* transgenic mice (infertile) in comparison with wild type mice was found to be reduced: 28% versus 44.5%. The proportion of sperm motility that exhibited progressive movement in *Piwil2* transgenic mice (infertile) was also reduced as compared

to those of wild type mice: 16.6% versus 26% (Table 2).

	Testis Weight(g)	Sperm Number(10^6) (epididymis)	Sperm Morphology[a] (abnormality)(%)	Motility [b](%) (Sperm incubated For 3.5h)	Progressive(%) (Sperm incubated For 3.5h)
#22 (Infertile)	0.087±0.07	0.12±0.03	10.2±1.13	28±9.3	16.6±2.1
#22 (fertile)	0.097±0.03	1.68±1.6	8.7±0.83	39±8.4	20±4.2
WT	0.108±0.05	4.6±1.1	3.7±0.41	44.5±14.8	26±3.25

a Percentage of sperm with abnormal morphology (three in each case).
b Percentage of sperm with straight motility (three in each case).

Table 2: Sperm analysis of *Piwil2* infertile, fertile and wild type mice.

3.11 Impairment of spermatogenesis in *Piwil2* transgenic mice

In hematoxylin and eosin-stained sections of testes from homozygous transgenic (infertile) males compared to wild type, all stages of spermatogenesis were normal (Fig.3.31 A and C). In 6 months old infertile transgenic mice, spermatogenesis looked apparently normal up till round spermatids in steps 2 and/or 3 of their development and then development stopped completely (Fig.3.31 B and D). This arrest was not accompanied by a massive apoptosis of the cells (Fig.3.31 F). Apoptosis did disappear, but gradually was observed in some tubules but somewhat sooner than in others. Tubules have preleptotene or leptotene spermatocytes surrounded by spermatogenic epithelium with vacuolated spaces of various sizes and these vacuolated spaces were thought to be the places where degenerated spermatocytes became eliminated (Fig. 3.31 B and D). What we see was that clumps were sometimes formed and sometimes apoptosis was observed in some of them (singles and clumps) (Fig.3.31 E). In

conclusion, a complete arrest at the level of round spermatids was observed. At this point, the acrosomic granules coalesce and should start to form an acrosomic cap. This arrest is characterized by degeneration and disappearance of pachytene or diplotene spermatocytes (Fig 3.31 B, D, F). In the normal testis (8 months old), seminiferous tubules at various spermatogenic stages were observed (Fig. 3.32 A and C). Whereas, there could no depletion of the epithelium and sertoli cells be observed in infertile male testis (8 month old). Round spermatids were not detected in advance to any further than in younger infertile mice (6 months old) (Fig. 3.32 B and D). In addition, histopathological analysis of testes of transgenic mice showed that the size of the seminiferous tubules was reduced (20-30% in diameter) although the number of tubules per testis appeared normal. (Fig. 3.32 A and B). Interestingly, depletion of germ cells of the transgenic testes did not appear to result from a markedly decreased number of dividing spermatogonia (Fig.3.32 D). In most cases, the arrested development was found to occur in late meiosis, either at pachytene or diplotene. No elongated spermatids were found except in those cases (partial) where mature spermatozoa occurred (Fig. 3.32 B and D).

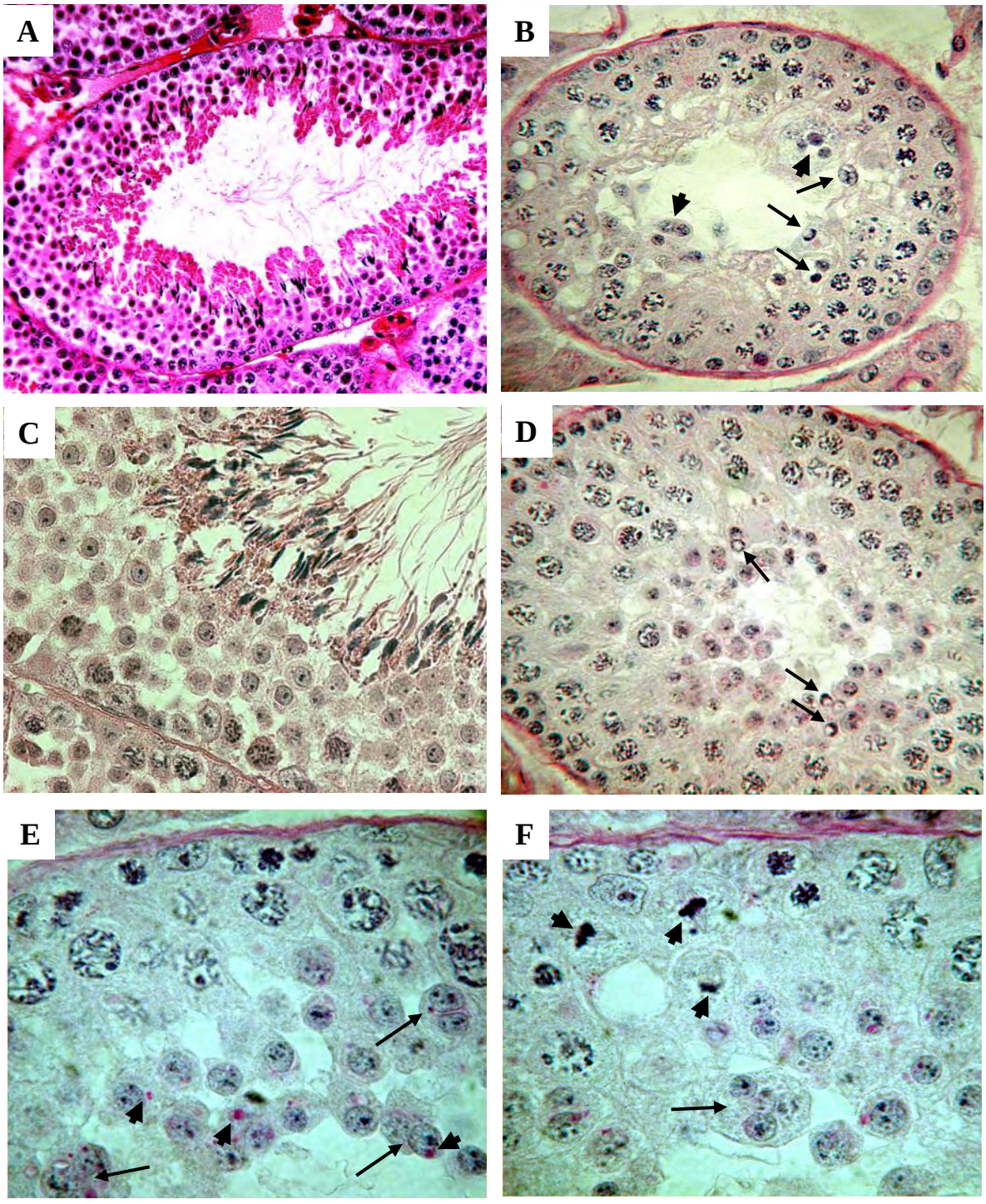
A
B
C
D
E
F

Figure 3.31: Histology of hematoxylin and eosin-stained sections of *Piwil2* transgenic mice. (A) The testis from 6 months old of normal littermate (X200) and (C) magnified normal testis (X600). (B, D, E, F) testis from transgenic mice (infertile) at 6 months of age. (B) Tubule where the round spermatids disappear more quickly (about stage IV). There is some apoptosis (small arrows) and 2 clumps (large arrows) (X200). (D) In stage VII-VIII, apoptosis (small arrows) and loosed round spermatids that may soon get sloughed off (X200). (E) In stage X-XI, there should no longer be round spermatids, but these still are present. The acrosome consists of an irregular dot or a couple of dots (large arrows). Therefore, there is no acrosomal cap in these spermatids. In stage IX-X, Some clumps of several spermatids are also present (small arrows) (X600). (F) In stage XII, the round spermatids present have become arrested in development in about stage III. Meiotic divisions (arrow heads) and clump of spermatids (small arrow) (X600).

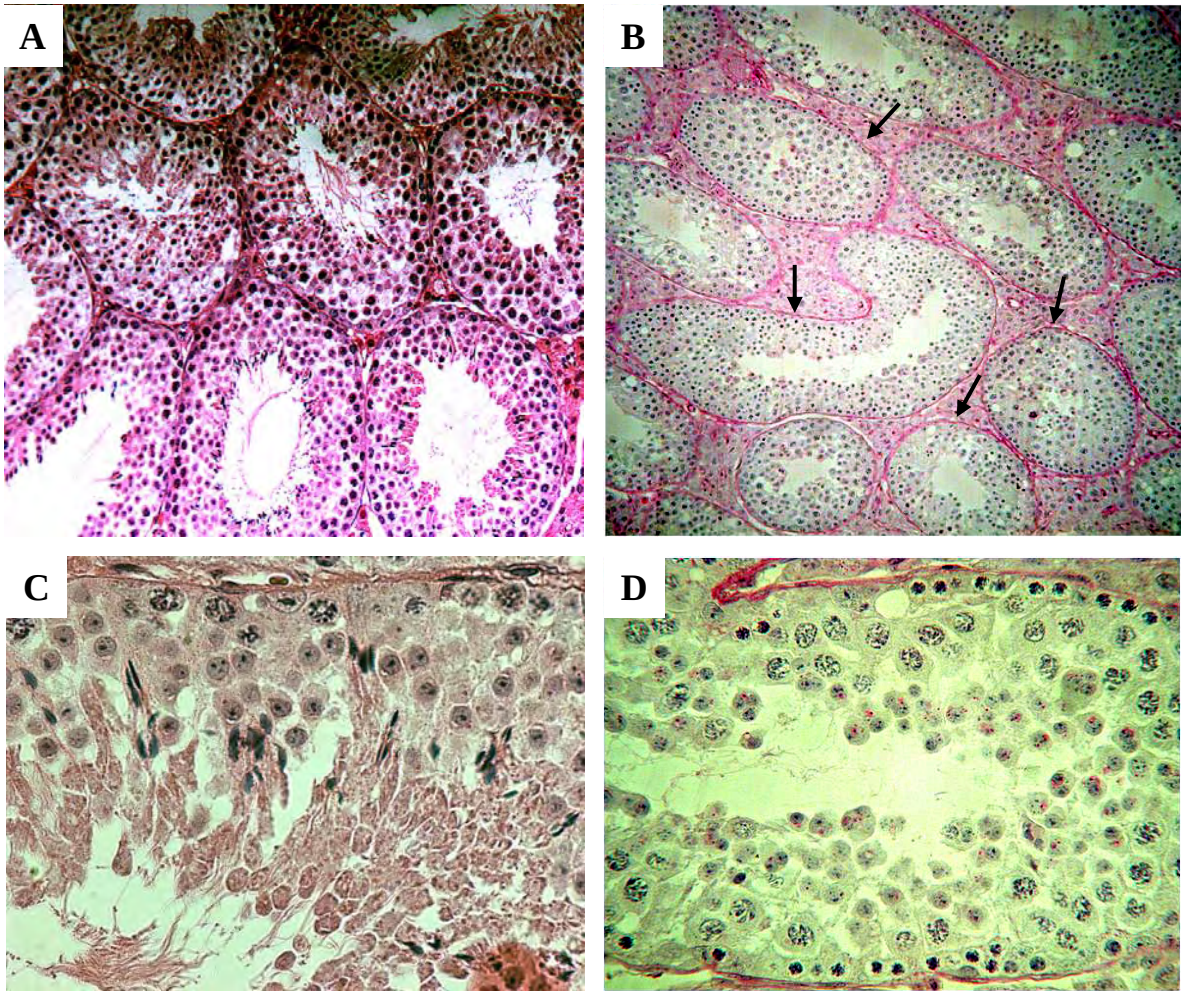

Figure 3.32: Histological sections of the testes. (A, C) Sections of testis from 8 months old wild type. hematoxylin and eosin staining, X100, X600, respectively. (B, D) Sections of testis from 8 months of age *Piwil2* transgenic mice (infertile). (B) No Sertoli cell only tubules and no depletion of the epithelium visible (arrows). Some spermatids can develop further than step 2-3 (X100). (D) In stage X-XI, this tubule was with zygotene and pachytene/diplotene spermatocytes (X600).

3.12 Electron microscopy of testis sections from infertile transgenic mice

The ultrastructure of testes from infertile *Piwil2* transgenic mice at the age of 8 months was examined by electron microscopy. Degenerated germ cells in the seminiferous tubules were identified (Fig. 3.33). Type A and B spermatogonia show normal morphology, but multivesicular vacuoles were generally observed in germ epithelium (Fig. 3.33 A and B). Furthermore, Leydig cells were bigger than normal and germ cells developed until round spermatids owing to degenerated meiotic pachytene spermatocytes (Fig. 3.33 C and D). In the seminiferous tubules, consecutive spermatogenic cycles are classically depicted as waves of differentiating germ cells (Fig. 3.33 E and F). In wild type mice, tubules containing elongated spermatids in the inner layer were easily detected, whereas these tubules were hardly detectable in transgenic mice. Even in the tubules containing round spermatids, they were few in number per section.

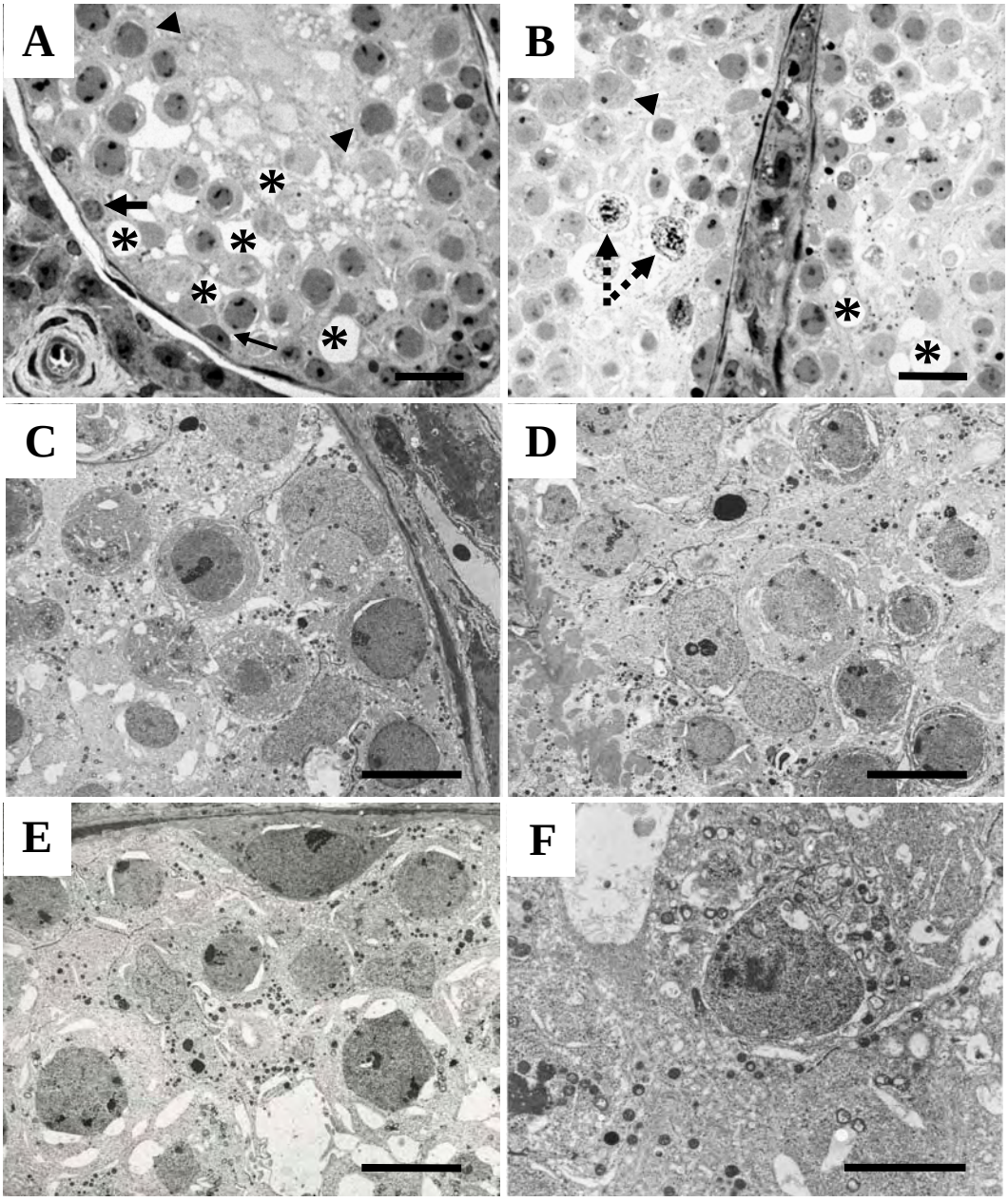

Figure 3.33: Electron microphotographs of an 8 months old *Piwil2*-overexpressing mice testis. (A and B) No pachytene spermatocytes are visible. Round spermatids: arrowheads, type B spermatogonia: large arrow, type A spermatogonia: small arrows, degenerated pachytene spermatocytes: dot arrows, vacuoles: asterisks. (C) Spermatogonia are normal but degenerative meiosis cells are observed. (D) Due to degenerated pachytene spermatocytes, germ cells arrested in round spermatids, sometimes in elongated spermatids. (E and F) Rarely, degenerated spermatogonia and degenerated germ cells were observed. Bars, (A and B) 7 µm, (C-E) 5 µm, (F) 2.5 µm.

3.13 Detection of apoptotic cells in transgenic mice

To analyse apoptosis, 3 months old testis section of wild type and transgenic mice were analysed by the TUNEL (Terminal dUTP Nick-End Labeling) labeling technique (Fig. 3.34). During normal spermatogenesis, sporadic apoptotic cell death is known to occur in normal spermatogenesis, where it has been described to be largely restricted to spermatogonia (Allan et al., 1992) (Fig. 3.34 A and E, arrows). However, significant numbers of apoptotic cells were observed in transgenic testis (Fig. 3.34 B and D, arrows). The apoptotic cells in the inner layers of the seminiferous tubules are in the most mature cells during the first wave of spermatogenesis. In the testis of transgenic mice, seminiferous tubules with vacuoles were observed. Vacuoles may have been created by elimination of the degenerated germ cells (Fig. 3.34 B, D, F, H). Labeled cells were found clustered in some tubules, whereas other tubules were totally devoid of TUNEL-positive cells (Fig. 3. 34 D). At higher magnification, the majority of labeled cells in the transgenic mice were ascertained to be pachytene and metaphase spermatocytes (Fig. 3.34 D and F), although round spermatids also exhibited labeling (Fig. 3.34 H). No staining was noted in elongated spermatids. In conclusion, apoptosis was mainly observed in premeiotic pachytene spermatocytes and much fewer in round spermatids. This indicates that ectopic *Piwil2* expression is not related directly with apoptosis.

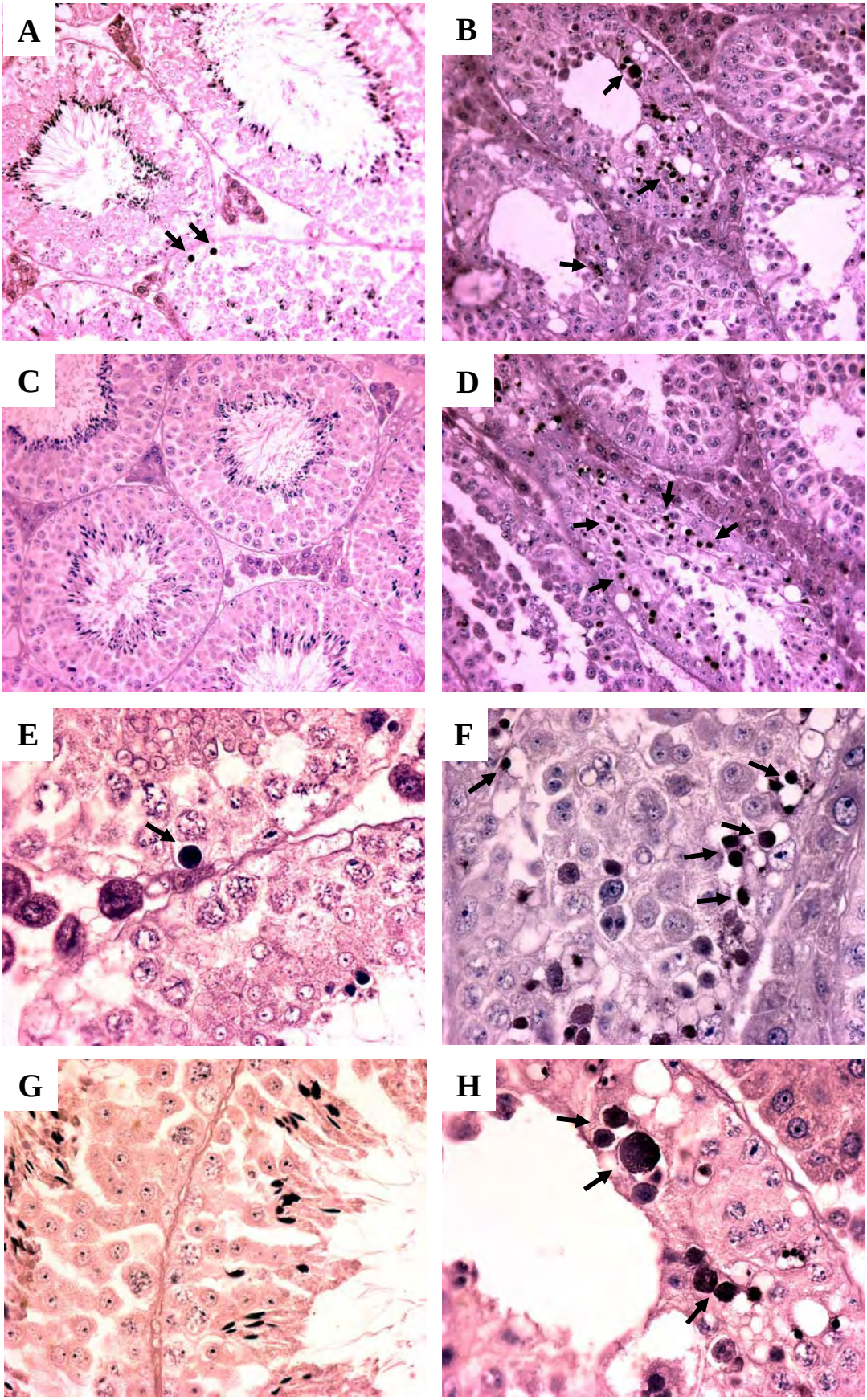
A
B
C
D
E
F
G
H

Figure 3.34: Apoptosis in transgenic testes. In situ 3'-end labeling by the TUNEL method using testes sections of a 3 months old transgenic mice. (A, C, E, G) Testes from wild type and (B, D, H, F) from transgenic mice. Apoptotic cells were stained violet (arrows). (A and C) Five apoptotic cells were observed in the testis of wild type mice (X200). (B and D) In contrast, apoptotic cells were abundant in 20-30% of seminiferous tubules (X200). (E and G) Magnification of wild type (X600). (F and H) Magnification of transgenic mice (X600).

3.14 Isolation and identification of downstream target genes of *Piwil2* involved in stem cell metabolisms

3.14.1 Stem cell gene array in NIH3T3-pcDNA and NIH3T3-pcDNA-*Piwil2* cell lines

To identify and characterize genes related to stem cell renewal and differentiation, expression profiles of NIH-3T3 cells expressing stably full length *Piwil2* was compared with control cell line NIH3T3-pcDNA using a stem cell array. The GEArray S series mouse stem cell gene array is designed to profile the expression of genes known to be important for the identification, growth and differentiation of mouse stem cells. It contains 258 known genes that encode markers expressed by stem cells at various stages of differentiation (91 genes), growth factors and cytokines known to regulate stem cell growth (99 genes), extra cellular matrix molecules expressed at appropriate developmental stages (38 genes), as well as other proteins such as cell cycle regulators that are thought to be involved in stem cell division. Positive controls and housekeeping genes are also included for normalization to generate relative expression profiles. The array is particularly useful in exploring neural stem cell development, but also contains markers for the identification and differentiation of embryonic, mesodermal and hematopoietic stem cells. This analysis revealed modulation or activation of genes (*GDNF/Ret, GFR α1, Cyclin D, Dazl, SCF/c-kit, Bax, Bcl-X_L, and Plzf*) related to stem cell renewal and differentiation (Fig. 3.35 and Table 3). *Pdgfrb* (Platelet derived growth factor receptor, beta polypeptide), *Slc2a1* (Solute carrier family 2

member 1, Glut1), *Gja7* (Gap junction membrane channel protein alpha 7) and spermatogonial cell surface markers *Itga6* (Integrin alpha 6) were overexpressed in NIH3T3-pcDNA-*Piwil2* cell line.

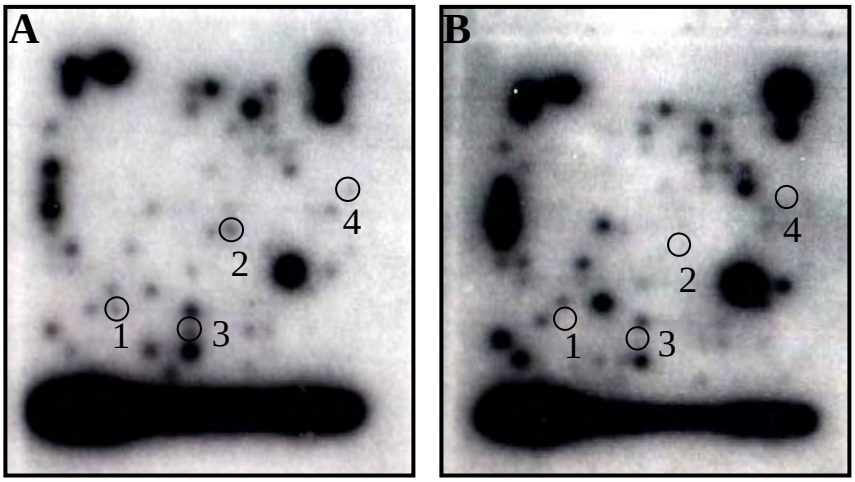

Figure 3.35: Modulation or activation of genes related to stem cell renewal and differentiation. Mouse stem cell array analysis was used for identification of genes regulated by *Piwil2*. 1: *Pdgfrb* (Platelet derived growth factor receptor, beta polypeptide) 2: *Itga6* (Integrin alpha 6) 3: *Slc2a1* (Solute carrier family 2 (facilitated glucose transporter), member 1) 4: *Gja7* (Gap junction membrane channel protein alpha 7); A: NIH3T3-pcDNA-*Piwil2*, B: NIH3T3-pcDNA.

	NIH3T3-pcDNA-Piwil2	NIH3T3-pcDNA
Gja7(Gap junction membrane channel protein alpha 7)	+	-
Pdgfrb (Platelet derived growth factor receptor, beta polypeptide)	+	-
Itga6 (Integrin alpha 6)	+	-
Slc2a1 (Solute carrier family 2 (facilitated glucose transporter), member 1)	+	-

Table 3: A summary of differentially expressed genes identified by stem cell array.

3.14.2 Characterization of upregulated genes using RT-PCR and Northern blotting

To confirm the results by stem cell array, expression of these genes was analysed by Northern blotting. Furthermore, expression of two other markers for spermatogonial stem cells (SSCs), *Thy-1* and *Egr3* (early growth response 3), was examined by Northern blot analysis. Activation of *Pdgfrb* and *Itga6* and overexpression of *Slc2a1*, *Gja7* and *Thy-1* were demonstrated (Fig. 3.36 A). A slight increase in expression level of *Itgb1* and *Egr3* was observed (Fig. 3.36 A). Expression of genes which had an increased expression level were analysed by RT-PCR using RNA isolated from testis of wild type and testis of W/W^v mutant mice which lack any germ cells. Expression of *Pdgfrb*, *Egr3*, *Gja7*, *Itga6* and *Thy-1* was detected in testis of wild type mice but not in testis of W/W^v mutant mice which is an indication for germ cell specific expression in testis (Fig. 3.36 B).

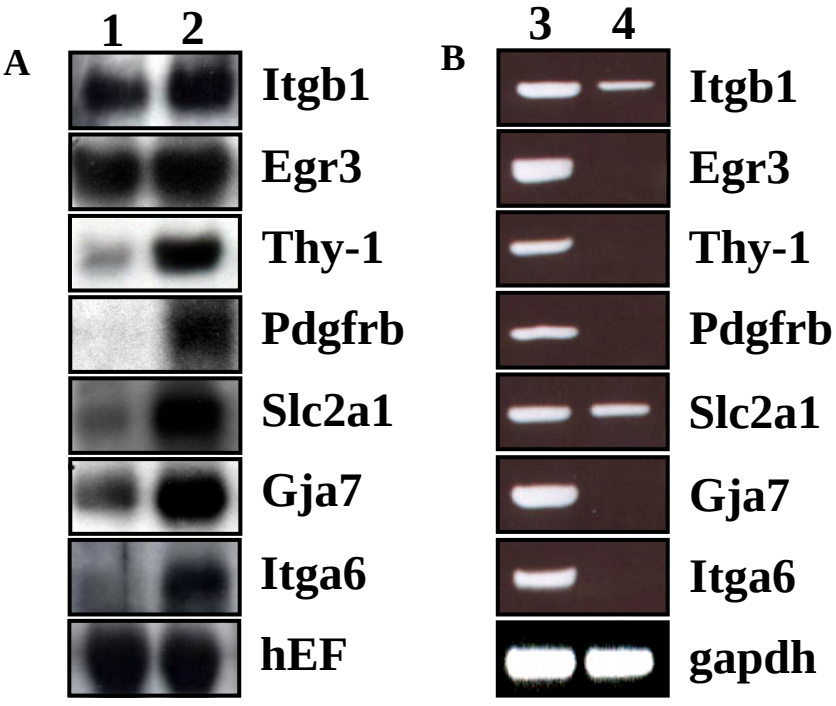

C

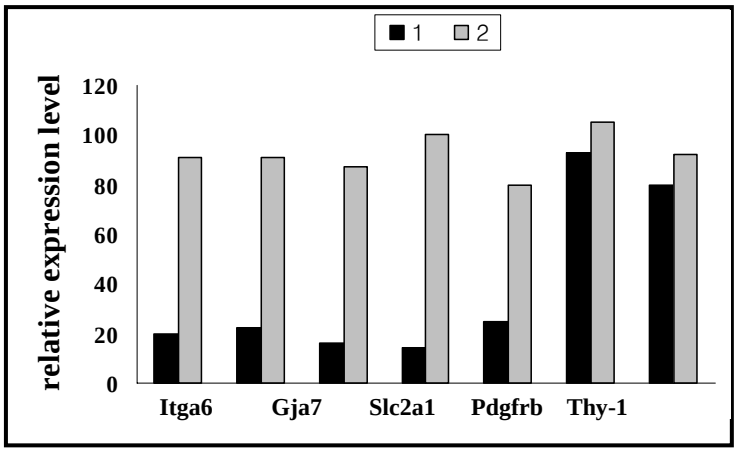

Figure 3.36: (A) Northern blot analysis using RNA isolated from NIH3T3-pcDNA cells (1), NIH3T3-pcDNA-*Piwil2* (2) cell lines hybridized with labelled specific probes for *Pdgfrb* (Platelet derived growth factor receptor, beta polypeptide), *Egr3* (early growth response 3), *Slc2a1* (Solute carrier family 2 member 1), *Gja7* (Gap junction membrane channel protein alpha 7) and spermatogonial cell surface markers Thy-*1*, *Itgb1* (beta1-integrin) and *Itga6* (Integrin alpha 6). The blots were rehybridized with *human elongation factor-2* (hEF-2) cDNA probe to ensure RNA integrity and equal loading. (B) RT-PCR analysis using RNA isolated from testis of wild type (3) and *W/W^v* (4) mice with primers specific for *Pdgfrb*, *Egr3*, *Slc2a1*, *Gja7*, and spermatogonial cell surface markers *Thy-1*, *Itgb1*, and *Itga6*. As control, for RT-PCR *glyceraldehyde-3-phosphate dehydogenase* (GAPDH) primers were used. (C) Quantification of expression of differentially expressed genes shown in (A), relative expression level in NIH3T3-pcDNA cells (1) compared to expression level in NIH3T3-pcDNA-*Piwil2* cells (2).

3.14.3 Analysis of spermatogonial stem cell markers in *Piwil2* expressing cells

To further confirm the spermatogonia characteristics of NIH3T3-pcDNA-*Piwil2* cells on molecular level, we investigated whether *Hsp90α*, *Stra8*, and *CD9* genes are expressed in

Piwil2 expressing cells. A germ cell marker (heat shock protein-90*α*, *Hsp90α*) and a marker of SSCs used to detect dividing cells showed that this proliferation was restricted to germ cells (Creemers et al., 2002; Nayernia et al., 2004). The spermatogonia-specific *Stra8* is sufficient to direct gene expression to the germinal stem cells (Giuili et al., 2002; Nayernia et al., 2004). *CD9* is involved in the common machinery in stem cells of many self-renewing tissues and the identification of a common surface antigen on spermatogonial stem cells (Shinohara et al., 1999; Kubato et al., 2003; Kanatsu-shinohora et al., 2004). As shown by RT-PCR, expression of these genes is induced in NIH3T3-pcDNA-*Piwil2* cells (Fig. 3.37).

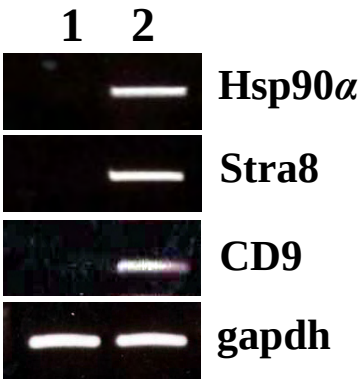

Figures 3.37: RT-PCR analysis using RNA isolated from NIH3T3-pcDNA cells (1) and NIH3T3-pcDNA-*Piwil2* cells (2) with primers specific for *Hsp90α*, *Stra8*, and *CD9* revealed induction of expression of these genes by *Piwil2*.

Furthermore, to determine expression of Itga6, Hsp90*α*, Stra8, and CD9 as spermatogonial stem cell markers (Creemers et al., 2002; Kanatsu-Shinohara et al., 2004; Nayernia et al., 2004) in cells expressing Piwil2, immunohistochemical analysis was performed using specific antibodies (Fig. 3.38 A). We used anti-Piwil2 (Fig. 3.38 A) and antibodies against

Itga6, Hsp90*α*, Stra8 and CD9 (Fig. 3.38 A) to demonstrate an antigen characteristic of spermatogonial stem cell in *Piwil2*-transfected cells (NIH3T3-pcDNA-*Piwil2*). As shown in figure. 3.31, most Piwil2 expressing cells are positive for Itga6, Hsp90*α*, Stra8 and CD9. Additionally, the expression of Hsp90*α* (28%) and Stra8 (24%) and CD9 (6.5%) was found to be induced in NIH3T3-pcDNA-*Piwil2* cells (Fig. 3.38 B).

A

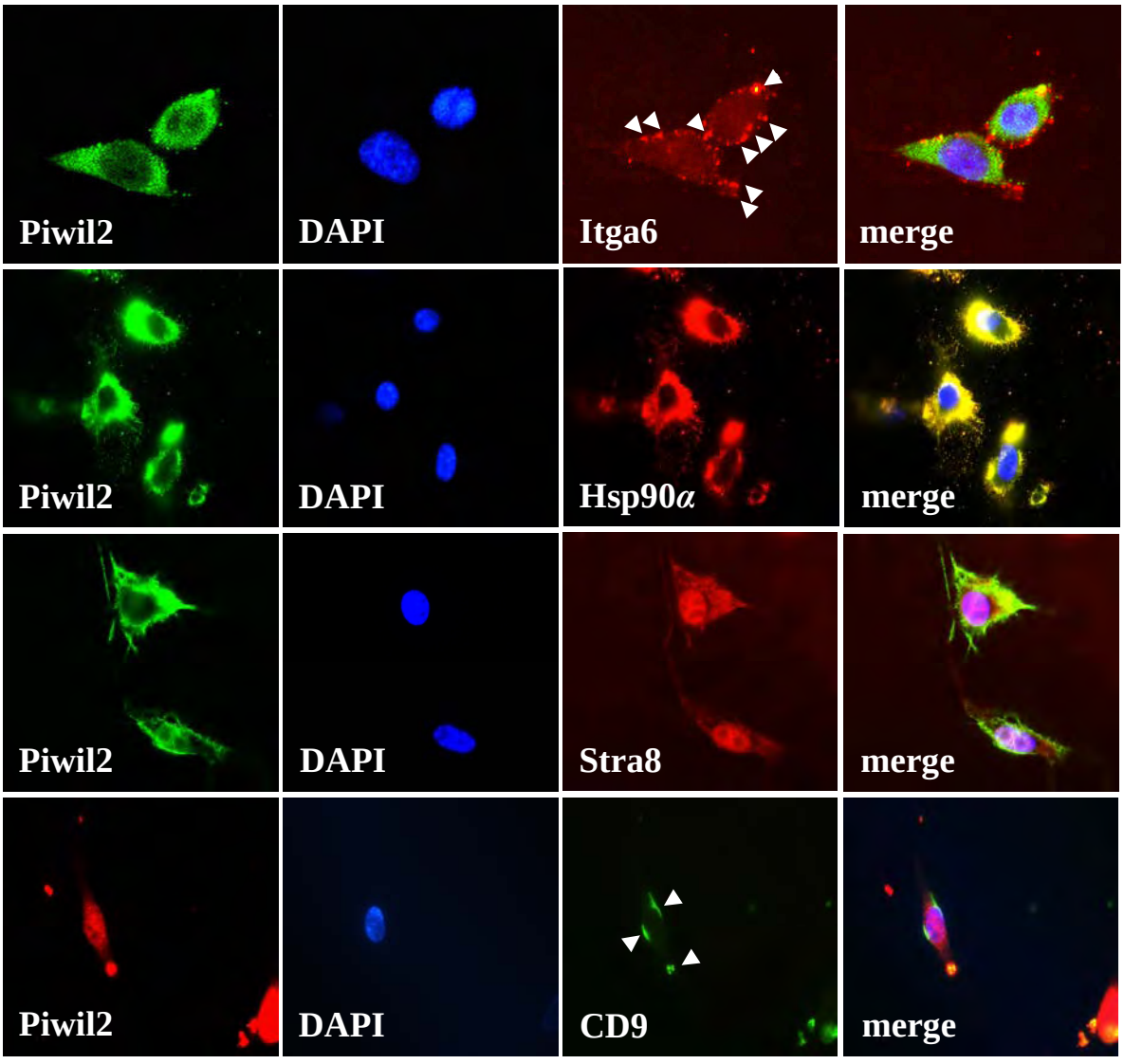

B

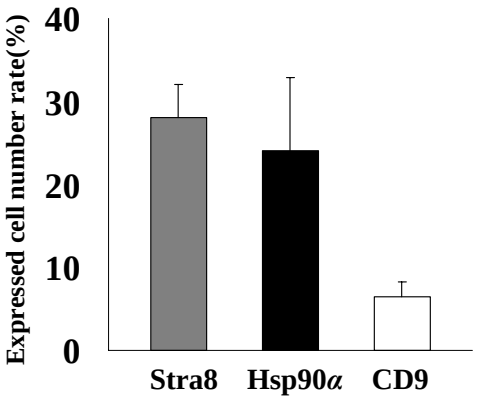

Figure 3.38: Expression of Itga6, Hsp90*α*, Stra8, and CD9 in cells expressing Piwil2 was shown using immunohistochemistry. (A) The expression of Piwil2 was detected in NIH3T3-pcDNA-*Piwil2* cells (green or red). Nucleus was counterstained with DAPI (blue). Itga6 and CD9, surface markers of spermatogonial stem cells, were expressed on the surface of NIH3T3-pcDNA-*Piwil2* cells (white arrows). Hsp90*α* and Stra8, spermatogonia specific markers, were observed in cytoplasm and nucleus in NIH3T3-pcDNA-*Piwil2* cells. Nearly all Piwil2 expressing cells show positive immunoreaction with Itga6, Hsp90*α*, Stra8 and CD9 (merge) (magnification X600). (B) Quantitative expression analysis of differentially expressed Stra8, Hsp90*α* and CD9 in NIH3T3-pcDNA-*Piwil2* cells show expression of Stra8 and Hsp90*α* genes in 20-30% of cells and an induction of CD9 expression in about 8% of cells.

3.15 Alerted morphology of NIH3T3-pcDNA-*Piwil2* cells

To characterize the morphological changes of the cells following *Piwil2* expression, cells were seeded at 2.5×10^4 cells per well and the morphology of cells was observed by an invert microscope. While most control cells, NIH3T3-pcDNA cells exhibited spindle-shaped morphology (Fig.3.39 A), more than 50% of NIH3T3-pcDNA-*Piwil2* cells showed a rounded morphology (Fig. 3.39 B), which resembles morphology of spermatogonia.

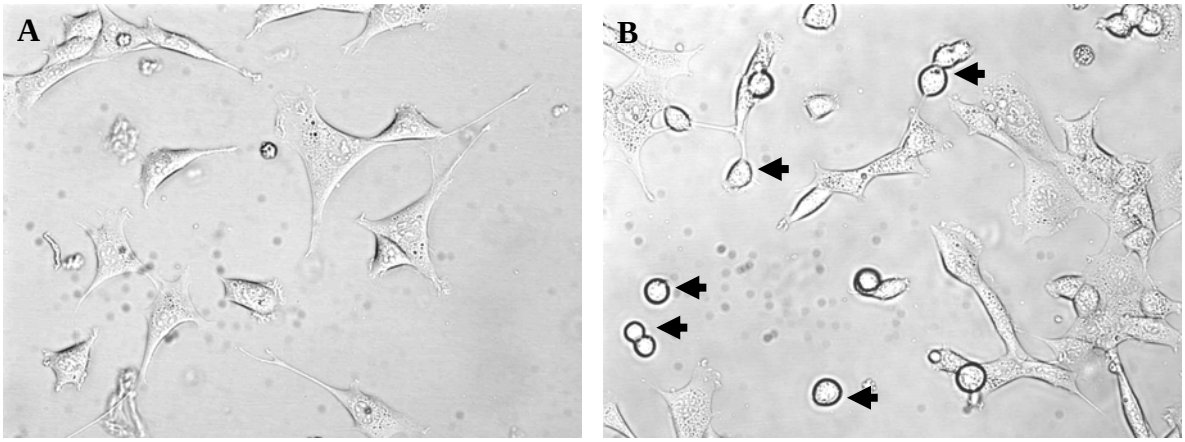

Figure 3.39: Expression of *Piwil2* causes morphological changes in NIH3T3 cells. (A) NIH3T3 cells transfected with control plasmid pcDNA. (B) NIH3T3 cells transfected with pcDNA-*Piwil2*. Arrows show appearance of round cells after *Piwil2* expression. Magnification X200.

4. DISCUSSION

4.1 Stem cell protein *Piwil2* is widely expressed in tumors and inhibits apoptosis through activation of *Stat3/Bcl-X_L* pathway

4.1.1 *Piwil2* is expressed specifically in testis and in a wide variety of tumors

We showed that *Piwil2* is specifically expressed in testis of mouse and human, in most tumors and in testis of mutant mice, except *W/W^V*. By immunohistochemical analysis we demonstrated that *Piwil2* is expressed specifically in spermatogonia and spermatocytes, but not in somatic cells. This expression pattern resembles expression of testis-cancer antigens, which are expressed in some tumor cells, tumor tissues and testis.

Therefore, *Piwil2* appears to fall in category of testis-cancer antigens (CTAs). Testis-cancer antigens were the first human tumor-associated antigens characterised at the molecular level (Scanlan et al., 2004). In testis, CTAs are exclusively present in the germ cell lineage, although there is a lot of variation in the expression profile during different stages of germ cell development (Zendman et al., 2003). CTAs are normally expressed by gametes and trophoblasts and are aberrantly expressed in a range of human cancers (Fig. 4.1). So far, 44 distinct CTAs families, some of which have multiple members, have been identified. CTAs are immunogenic and, as a result, have the potential to be used as tumor vaccines. CTAs can be divided into those that are encoded on the X chromosome (CT-X antigens) and those that are not (non-X CT antigens). CT-X antigens tend to form recently expanded gene families that are usually highly expressed in the spermatogonia (mitotically proliferating germ cells). The CT-X genes are frequently co-expressed in cancer cells which tend to express several CT antigens. The genes for the Non-X CT antigens are distributed throughout the genome. In testis, they are usually expressed in the spermatocytes and many have roles in meiosis. Their aberrant expression in cancer cells might cause abnormal chromosome segregation and aneuploidy. Methylated CpG islands associated with the CT-

X genes in normal somatic cells become demethylated in cancer cells, indicating activation of their expression in somatic cells (Simpson et al., 2005).

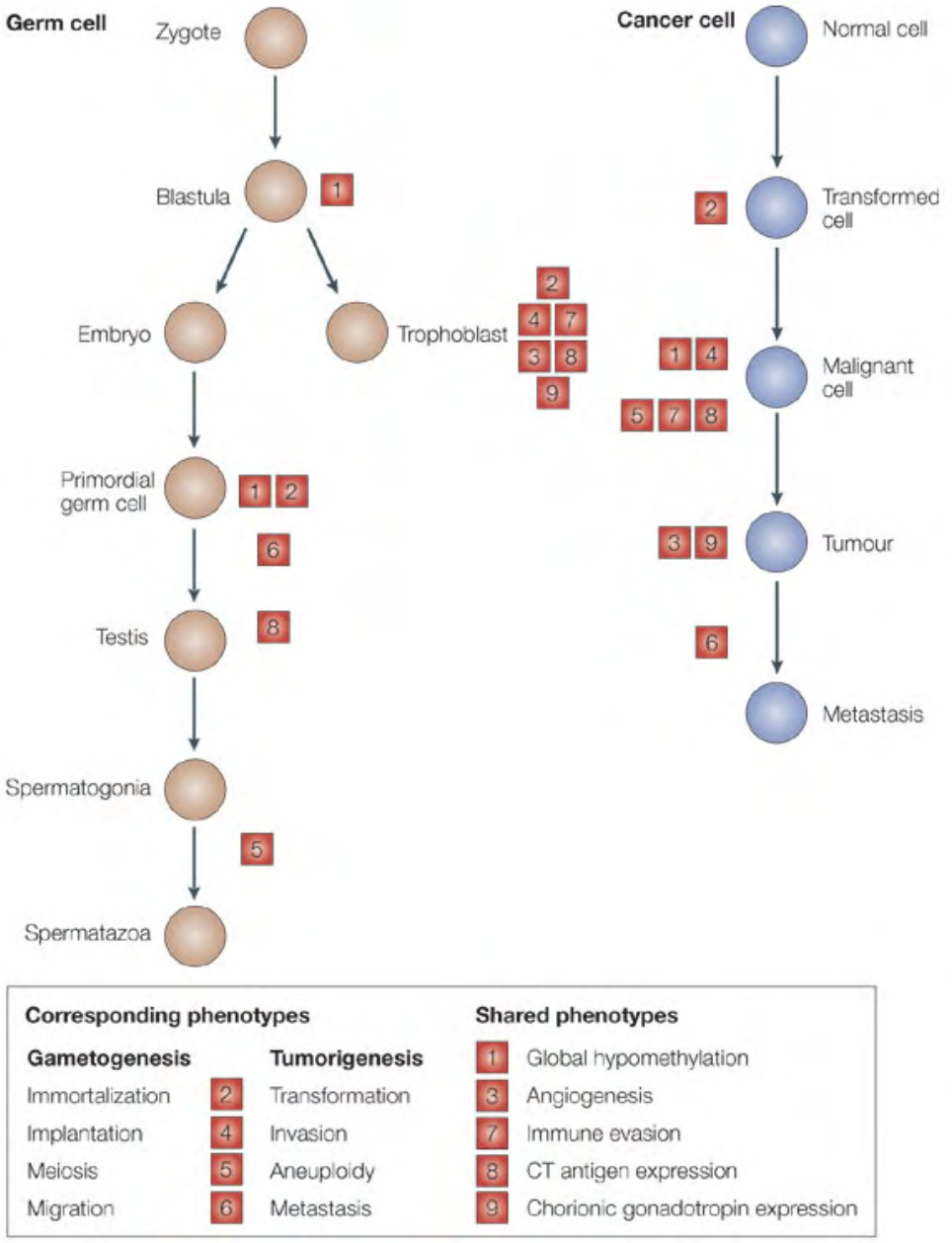

Figure 4.1: Shared characteristics of germ cells and cancer cells. Activation of the gametogenic programme (shown by brown cells) might contribute to properties of tumor formation and progression (shown by blue cells). Corresponding features between cancer cells and those in the germ cell/gamete/trophoblast differentiation pathways include: immortalization (involved in transformation), invasion, induction of meiosis (can lead to aneuploidy) and migration (contributes to metastasis). Shared phenotypes between germ cells and cancer cells include demethylation, angiogenesis induction, downregulation of the major histocompatibility complex (immune evasion) and expression of chorionic gonadotropin. The numbers (1–9) indicate gametogenesis- and tumorigenesis-related phenotypic traits and the stages at which these events occur (adapted by Simpson et al., 2005).

As germline stem cells and their trophoblastic derivatives share many characteristics with tumor cells, the activation of normally silent germline-specific genes in cancer stem cells (gametic recapitulation) could mediate the malignant phenotype in the absence of mutations in known oncogenes and tumor-suppressor genes.

However, literature regarding the biological properties of *Piwil2* is very limited and, furthermore, the role of *Piwil2* in solid cancer is completely unknown. The aim of our present work was to investigate *Piwil2* expression in human and mouse cancer and to identify potential roles for *Piwil2* in the genesis of cancer. We screened 10 human cancer cell lines and 8 mouse cancer cell lines for *Piwil2* expression. 9 of 10 human cancer cell lines and 7 of 7 mouse cancer cell lines showed *Piwil2* mRNA expression. In addition, three types of tumors with their corresponding normal tissues were examined in mouse. Whereas in breast tumor, rhabdomyosarcoma and medulloblastoma expression of Piwil2 was detected, no expression was observed in normal breast, muscle and cerebellum tissue. In human, in different tumor types expression of *Piwil2* was detectable by using RT-PCR. In 3 of 4 different ovarian tumors, in 4 of 4 prostate carcinomas, in 4 of 4 tumors in lymphatic gland and in 7 of 7 breast tumors, expression of *Piwil2* was detected by RT-PCR analysis. These data suggest that *Piwil2* is expressed in most human and mouse cancer tissues and it may play an important role in cancer development.

In order to investigate expression of Piwil2 on protein level, we generated a rabbit polyclonal antibody against mouse Piwil2 and a human monoclonal antibody against human PIWIL2. The specificity of the antibodies was examined with *Piwil2* gene

transfection in NIH3T3 cells and immunostaining on paraffin-embedded tissue sections of each human and mouse testis. In mouse, we used this specific antibody for immunohistochemistry to examine the expression of *Piwil2*. In mouse and human testis, the Piwil2 protein was detected in spermatogonia and early spermatocytes. While expression of Piwil2 was not detected in normal skeletal muscle and cerebellar tissues, Piwil2 was detectable in corresponding tumor tissues, rhabdomyosarcoma and medulloblastoma. In human, Piwil2 was found in cytoplasm of breast tumor cell line MDA-MB-231. In all seven breast tumor tissues from different patients, expression of Piwil2 was observed. No expression was detectable in normal breast tissue. Furthermore, immunohistochemical analysis showed expression in other tumors either in dispersed or in clonal form. These results indicate that Piwil2 is specifically expressed in spermatogonia of testis and ectopically in most tumor cell lines and tumor tissues.

Our immunohistochemical results indicate that Piwil2 is a potential marker for cancer cell proliferation. Likewise, we used proliferation assay and soft agar assay in Piwil2 expressing cell line in order to estimate the proliferation status of the cells in this study.

In human, an elevated expression of *Piwil2* was observed in testicular germ cell tumors (Fig. 3.11). This expression pattern mimics expression pattern of *Piwil1* in testicular germ cell tumors. In normal human testis, *Piwil1* (*hiwi*) is specifically expressed in germ cells, with its expression detectable in spermatocytes and round spermatids during spermatogenesis (Qiao et al., 2002). Enhanced expression of *Piwil1* was found in 12 out of 19 sampled testicular seminomas originating from embryonic germ cells with retention of germ cell phenotype. In contrast, no enhanced expression was detected in 10 nonseminomatous testicular tumors that originate from the same precursor cells as seminomas (Qiao et al., 2002).

Moreover, the specific correlation between *Piwil2* overexpression and seminomas but not nonseminomas suggests that *Piwil2* can function in spermatogonia or their precursors. Seminomas could be caused by the ectopic expression of *Piwil2* in spermatogonia. Both possibilities may reflect a functional evolution of the *piwi* family genes from *Drosophila* to mammalian systems. In this context it is also interesting to note that there are multiple human homologs of *piwi*. It is therefore possible that the various *Piwil2* homologs became specialized in subsets of the *piwi* functions, with *Piwil2* in particular concentrating on and

further enhancing the cell-autonomous function of *piwi* in promoting the division of stem cells and/or their differentiating daughter cells in the germline.

Nonseminomas do not show enhanced *Piwil2* expression, likely because these tumors have lost their germline properties, even though they also originate from the same precursor cells as seminomas, i.e. CIS (Carcinoma In Situ). The results presented in this study allow us to conclude that the overexpression of *Piwil2* probably does not lead to the development of spermatocytic seminomas but might be involved in the formation of TGCTs (Testicular Germ Cell Tumor). Several studies have identified genetic components in the development of TGCTs. It has been suggested that up to 30% of TGCTs are affected by genetic predisposition (Nicholson and Harland, 1995). In fact, the development of TGCTs has been found to show linkage to a number of chromosomal regions, suggesting the involvement of more than one gene, for which both a dominant and a recessive model might be applicable (Bishop, 1998). The specific correlation between *Piwil2* overexpression and seminomas is likely due to the fact that these cells retain the phenotype of CIS cells. Yet, varied levels of *Piwil2* expression in different seminomas or even within the same tumor might be related to the heterogeneity of the tumor cells. This heterogeneity is not correlated to the mitotic or apoptotic frequency of these cells. It thus remains to be elucidated whether it might be explained by the difference in other aspects of cellular metabolism or the heterogeneity of tumor cells in activating various *Piwil2* homologies. More specific antibodies against PIWIL2 and its *Piwil2* homologs of human could be informative to investigate this hypothesis. This intriguing expression pattern of *Piwil2*, as well as its expression in cancer cell lines and tissues, offer novel opportunities for studying the mechanisms of stem cell divisions and oncogenesis.

These results show a possible synergistic effect of *piwi* genes on initiation and progression of testicular germ cell tumors.

Therefore, the wide range of tumors in which *Piwil2* has been detected urges further efforts to develop effective specific immunotherapeutic procedures.

Based on these results in cancer samples, it would be interesting to analyse the relationship between *Piwil2* expression and clinical parameters. It is possible that the number of samples used in this study may not be large enough to evaluate the link between *Piwil2* expression and clinical parameters.

4.1.2 Identification of *Piwil2* Downstream Targets

Herewith, the establishment of the cell lines expressing *Piwil2* which show some mouse spermatogonial stem cell characteristics is described. It proved possible to establish the cell lines expressing *Piwil2* by the use of transfection with pcDNA-*Piwil2* and pcDNA in NIH3T3 cells. We ended up with cell lines, which have now been cultured for over 1 month under permanent selection of G418, indicating that these cell lines are very stable. *Piwil2* is not expressed in the NIH3T3 cells (Fig. 3.7). Transfection with pcDNA and pcDNA-*Piwil2*, respectively, revealed a subcellular localization of the Piwil2 protein in the cytoplasm (Fig. 3.14).

In the present study, we applied microarray gene expression profiling to identify candidate Piwil2-regulated genes that may confer resistance to apoptosis in NIH3T3-pcDNA-*Piwil2* cells. *Bcl-X_L*, an antiapoptotic gene, is frequently expressed in various tumors and is identified as a Piwil2-regulated gene in NIH3T3-pcDNA-*Piwil2* cells. We demonstrated that *Piwil2* activates expression of *Bcl-X_L*. *Bcl-X* belongs to the *bcl-2* gene family. Members of the *bcl-2* family of genes serve as regulators of cell death, either promoted by *Bax*, *Bak*, *Bok*, *Bik*, *Blk*, *Hrk*, *Bad*, *Bid*, *Diva* and *EGL-1* or inhibited by *Bcl-2*, *Bcl-X*, *Bcl-w*, *Mcl-1* and *CED-9* (Reed, 1998; Zamzami et al., 1998; Ke et al., 2004). Furthermore, we showed that *Piwil2* is able to induce the expression of signal transducers and activators of transcription 3 (*Stat3*) and to slightly enhance expression of *Akt*, two upstream regulators of *Bcl-X_L* (Jost et al., 2001; Umeda et al., 2003). The signal transducers and activators of transcription (STAT) factors function as downstream effectors of cytokine and growth factor receptor signaling. In mouse, STAT3 activation is required and sufficient to maintain the undifferentiated state of ES cells (Niwa et al., 1998; Matsuda et al., 1999). Stable expression of a dominant negative mutant of STAT3 induces morphological differentiation of ES cells despite continuous LIF supply. STAT3 is a critical target of the LIF signaling pathway, which maintains pluripotent cell proliferation. Along with recent reports showing that dominant-negative forms of STAT3 lead to differentiation of ES cells (Boeuf et al., 1997; Niwa et al., 1998), our findings indicate that STAT3 activation is required for self-renewal of ES cells. In addition to the requirement of STAT3 activation, we showed further that STAT3 activation is sufficient to maintain the undifferentiated state of ES cells (at

least in the presence of fetal calf serum (FCS)), determined using a conditionally active form of STAT3. This is apparently the first report demonstrating the sufficiency of STAT3 activation in differentiation-suppression signaling.

Compared with normal cells and tissues, constitutively activated STATs have been detected in a wide variety of human cancer cell lines and primary tumors (Buettner et al., 2002). STATs are activated by tyrosine phosphorylation, which is normally a transient and tightly regulated process. In tumor cells, constitutive activation of STATs is linked to persistent activity of tyrosine kinases, including Src, epidermal growth factor receptor, Janus kinases, Bcr-Abl and many others (Buettner et al., 2002). Such oncogenic tyrosine kinases are often activated as a consequence of permanent ligand/receptor engagement in autocrine or paracrine cytokine and growth factor signaling. Autonomous constitutively active enzymes were represented as a result of genetic alterations found in tumor but not in normal cells. Persistent signaling of specific STATs, in particular Stat3 and Stat5, has been demonstrated directly to contribute to oncogenesis by stimulating cell proliferation and preventing apoptosis. STATs participate in oncogenesis through up-regulation of genes encoding apoptosis inhibitors and cell cycle regulators such as *Bcl-X_L*, *Mcl-1*, *Cyclins D1/D2* and *c-Myc* (Buettner et al., 2002). These results demonstrate that *Piwil2* independently targets two important cellular signaling pathways, *Stat3/Bcl-X*, and therefore can act as an oncogenic factor in tumorigenesis of different tissues. Block of constitutive Stat3 signaling results in growth inhibition and apoptosis of Stat3-positive tumor cells in vitro and in vivo. The observation that diminished Stat3 expression is associated with oncogenesis, suggests that the Stat3 signaling pathway is a potential therapeutic target in cancer.

Association of *Piwil2* expression and expression of *Stat3*, *Bcl-X_L*, *Cyclin D1* and *Akt* was demonstrated in testicular germ cell tumor cell lines, Tera-1 (Fig. 3.17), GC-1 (Fig. 3.20) and mouse breast tumor tissue (Fig. 3.17). In Tera-1 cells, an association was found between elevated *Piwil2* expression and increased expression of *Stat3*, *Bcl-X_L*, *Cyclin D1* and *Akt*, whereas in mouse breast tumor, this association was found only with *Stat3* and *Cyclin D1*, but not with *Bcl-X_L*. This indicates that *Piwil2* acts through different signaling pathways in tumors with epithelial and stromal origins. Interestingly, while there are differences between *Piwil2* expression and expression of *Bcl-X_L*, *Cyclin D1* and *Akt* in stromal cell line NIH3T3 (Fig. 3.16) and epithelial tumors (Fig. 3.17 and 3.20), no

differences were observed between elevated Piwil2 expression and increased Stat3 expression in stromal and epithelial derived tumors and cancer cell lines. These findings suggest that elevated levels of Piwil2 activity and consequently Stat3 expression in tumor cells are key factors in promoting the survival of tumor cells and determining their response to chemotherapy.

In order to examine whether other signaling pathways are also involved in *Piwil2*-mediated increase of *Bcl-X_L* and *Cyclin D1*, we investigated changes in expression level of *Stat2*, *RelA*, *Ets2* and *NFkB2* in NIH3T3 cells expressing constitutively *Piwil2*. All these proteins are known as regulatory factors of *Bcl-X_L* and *Cyclin D1* (Sevilla et al., 1999; Chen et al., 2000; Calo et al., 2003). A slight increase in *Stat2* expression and a slight reduction in expression of *RelA* and *NFkB2* were observed. No change in expression level of Ets2 was obtained. These results indicate that *Stat2*, *RelA*, *Ets2* and *NFkB2* are not mainly involved in *Piwil2*-mediated regulation of *Bcl-X_L* and *Cyclin D1* in NIH3T3-pcDNA-*Piwil2* cells.

In order to examine whether direct inhibition of activated Stat3 signaling with siRNA of *Piwil2* inhibits *Stat3*, *Bcl-X_L* and *Cyclin D1* expression. Moreover, blockade of constitutively active *Piwil2* expression by siRNA of *Piwil2* induces apoptosis, which is consistent with the critical role of *Piwil2*-mediated *Stat3* and *Bcl-X_L* expression is correlated with GC-1 cell and MDA-MB-231 cell lines survival.

This conclusion is further strengthened by our finding that inhibition of *Piwil2* and downstream *Stat3* expression induces apoptosis in mouse transformed germ cell line and human breast cancer cell line harboring constitutively active Stat3. Therefore, small molecule inhibitors of *Stat3* and *Piwil2* could be used in combination with conventional chemotherapy or with other signal transduction blockers for increased therapeutic benefits in breast cancer patients.

4.1.3 PPD (PAZ Piwi domain) proteins and development

The question to be discussed is how Piwil2 regulates expression of the genes which are involved in apoptosis and proliferation, especially in *Piwil2/Bcl-X_L* pathway. Piwil2

belongs to the PPD (PAZ Piwi domain) proteins. These proteins have well established roles in RNAi (RNA interference) metabolism. RNAi is a process utilized by eukaryotes to modulate gene expression at pre- and post-transcriptional levels (Hannon, 2002). The Piwi domain, comprising approx. 300 amino acids, has been shown to mediate the interaction of PPD proteins with Dicer (Doi et al., 2003). Recent structural and bioinformatic analyses suggest that Piwi domains share similarity with endonucleases, an observation that led to the discovery that PPD proteins are directly involved in cleavage of targeted mRNAs during the effector stage of RNAi (Song et al., 2004).

In vertebrates, PPD proteins appear to be important for regulating multiple developmental pathways, and certain family members are highly expressed in undifferentiated cells and germline stem cells. Similarly, *Piwil2* is preferentially expressed in germ cells and is essential for spermatogenesis in mice. Interestingly, *Piwil2−/−* strains of mice resemble *MVH−/−* (Mouse Vasa Homolog) strains in that they are developmentally normal, but are sterile owing to arrest of spermatogenesis at the spermatocyte stage (Kuramochi-Miyagawa et al., 2001). *MVH* is the mammalian homologue of *Vasa*, an ATP-dependent DEAD-box RNA helicase that was previously found to colocalize with the PPD protein Aub in germline-specific granules (Findley et al., 2003) and in a RISC-like complex (Caudy et al., 2002). Expression and localization of *Vasa* mRNA is an important determinant of germline fate commitment (Yoon et al., 1997; Knaut et al., 2000). Accordingly, since Piwil2 associates with MVH, it is likely that these two proteins function together as a complex that regulates cell differentiation. Finally, mouse *Ago2* was demonstrated recently to play a critical role in embryogenesis. Targeted disruption of the *ago2* gene results in embryonic lethality owing to multiple developmental abnormalities, the most severe of which are defects in neural tube closure and cardiac failure (Liu et al., 2004). Taken together, these data suggest that it is not only the level of expression and/or activity of PPD family members, but also their intracellular localization that dictates specific developmental processes.

Accordingly, it seems likely that the majority of the developmental defects exhibited by PPD mutants results from aberrant expression of transcription factors that determine cell fate. However, it is important to consider the possibility that at least some of the developmental roles of PPD proteins are unrelated to gene silencing. In *A. thaliana*, for

instance, some allelic mutants of *ago1* are defective for RNAi, but are developmentally normal (Morel et al., 2002). This study indicates that the gene-silencing functions of PPD proteins can be genetically uncoupled from their roles in development.

D. melanogaster has also served as an excellent experimental system to study the roles of PPD proteins in signaling pathways that control cell fate and developmental patterning. For example, *dAGO1* was isolated in a genetic screen for dominant activators of the *Wingless* signal transduction pathway (Kataoka et al., 2001). Moreover, the phenotypes of *piwi* mutants can be rescued by overexpression of *Hedgehog*, a secreted signaling protein that is not implicated in RNAi (King et al., 2001). Of course, these results do not discount the possibility that *Wingless* and *Hedgehog* function downstream of *dAgo1* and *Piwi*, respectively. In this case, overexpression of *Hedgehog* may simply bypass the need for *Piwi* at an upstream miRNA (microRNA)-dependent step.

The mechanisms by which PPD proteins mediate translational suppression and chromatin silencing are not known at this time. Accordingly, it is possible that overexpression of *Piwil2* activates endogenous RNAi machinery which induces indirectly expression of *Stat3/Bcl-X_L*.

4.1.4 *Piwil2* Inhibits apoptosis and stimulates cell proliferation

Another interesting observation is the increase of *Piwil2* expression in proliferating cells (Fig. 3.9 and 3.27). It is not hard to imagine how Piwil2 may indirectly affect cell-cycle progression through its involvement in gene-silencing pathways that regulate expression of transcription factors like Stat3. It has recently become evident that PPD proteins and Dicer also function in siRNA-independent pathways that regulate cell cycle events (Carmichael et al., 2004). Accordingly, it is important to consider the aberrant expression of PPD proteins and Dicer in human cancers. We observed a difference between NIH3T3-pcDNA-*Piwil2* and NIH3T3-pcDNA cells, when we started from 9500 cells per well. This suggested that the role of cell-cell interaction in *Piwil2* mediated cell proliferation, because the possibility for cells to form aggregates is greater with this starting cell number (Fig. 3.25).

Of particular significance is the observation that seminoma tumors are often associated with increased levels of *Hiwi* mRNA (Qiao et al., 2002). Coincidentally, *Hiwi* was first reported as a gene that is expressed in undifferentiated haematopoietic stem cells, but not in differentiated cells (Sharma et al., 2001). Likewise, expression of the *D. melanogaster* orthologue of *Piwi*, has previously been reported to promote mitosis in stem cells (Cox et al., 2000). In addition, the chromosomal locus 12q24.33 that includes the *Hiwi* gene has been linked to testicular germ cell tumors (Summersgill et al., 2001). Together, these observations are consistent with a scenario in which overexpression of certain PPD proteins like Piwil2 is associated with increased mitosis in undifferentiated cells. The role of other PPD protein family members in this process is less clear.

Antisense RNA and DNA techniques have been developed as an approach to modulate gene expression in vitro and in vivo (Neckers et al., 1993). RNA interference (RNAi) can reduce target gene expression in mammalian cells and is widely used for functional studies of novel genes (Elbashir et al., 2002; Hannon et al., 2002). Here we report that the use of siRNA *Piwil2* reduced successfully *Piwil2* expression in GC-1 and MDA-MB-231 cell lines and thus induced an increase of apoptosis in siRNA *Piwil2* treated cells. These findings may indicate that *Piwil2* is essential for the proliferation of cancer cells.Our results demonstrate that *Piwil2* inhibits apoptosis and stimulates proliferation through activation of *Stat3*/*Bcl-*X_L and enhancement of *Stat3*/*Cyclin D1* signaling pathways (Fig.4.2). Inhibition of constitutively signaling pathways by repression of *Piwil2* expression can inhibit tumor cell growth in vitro and provides a novel mean for therapeutic intervention in human cancer. Furthermore, specific expression of *Piwil2* in testis and its aberrant expression in various tumors make this molecule an attractive candidate as a cancer prognostic and diagnostic marker.

In summary, the present data report for the first time, that *Piwil2* is overexpressed in cancer cell lines and cancer tissues, consistent with precancerous development. Furthermore, the downregulation of endogenous *Piwil2* by siRNA effectively inhibits the proliferation of cancer cells (GC-1, MDA-MB-231) and induces apoptosis. These results suggest that *Piwil2* may play an important role in the development of cancer and is a potential target for cancer biotherapy.

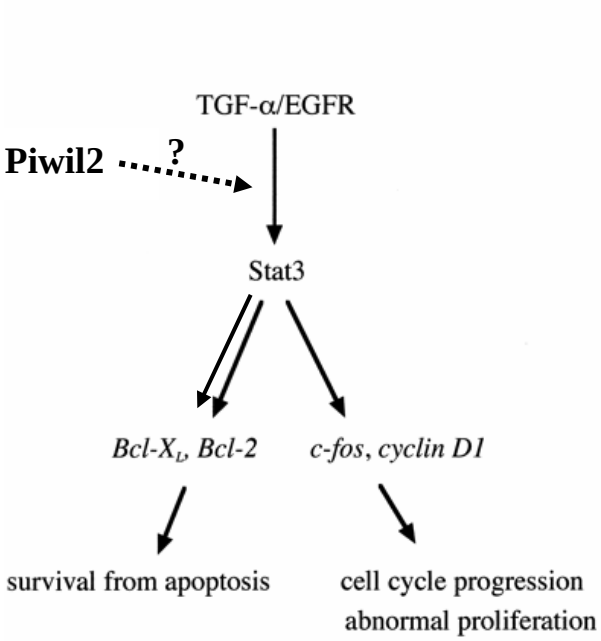

Figure 4.2: A hypothetical mechanism by which Piwil2 induces growth and inhibits apoptosis. The Piwil2 activates Stat3, thus leading to activation of the Stat3 pathways. Activated Stat3 signals induce strongly Bcl-X_L and Bcl-2 pathway and slightly Cyclin D1 pathway; therefore, tumor growth is enhanced and/or normal cells can be transformed to malignant cells. Piwil2 is involved in these signal transduction pathways and thereby inhibits G_1 arrest and apoptosis (adapted by Masuda et al., 2001).

4.2 Spermatogenesis arrest in *Piwil2* overexpressing mice

4.2 1 Aberrant spermatogenesis in *Piwil2* transgenic mice

Spermatogenesis is the differentiation process of male germ cells to produce mature spermatozoa and is divided into three distinct stages: the mitotic proliferation of spermatogonial stem cells, meiotic division of spermatocytes and differentiation of haploid spermatids (Zirkin, 1993). In mice, the proliferation of spermatogonia occurs soon after birth, at around 5 days post-partum (dpp) and this is followed by the first wave of spermatogenic differentiation, which gives rise to primary spermatocytes at around 10 dpp, to haploid round spermatids at 20 dpp and to mature spermatozoa at 35 dpp (Bellve et al., 1977 ; Zhao et al., 2002). This differentiation takes place in the seminiferous tubules, in which spermatogonia and Sertoli cells sit on the basement membrane, with spermatocytes, spermatids and mature spermatozoa facing the lumen (Fig. 4.3 A and B). Through the continuous proliferation of spermatogonia and subsequent differentiation, functional spermatozoa are produced throughout male life. Studies of genes that regulate spermatogenesis are being carried out mostly via the production and analysis of mutant mice carrying transgenes or targeted gene disruptions (Escalier, 1999).

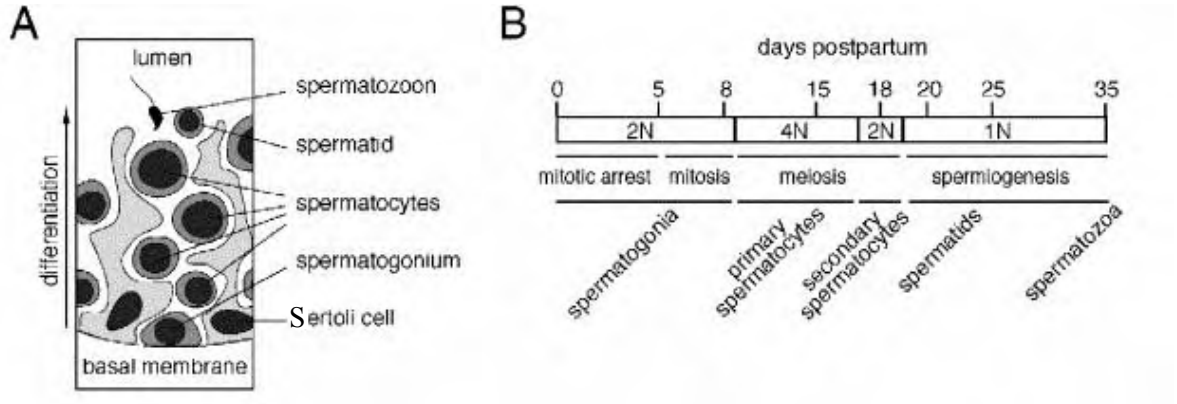

Figure 4.3: Spermatogenesis in vivo. (A) Schematic representation of spermatogenesis in mouse seminiferous tubule. (B) Differentiation time course of the first wave of spermatogenesis (adapted by Masanobu et al., 2005).

We have generated transgenic mice which ectopically express the *Piwil2* transgene in germ cells. The *hEF-1α*/*Piwil2* fusion gene in these mice was highly expressed in testis but not detected in other examined tissues. Although only one line of *Piwil2* transgenic mice has been analysed in the present report, several data support the assumption that the spermatogenic disorder is caused by *Piwil2* overexpression rather than by an insertional mutation. First, another independent transgenic line showed similar pattern of expression. Second, it has been demonstrated that *Piwil2* transgenic line presented reduced fertility. Third, *Piwil2* expression was shown stronger in *Piwil2* transgenic mice than in wild type mice. Fourth, the transgenic Piwil2 protein accumulated in the pachytene spermatocytes in the most afflicted tubules. Fifth, EGFP signals were observed only in *Piwil2* transgenic mice. Although the *EF-1α* gene is normally expressed in most tissues (Uetsuki et al., 1989; Mizushima et al., 1990) and the regulatory region of the gene which was used for the transgene construct can direct strong expression in various cultured cells (Mizushima et al., 1990), the truncated regulatory region apparently activates transcription preferentially in germ cells in a physiological context.

In fact, the presence of the Piwil2 protein in pachytene spermatocytes and metaphase cells in *Piwil2* transgenic mice and their accumulation in those tubules presenting arrest of spermatogenesis suggest that the excess of *Piwil2* causes meiotic arrest and cellular degeneration. Nevertheless, the parallel increase of the endogenous *Piwil2* in transgenic mice raises the possibility that the exogenous Piwil2 protein is not active in mice and could antagonize the effect of the endogenous protein. Thus, it might be the lack rather than the excess of *Piwil2* that is responsible for the interruption of spermatogenesis.

The *Piwil2* transgene was found to be arrested in round spermatids and expressed in pachytene spermatocytes in seminiferous tubules under the *hEF-1α* promoter. Although the latter finding confirms to the inducibility of *Piwil2* gene under the *hEF-1α* promoter, the arrest in round spermatids is somewhat surprising.

To our knowledge, the presented results of the *Piwil2* transcriptional activity studies suggest that the regulation of *Piwil2* is more complex than previously supposed. Interestingly, the infertility of Piwil2 mice is probably due to effects of *Piwil2* on the testis. The finding of *Piwil2* in pachytene spermatocytes and spermatogonia suggests that *Piwil2* can act directly on spermatogenic cells. The arrest in the round spermatids, which are only

beginning to elongate, is of particular interest as the observed spermatogenic arrest occurred at this point.

Altogether, our results show that overexpression of *Piwil2* under the *hEF-1α* promoter in the testis of transgenic mice results in infertility. However, the *Piwil2* transgenic mice were fertile until 3-6 months old, whereas the *Piwil2* transgenic mice older than 8 months old never sired any litters. Although the exact functions of *Piwil2* in the male genital tract remain to be elucidated, it is likely to play an important role in male fertility.

The present data are consistent with the interpretation that overexpression of *Piwil2* gene in transgenic mice result in the existence of fertility disturbances, including arrest of spermatogenesis during the second meiotic division and an increase in germ cell degeneration.

4.2.2 Germ cell apoptosis in *Piwil2* transgenic mice

We demonstrated that pachytene spermatocytes and metaphase cells are the most susceptible cells for undergoing apoptosis in *Piwil2* transgenic mice. However, the increase in the number of pachytene spermatocytes and metaphase cells and the decrease in or even the absence of cells at later maturation steps in some tubules suggested the existence of a partial arrest during the first meiotic division. Although 6 months old testes of the transgenic mice seemed to be normal, exogenous *Piwil2* was expressed mainly in spermatogonia and in some spermatocytes (Fig. 3.30 H) and TUNEL positive cells apparently increased (Fig. 3.34 B and D). However, there was a significant number of TUNEL-positive cells in normal testes and some of these cells were spermatogonia, judging from their morphology (Fig. 3.34 A and E). These observations indicate that *Piwil2* ectopically expressed under *hEF-1α* promoter induces apoptosis.

In general, several studies have demonstrated the existence of germ cell apoptosis during normal spermatogenesis (Kerr, 1992; Brinkworth et al., 1995). Spontaneous germ cell loss occurs during the mitotic division of spermatogonia, the meiotic division of spermatocytes and during spermiogenesis. Generally, the fertility disturbances and the abnormal

spermatogenesis observed in several lines of transgenic mice are produced by the gain of specific gene functions regulating spermatogenesis (Huckins, 1978; De Rooij and Lok, 1987; Allan et al., 1992). In particular, the prophase of the first meiotic division and the number of primary spermatocytes entering meiosis seem to be apoptosis regulated (Stephan et al., 1996). During meiosis, as occurs in mitosis, DNA damage is detected at specific checkpoints, providing the cell with a control mechanism that may result in cell cycle arrest (Elledge, 1996; Sassone-Corsi, 1997) and ultimately, in genomic instability and/or cell death (Rubin et al., 1993; King and Cidlowski, 1995). Although most of our knowledge about the genes that control meiosis comes from cell cycle division mutants in yeast (Elledge, 1996; Paulovich et al., 1997); transgenic animals have proven to be a useful tool for studying meiotic regulation in mammals (Reventos and Munell, 1997; Sassone-Corsi, 1997).

Considering that deficiencies in different genes leads to cell death, it might be plausible that a sensitive checking mechanism for differentiation progression operates during spermatogenesis. Thus, it is conceivable that *Piwil2* plays an important role in meiotic prophase. In the *Piwil2*–/– testis, the expression of genes that are involved in spermiogenesis was undetectable (Kuramochi-Miyagawa et al., 2004). The *Dmc1* gene, whose expression is restricted to leptotene and to zygotene stage spermatocytes (Yoshida et al., 1998), was expressed normally in the *Piwil2*–/– testis. By contrast, the expression levels of *Sycp1* and *Sycp3*, both of which are transcribed predominantly in the zygotene to diplotene stages (Meuwissen et al., 1992; Dobson et al., 1994; Lammers et al., 1994), were slightly reduced. *A-myb*, which is expressed in early primary spermatocytes (Mettus et al., 1994; Trauth et al., 1994), showed similar low-level expression. To summarize, these results suggest that spermatogenesis in *Piwil2*–/– mice are arrested from the zygotene to early pachytene stages.

We could not obtain evidence for tumor in *Piwil2* transgenic mice. Our findings are consistent with previous studies of the *piwi* gene, (Cox et al., 1998), which indicated that a certain level of somatic *piwi* activity is required to establish or maintain the stem cell identity, but a higher level of somatic *piwi* expression will not increase the number of germ stem cells. These findings may indicate that endogenous *Piwil2* is essential for the proliferation of germ stem cells, but the exogenous *Piwil2* does not significantly influence

proliferation. Sharma et al. reported that overexpression of *Piwil1* in KG1 cells (chronic myeloid cell line) resulted in a marked reduction in cell growth and led to programmed cell death (Sharma et al., 2001). One explanation for this difference is that misexpression of *Piwil2* at a high level in cells lacking endogenous *Piwil2* expression may induce the programmed cell death. This is consistent with previous studies showing that the elevated levels of a gene may perturb the normal development (Hay et al., 1997; Yang et al., 1999) and *hEF-1α* promoter can not strongly drive to overexpress Piwil2 in spermatogonia (Furuchi et al., 1996). Another possible explanation would be that there is a changing genetic background with 129/Sv for proliferation in cells; it might not be sufficient to exert an effect alone on cell proliferation. The advantages of the 129/Sv strain for studying TGCTs include its availability in large numbers, its genetic uniformity, and its short generation time (Lam and Nadeau, 2003). In addition, the normal interaction between Sertoli cells and spermatogonia, which is known to be important for their growth and differentiation (de Franca et al., 1993), may be disrupted in the transgenic mice, and this could lead to abnormal differentiation of spermatogonia. Similarly, Sertoli cells were observed and spermatogenesis was disrupted in *Piwil2* transgenic mice. As described in figure 3.32 B, spermatogenesis was unrecovered in seminiferous tubules in older mice due to increased expression of the exogenous *Piwil2* in the germ cells.

Based on morphological criteria and *in situ* end labeling of DNA fragmentation, pachytene spermatocytes and metaphase-cells appear to be frequently afflicted cell types in transgenic mice (Selva et al., 2000). In *Piwil2* transgenic mice, we demonstrated by *in situ* end labeling of DNA fragmentation that most labeled cells were indeed pachytene spermatocytes and metaphase cells. Although some of these cells apparently looked normal under light microscopic examination, a subset of them exhibited clear evidence of apoptosis, chromatin condensation over the chromosome axes, abnormal disposition of the chromatin and loss of intercellular contacts. Cellular swelling with decondensed chromatin and homogeneous nuclear staining were also evident in our model. The high amount of apparently normal pachytene and metaphase cells labeled for DNA fragmentation does not seem to be the product of nonspecific labeling of the DNA by terminal transferase (Brinkworth et al., 1995). However, when a low concentration of the enzyme was used, almost no labeled cells were found in controls. These cells were most likely cells in an early

stage of degeneration, bearing DNA fragments but still maintaining their overall morphology.

These results lead us to speculate that in *Piwil2* transgenic mice pachytene spermatocytes and metaphase cells of most damaged tubules arrest their differentiation program and degenerate by apoptosis and show the consequence of ectopic expression of *Piwil2* in spermatogonia and pachytene spermatocytes. These results provide evidence that the renewal, differentiation and apoptosis of germ cells are closely correlated and that a pathway affected by *Piwil2* plays a major role in switching the developmental fates of spermatogonia. Our transgenic mice thus provide a model for studying the choice between death and survival in spermatogonia.

4.3 Stem cell protein Piwil2 modulates expression of murine spermatogonial stem cell specific genes

Spermatogenesis depends on stem cells, which have the ability to self-renewal and generation of a large number of differentiated germ cells in most species. In mammals, millions of spermatozoa are produced every day from spermatogonial stem cells (SSCs), the germ-line stem cells in the testis (Russell et al., 1990; Olive and Cuzin, 2005). SSCs are infrequent in the testis, presumably ~1 in 3,000-4,000 cells in adult mouse testis (Olive and Cuzin, 2005). To maintain spermatogenesis, the processes of self-renewal and differentiation of SSCs must be precisely regulated by intrinsic gene expression in the stem cells and extrinsic signals, including soluble factors or adhesion molecules from the surrounding microenvironment, the stem cell niche (Kubota et al., 2004).

It is postulated that piwi proteins may be involved in the development and maintenance of stem cells through the RNA-mediated gene-quelling mechanisms associated with Dicer. Piwi proteins together with the RNA cleavage products of Dicer form ribonucleoprotein complexes called RNA-induced silencing complexes (RISCs). RNA silencing regulates gene expression through mRNA degradation, translation repression and chromatin remodelling. The clear-cut arrest of spermatogenesis at the beginning of spermiogenesis in

Piwil2 mutants suggests that *Piwil2* may play a key role in the initiation of the entire spermatogenesis (Kuramochi-Miyagawa et al., 2004). Normally, spermatogenesis is controlled by both inter- and intracellular mechanisms. Intercellular signaling pathways can eventually influence spermatogenesis through the intracellular regulatory molecules at important control points. These control points are often revealed by clean-arrest phenotypes, as suggested by extensive genetic analysis. (Hartwell et al., 1989).
In order to characterize stem cell-related genes regulated by *Piwil2*, an in vitro gain of function model was established and differentially regulated genes were characterized.

4.3.1 Mouse stem cell array and analysis of differentially expressed genes

By using mouse stem cell gene arrays with isolated total RNA from NIH3T3-pcDNA-*Piwil2* and NIH3T3-pcDNA cells were selected for differentially expressed 4 genes (*Pdgfrb*, *Slc2a1*, *Gja7 and Inta6*) involved in the regulation of stem cell.
We demonstrated that *Piwil2* induces or modulates expression of some stem cell related and spermatogonia markers like *Stra8*, *Hsp90α*, *CD9*, *Pdgfrb*, *Slc2a1*, *Gja7*, *Intgb1*, *Inta6* and *Thy-1*. *Stra8* and *Hsp90α* are spermatogonia markers (Oulad-Abdelghadi et al., 1996; Creemers et al., 2002; Nayernia et al., 2004). During mouse embryogenesis, *Stra8* expression was restricted to the male developing gonads, and in adult mice, the expression of *Stra8* was restricted to the premeiotic germ cells (Oulad-Abdelghadi et al., 1996). *Hsp90α* is highly expressed in PGCs and continues to be expressed in both male and female pre-meiotic germ cells. Induction of *Stra8* and *Hsp90α*, two spermatogonia markers, supports the hypothesis that *Piwil2* is able to differentiate the NIH3T3 cells toward spermatogonia. This hypothesis was substantiated by morphological changes of NIH3T3 cells after *Piwil2* expression. In cells expressing *Piwil2*, many cells with a spermatogonia-like morphology were observed (Fig. 3.39). In addition, we showed that *Piwil2* induces or modulates expression of some stem cell related genes like *Pdgfrb*, *Scl2a1* and *Gja7*.
Platelet-derived growth factors (*PDGF*s) are paracrine growth factors mediating epithelial-mesenchymal interactions and exerting multiple biological activities which include cell

proliferation, motility and differentiation. Expression of *Pdgfrb* was demonstrated in gonocytes, a developmental stage before spermatogonial stem cells (Puglianiello et al., 2004). The *PDGF* alpha-receptor is ubiquitously expressed during differentiation of neural stem cells. In contrast, the *PDGF* beta-receptor is hardly detectable in uncommitted cells, but its expression increases during differentiation. It is suggested that *PDGF* acts as a mitogen in the early phase of stem cell differentiation to expand the pool of immature neurons (Erlandsson et al., 2001). Expression of *Piwil2* in primordial germ cells and gonocytes and activation of *Pdgfrb* by *Piwil2* may play a role in differentiation of gonocytes toward spermatogonial stem cells.

Solute carrier family 2 member 1 (*Slc2a1* or *Glut1*) is believed to play a key role in maintaining basal glucose uptake for metabolism in many cell types. Its expression is detectable throughout preimplantation development from the oocyte through the blastocyst stage and it increases 11-fold in developing embryos from the two-cell stage to the blastocyst (Pantaleon et al., 2001). An increased expression of *Slc2a1/Glut1* in NIH3T3 cells by *Piwil2* revealed the elevated rate of glucose uptake. For other stem cells it was demonstrated that *Glut1* expression is regulated in a very complex manner and *Glut1* would play some important roles in stem cell differentiation (Cai et al., 2004).

Gja7 (Gap junction membrane channel protein alpha 7) belongs to the junction channel proteins. These proteins are macromolecular complexes that allow the direct exchange of small molecules and ions between neighbouring cells (Loewenstein, 1981); thus, these channels have an important role in maintaining homeostasis within tissues. Increased expression of *Gja7* in NIH3T3-pcDNA-*Piwil2* cells and the fact that differentiation of mouse embryonic stem cells is characterized by a sequential upregulation of some channel proteins and connexins (van Kempen et al., 2003) provide another argument for phenotypic changes mediated by Piwil2 protein.

The differential expression of *Pdgfrb*, *Scl2a1* and *Gja7* in NIH3T3-pcDNA-*Piwil2* cells was compared with those in NIH3T3-pcDNA cells. The finding that *Piwil2* modulates *Pdgfrb*, *Scl2a1* and *Gja7* expression provides a potential new therapeutic approach based on SSC differentiation. In this regard, we are currently developing novel downstream targets of *Piwil2* for SSC differentiation. Our results presented here encourage further exploration of the potential therapeutic value of targeting genes through expression of

Piwil2. This approach may have dual benefits for screening markers of SSC differentiation and for characterization of regulated downstream genes by directly inducing *Piwil2*.

4.3.2 Spermatogonial stem cell specific markers are expressed in the *Piwil2* expressing cells

Till now, four cell surface markers, beta1-integrin (*Itgb1*), alpha6-integrin (*Itga6*), *Thy-1* (*CD90*) and *CD9* were identified on the surface of spermatogonial stem cells (Shinohara et al., 1999; Kubato et al., 2003; Kanatsu-shinohora et al., 2004). We found *CD9* and *Itga6* expression in *Piwil2* expressing NIH3T3 cells (Fig. 3.38). Studies have begun to reveal the phenotype of mouse spermatogonial stem cells. Their surface phenotype is side $scatter^{low}$, $\alpha 6\text{-}integrin^{+}$, $\beta 1\text{-}integrin^{+}$, $CD24^{+}$, $thy\text{-}1^{+}$, α5-integrin^{-}, $c\text{-}kit^{-}$ and MHC^{-} (Shinohara et al., 1999; Shinohara et al., 2000; Kubota et al., 2003). These stem cells also express *Oct-4* and *Stra8* (Giuili et al., 2002; Tadokoro et al., 2002). Interestingly, Piwil2 and Stra8 protein expression was detected in about 30% of NIH3T3-pcDNA-*Piwil2* cells. Some of side $scatter^{low}$, $\alpha 6\text{-}integrin^{+}$, $\beta 1\text{-}integrin^{+}$, $CD24^{+}$, $thy\text{-}1^{+}$, α5-integrin^{-}, $c\text{-}kit^{-}$ and MHC^{-} are also expressed on other types of stem cells. For example, *Thy-1* and *ß1-integrin* are expressed on hematopoietic stem cells (Spangrude et al., 1988; Williams et al., 1991) and *Oct-4* and *Itga6* are expressed on ES cells (Xu et al., 2001). However, spermatogonial stem cells are not identical with other stem cells. Hematopoietic stem cells express *Itga4* and *c-kit* (Williams et al., 1991; Ikuta et al., 1992), which are absent on spermatogonial stem cells (Shinohara et al., 1999). *Oct-4*, a marker of ES cells, is not expressed on hematopoietic stem cells (Pesce et al., 2001). Nonetheless, the search for common molecules for different stem cells has facilitated the identification of stem cell surface markers (Shinohara et al., 1999; Kubota et al., 2003).

CD9 can now be added to the list of molecules that are expressed on several types of stem cells. *CD9* is a type III membrane protein with four transmembrane domains and is involved in cell adhesion, migration, proliferation and fusion (Ikeyama et al., 1993; Masellis-Smith et al., 1994; Hadjiargyrou et al., 1995). It is expressed on many types of

cells, including bone marrow, brain and muscle cells (Ikeyama et al., 1993; Masellis-Smith et al., 1994; Hadjiargyrou et al., 1995). It is also expressed on oocytes and plays an important role in fertilization; disruption of the *CD9* molecule by gene targeting results in female infertility (Miyado et al., 2000). *CD9* associates with integrins, including *ß1-* and *α6-integrin* (Park et la., 2000), and it may play a role in signal transduction and in regulating cellular adhesion (Wright et al., 1994). As these integrin molecules are involved in the binding of cells to the basement membrane, this complex of molecules may be expressed on spermatogonial stem cells and may regulate cell adhesion. In a previous study, the addition of leukemia inhibitory factor (LIF) or STAT3 was found to result in CD9 expression in ES cells, which indicates that the LIF/STAT3 pathway is critical for maintaining CD9 expression. The LIF/STAT3 pathway is essential for maintaining the undifferentiated state of ES cells (Niwa et al., 1998; Matsuda et al., 1999). A weak CD9 expression was detected in *Piwil2* expressing NIH3T3 cells (Fig. 3.38).

An increase of Itga6 expression and a slight change in expression of *Itgb1* was observed in NIH3T3-pcDNA-*Piwil2* cells. Testicular germ cells selected by anti-*α* 6-integrin antibody appeared to be twice as effective in stem cell activity as those selected by anti-ß1-integrin antibody (Shinohara et al., 1999). Integrins are heterodimeric transmembrane receptors consisting of one *α* and one ß subunit. The two subunits collaborate to bind ligands, which are extracellular matrix proteins or counter-receptors of the Ig superfamily. It was reported that the stem cell or progenitor cell populations of other self-renewing tissues express also integrin molecules. For example, extracellular matrix receptors of the integrin family have been identified as important regulators of epidermal homeostasis, influencing the balance between stem cell renewal and differentiation (Watt, 2002).

Thy-1 (*CD90*) is a glycoprotein of the immunoglobin superfamily, which is expressed in a variety of stem cells, including mouse SSCs (Goldschneider et al., 1978; Beech et al., 1983; Sprangrude et al., 1988; Baum et al., 1992; Ling and Neben, 1997; Jiang et al., 2002; Kubota et al., 2003). By flow cytometric analysis and the testicular transplantation assay, it was demonstrated that *Thy-1* is a unique surface marker of SSCs in neonatal pup and in adult testes of wild type mouse (Kubota et al., 2004). Increased expression of two stem cell surface markers, *Thy-1* and *Itga6*, supports again the hypothesis that Piwil2 protein is able to induce normal NIHT3T cells towards cells with stem cell-like characters.

Taken together, our data suggest a crucial role of stem cell protein Piwil2 in regulation or modulation of other stem cell proteins which are involved in proliferation (*Pdgfrb*), energy metabolism (*Slc2a1*), cell adhesion (*Intga6*) and cell signaling (*Thy-1*). These findings suggest that *Piwil2* modulates cells towards cells with spermatogonial stem cell phenotype.
Therefore, immunological separation using surface antigenic properties (anti-Thy-1, CD-9, Stra8, Hsp90 antibody) is a major approach for enrichment of SSCs. These cells selected by using anti-piwil2 and anti-Itga6 antibody can be useful to determine the degree of enrichment by using flow cytometric analysis.
In our future works, to obtain a pure or highly enriched stem cell population, it is critical to identify unique markers that are expressed on SSCs because the antigenic profile of SSCs establishes the basis for selective separation. Particularly, identification of markers that are expressed uniquely on SSCs, but not on other somatic cells or differentiated spermatogenic cells, facilitates enrichment of SSCs. It is also important to notice that expression of spermatogonial stem cell markers is conserved during development, indicating possible association with biological properties of the SSCs.
In conclusion, the present data report for the first time, that the expression of *Piwil2* is specifically restricted to testes of mouse and human. However, *Piwil2* expression was highly detected in various cancer cell lines and cancer tissues of mouse and human. The correlation between *Piwil2* expression and the germline property is also supported by the finding that *Piwil2* is only overexpressed in seminomas, but not in nonseminomas or in somatic tumors of the adult testis in human. Nonseminomas do not show enhanced *Piwil2* expression because these tumors have lost their germline properties, even though they also originate from the same precursor cells as seminomas. The expression of *Piwil2* ectopically in fibroblast mouse cells supports the hypothesis that *Piwil2* expression is highly upregulated by the *Stat3*/*Bcl-*X_L signaling pathway. Furthermore, we investigated the role of *Piwil2* in cell metabolism using siRNA of *Piwil2* in mouse spermatogonia tumor cells and human breast cancer cells. Candidate *Piwil2*-regulated genes were found to be involved in preventing apoptosis of mouse tumor germ cells and human breast cancer cells. Among the genes of which expression changed on silencing *Piwil2* is *Stat3*/*Bcl-*X_L, an antiapoptotic genes. Stat3 proteins are persistently activated in breast cancer and promote tumor cell survival (Gritsko et al., 2006).

By contrast, dramatic overexpression of *Stat3* has been shown in antiapoptotic cells, in which *Piwil2* was not expressed. Our results provide first finding that *Piwil2* directly regulates the *Stat3* expression. Notably, *Stat3* expression in antiapoptotic cells is significantly correlated with decreased *Piwil2* expression in GC-1 and MDA-MB-231 cells and our findings presented here indicate that *Piwil2* expression in NIH3T3-pcDNA-*Piwil2* cells induces *Stat3*/*Bcl-*X_L expression and increases proliferation. Thereby apoptosis is prevented.

Piwil2 transgenic mice that are homozygous for this targeted allele are viable, normal in size and do not display any severe physical abnormalities. Homozygous males are subfertile and have smaller testes than wild type controls. Decreased numbers of sperms are produced in response to degenerated spematocytes. The testes of the *Piwil2* transgenic mice exhibit round spermatid arrest and spermatogenesis looks apparently normal up till round spermatids. Histological analysis and TUNEL assay for apoptotic cells in *Piwil2* testis showed an increase of apoptosis compared with wild type.

We have confirmed *Piwil2* expression in SSCs and shown that alpha6-integrin (*Itga6*), *Thy-1* (*CD90*), *Stra8*, *Hsp90* and *CD9* antibodies can be used to obtain enriched fractions of SSCs by MACS. Our results indicate the existence of a distinct subpopulation of SSCs in the mouse pup testis that expresses a higher level of alpha6-integrin (*Itga6*), *Thy-1* (*CD90*), *Stra8*, *Hsp90* and *CD9*. This subpopulation is also positive for the pluripotency marker *Piwil2*. It will be interesting in future studies to confirm the existence of subpopulations of SSCs that maintain different degrees of developmental potential.

4.4 Future studies

In further studies, we were going to challenge the cells by transplanting Piwil2 expressing NIH3T3 cells into a recipient mouse testis or we might look whether they can repopulate the epithelium after a moderate dose of irradiation to observe a stem cell defect.

Likewise, in order to determine the role of *Piwil2* in ES cells, we will design a construct in which *Piwil2* is ubiquitously expressed under the human CMV promoter. Reported data together with our data (data not shown) in the present study shows that *Piwil2* is not expressed in ES cells but expressed in primordial germ cells (PGC). For example, it is a good approach to characterize or to identify regulated genes in Piwil2 expressing ES cells by using microarray. We have a keen interest in the specification of germ cells during early development and the establishment of methods to derive such cells from an embryonic stem cell starting point by using PIWIL2 marker protein.

Our future projects also involve determination of important genes and factors of proliferation for mouse germ cell cancer cells and human breast cancer cells with *Piwil2* RNA interference strategies. To do experiments, stable cell lines (MDA-MB-231, GC-1) will be established by using Tet-on system. Later, these approaches follow the injection in nude mice and these are therapeutically helpful to elucidate cancer mechanism (so called, cancer therapy).

Piwil1 (*hiwi*), a novel human homologue of *piwi*, was also found to be present in human CD34(+) hematopoietic progenitor cells but not in more differentiated cell populations (Sharma et al., 2001). We wonder whether *Piwil2* is also expressed in normal blood and patient blood. To check our proposal, a specific antibody has to be generated against Piwil2 to be investigated by the immunofluorescence study, ELISA and RT-PCR analysis. *Piwil2* regulates the proliferation and apoptosis in vivo and in vitro.

The genetic control of TGCT susceptibility in 129/Sv mice is complex. Crosses between 129/Sv and other inbred strains revealed only one affected individual in ~11000 males (Stevens, 1967), suggesting that many genes with low penetrance are involved in TGCT development. Spontaneous and engineered mutations in genes on the 129/Sv inbred background have found to increase the frequency of spontaneous TGCTs (Stevens, 1967; Stevens, 1973; Jiang et al., 2001), either by increasing the penetrance of TGCT

susceptibility genes, or by reducing the number of 129-derived alleles required for tumorigenesis, or both (Matin et al., 2002).

Therefore, we try to breed *Piwil2* transgenic mice with other background strains (129/Sv) to obtain more severe phenotype of *Piwil2* transgenic mice.

5. SUMMARY

In this work, the role of *Piwil2* gene in turmorigenesis and germline stem cell metabolisms was investigated.

The genes of the *piwi* family are defined by conserved PAZ and Piwi domains and play important roles in stem cell self-renewal, RNA silencing and translational regulation in various organisms. Both, mouse and human *Piwil2* genes, members of the *piwi* gene family, are specifically expressed in testis. We report here enhanced expression of the human *Piwil2* gene in testicular seminomas, but not in testicular nonseminomatous tumors. Expression of the *Piwil2* gene was also found in different examined tumors, including prostate, breast, gastrointestinal, ovarian and endometrial cancer of human and in breast tumors, rhabdomyosarcoma and medulloblastoma of mouse. Therefore, *Piwil2* can be categorized as a novel member of cancer/testis antigens. To identify genes activated by *Piwil2*, RNA isolated from NIH3T3 cells expressing constitutively *Piwil2* was compared with RNA samples from control NIH3T3 cells using a cancer gene array. Induction of high level expression of the antiapoptotic gene *Bcl-X_L* was observed in cells expressing *Piwil2*. Furthermore, increased *Bcl-X_L* expression correlated with an increase of signal transducer and activator of transcription 3 (*Stat3*) expression. Gene silencing of *Piwil2* with its siRNA (small interference RNA) suppressed *Stat3* and *Bcl-X_L* expression and induced apoptosis. A causal link between *Piwil2* expression and inhibition of apoptosis and enhanced proliferation was demonstrated in cells expressing *Piwil2*. Furthermore, results of a soft agar assay indicated that *Piwil2* overexpression induced transformation of fibroblast cells. In summary, our results demonstrate that *Piwil2* is widely expressed in tumors and acts as an oncogene by inhibition of apoptosis and promotion of proliferation via Stat3/Bcl-X_L signalling pathway. Expression of *Piwil2* in a wide variety of tumors could be a useful prognostic factor that could have also diagnostic and therapeutic implications.

In this study, we were attempting to determine putative functions for *Piwil2* in vivo. To address functions of *Piwil2*, a transgenic mouse was generated under the testis-specific *human elongation factor-1α* (*EF-1α*) promoter. *Piwil2* transgenic mice who are

homozygous for this targeted allele are viable, normal in size and do not display any gross physical abnormalities. Homozygous males were subfertile, producing smaller testes than wild type controls. Decreased numbers of sperms were also produced in response to degenerated spematocytes. The testis of the transgenic mice exhibited round spermatid arrest and spermatogenesis looked apparently normal up till round spermatids. This arrest did not result from a massive apoptosis of the cells but in some tubules the arrest appeared somewhat sooner than in others. Some clumps were observed and some of them (single cells and clumps) were detected in apoptosis. Germ cells seem to lie rather loose near the lumen and many of them just get sloughed off and disappear via the lumen. Presumably, we guess that round spermatids will be detected in the epididymis of these mice. In Histological analysis and TUNEL assay for apoptotic cells, *Piwil2* transgenic testes showed an increase of apoptosis compared with wild type. In conclusion, a complete arrest was shown at the level of round spermatids, the acrosomic granules coalesce at the point and start to form an acrosomic cap.

Piwil2, known also as *Mili* gene, is one of three mouse homologues of *piwi*. *Piwil2* was found in germ cells of adult testis, suggesting that this gene functions in spermatogonial stem cell self-renewal. In order to find molecular mechanisms underlying stem cell activity mediated by *Piwil2* gene, an in vitro gain of function cell culture model was established. Messenger RNAs isolated from cells expressing *Piwil2* and mRNAs isolated from cells without *Piwil2* expression were compared using a stem cell array technique. It was shown that *Piwil2* modulates expression of stem cell specific genes, including *Pdgfrb* (Platelet derived growth factor receptor, beta polypeptide), *Slc2a1* (Solute carrier family 2 member 1), *Gja7* (Gap junction membrane channel protein alpha 7) and spermatogonial cell surface markers *Thy-1* (*CD90*), *Itga6* (Integrin alpha 6), *CD9* and spermatogonia specific markers *Hsp90α* (Heat shock protein 90 alpha) and *Stra8* (Stimulated by retinoic acid gene 8). These molecules play essential roles in stem cells proliferation (*Pdgfrb*), energy metabolism (*Slc2a1*), cell adhesion, cell-cell interaction (*Itga6*, *Gja7*, *Thy-1* and *CD9*) and germ cell differentiation (*Stra8*). The expression of these markers in spermatogonial stem cells and other non-germinal stem cells suggests that these cells share elements of common

molecular machinery with stem cells in other tissues which are modulated by stem cell protein Piwil2.

6. REFERENCES

Al-Hajj, M., Becker, M.W., Wicha, M., Weissman, I., and Clarke, M.F. (2004). Therapeutic implications of cancer stem cells. *Curr Opin Genet Dev* **14**: 43-7.

Allan, D.J., Harmon, B.V., and Roberts, S.A. (1992). Spermatogonial apoptosis has three morphologically recognizable phases and shows no circadian rhythm during normal spermatogenesis in the rat. *Cell Prolif* **25**: 241-50.

Baum, C.M., Weissman, I.L., Tsukamoto, A.S., Buckle, A.M., and Peault, B. (1992). Isolation of a candidate human hematopoietic stem-cell population. *Proc Natl Acad Sci U S A* **89**: 2804-8.

Beech, J.N., Morris, R.J., and Raisman, G. (1983). Density of Thy-1 on axonal membrane of different rat nerves. *J Neurochem* **41**: 411-7.

Bellve, A.R., Cavicchia, J.C., Millette, C.F., O'Brien, D.A., Bhatnagar, Y.M., and Dym, M. (1977). Spermatogenic cells of the prepubertal mouse. Isolation and morphological characterization. *J Cell Bio* **74**: 68-85.

Bishop, G.A. (1998). Brainstem origin of corticotropin-releasing factor afferents to the nucleus interpositus anterior of the cat. *J Chem Neuroanat* **15**: 143-53.

Boeuf, H., Hauss, H., De Graeve, F., Baran, N., and Kedinger, N. (1997). Leukemia inhibitory factor-dependent transcriptional activation in embryonic stem cells. *J Cell Biol* **138**: 1207-17.

Bohmert, K., Camus, I., Bellini, C., Bouchez, D., Caboche, M., and Benning, C. (1998). AGO1 defines a novel locus of Arabidopsis controlling leaf development. *EMBO J* **17**: 170-80.

Bradford, M.M. (1976). A rapid and sensitive method for the quantitation of microgram quantities of protein utilizing the principle of protein-dye binding. *Anal Biochem* **72**: 248-54.

Brinkworth, M.H., Weinbauer, G.F., Schlatt, S., and Nieschlag, E. (1995). Identification of male germ cells undergoing apoptosis in adult rats. *J Reprod Fertil* **105**: 25-33.

Buettner, R., Mora, L.B., and Jove, R. (2002). Activated STAT signaling in human tumors provides novel molecular targets for therapeutic intervention. *Clin Cancer Res* **8**: 945-54.

Cai, J., Cheng, A., Luo, Y., Lu, C., Mattson, M.P., Rao, M.S., and Furukawa, K. (2004). Membrane properties of rat embryonic multipotent neural stem cells. *J Neurochem* **88**: 212-26.

Calin, G.A., Dumitru, C.D., Shimizu, M., Bichi, R., Zupo, S., Noch, E., Aldler, H., Rattan,

S., Keating, M., and Rai, K. (2002). Frequent deletions and down-regulation of micro-RNA genes miR15 and miR16 at 13q14 in chronic lymphocytic leukemia. *Proc Natl Acad Sci USA* **99**: 15524-29.

Calo, V., Migliavacca, M., Bazan, V., Macaluso, M., Buscemi, M., Gebbia, N., and Russo, A. (2003). STAT proteins: from normal control of cellular events to tumorigenesis. *J Cell Physiol* **197**: 157-68.

Carmell, M., Xuan, Z., Zhang, M., and Hannon, G. (2002). The Argonaute family: tentacles that reach into RNAi, developmental control, stem cell maintenance, and tumorigenesis. *Genes Dev* **16**: 2733-42.

Carmichael, J.B., Provost, P., Ekwall, K., and Hobman, T.C. (2004). ago1 and dcr1, two core components of the RNA interference pathway, functionally diverge from rdp1 in regulating cell cycle events in *Schizosaccharomyces pombe*. *Mol Biol Cell* **15**: 1425-35.

Catalanotto, C., Azzalin, G., Macino, G., and Cogoni, C. (2000). Gene silencing in worms and fungi. *Nature* **404**: 245.

Caudy, A.A., Myers, M., Hannon, G.J., and Hammond, S.M. (2002). Fragile X-related protein and VIG associate with the RNA interference machinery. *Genes Dev* **16**: 2491-6.

Cerutti, L., Mian, N., and Bateman, A. (2000). Domains in gene silencing and cell differentiation proteins: the novel PAZ domain and redefinition of the Piwi domain. *Trends Biochem Sci* **25**: 481-2.

Chalifour, L.E., Fahmy, R., Holder, E.L., Hutchinson, E.W., Osterland, C.K., Schipper, H.M., and Wang, E. (1994). A method for analysis of gene expression patterns. *Anal Biochem* **216**: 299-304.

Chen, C., Edelstein, L.C., and Gelinas, C. (2000). The Rel/NF-kappaB family directly activates expression of the apoptosis inhibitor Bcl-x(L). *Mol Cell Biol* **20**: 2687-95.

Chien, A., Edgar, D.B., and Trela, J.M. (1976). Deoxyribonucleic acid polymerase from the extreme thermophile Thermus aquaticus. *J Bacteriol* **127**: 1550-7.

Chomczynski, P., and Sacchi, N. (1987). Single-step method of RNA isolation by acid guanidinium thiocyanate-phenol-chloroform extraction. *Anal Biochem* **162**: 156-9.

Cogoni, C., and Macino, G. (2000). Post-transcriptional gene silencing across kingdoms. *Curr Opin Genet Dev* **10**: 638-43.

Collins, J.A., Schandi, C.A., Young, K.K., Vesely, J., and Willingham, M.C. (1997). Major DNA fragmentation is a late event in apoptosis. *J Histochem Cytochem* **45**: 923-34.

Costa, G.L., and Weiner, M.P. (1994). Protocols for cloning and analysis of blunt-ended PCR-generated DNA fragments. *PCR Methods Appl* **3**: 95-106.

Cox, D.N., Chao, A., Baker, J., Chang, L., Qiao, D., and Lin, H. (1998). A novel class of evolutionarily conserved genes defined by piwi are essential for stem cell self-renewal. *Genes Dev* **23**: 3715-27.

Cox, D.N., Chao, A., and Lin, H. (2000). Piwi encodes a nucleoplasmic factor whose activity modulates the number and division rate of germline stem cells. *Development* **127**: 503-14.

Creemers, L.B., den Ouden, K., van Pelt, A.M., and de Rooij, D.G. (2002). Maintenance of adult mouse type A spermatogonia in vitro: influence of serum and growth factors and comparison with prepubertal spermatogonial cell culture. *Reproduction* **124**: 791-9.

de Franca, L.R., Ghosh, S., Ye, S.J., and Russell, L.D. (1993). Surface and surface-to-volume relationships of the Sertoli cell during the cycle of the seminiferous epithelium in the rat. *Biol Reprod* **49**: 1215-28.

Denhardt, D.T. (1966). A membrane-filter technique for the detection of complementary DNA. *Biochem Biophys Res Commun* **23**: 641-6.

Deng, W., and Lin, H. (2002). Miwi, a murine homolog of piwi, encodes a cytoplasmic protein essential for spermatogenesis. *Dev Cell* **2**: 819-30.

De Rooij, D.G., and Lok, D. (1987). Regulation of the density of spermatogonia in the seminiferous epithelium of the Chinese hamster. II. Differentiating spermatogonia. *Anat Rec* **217**: 131-6.

Ding, X.Z., Hennig, R., and Adrian, T.E. (2003). Lipoxygenase and cyclooxygenase metabolism: new insights in treatment and chemoprevention of pancreatic cancer. *Mol Cancer* **7**: 2-10.

Dobson, M.J., Pearlman, R.E., Karaiskakis, A., Spyropoulos, B., and Moens, P.B. (1994). Synaptonemal complex proteins: occurrence, epitope mapping and chromosome disjunction. *J Cell Sci* **107**: 2749-60.

Doi, N., Zenno, S., Ueda, R., Ohki-Hamazaki, H., Ui-Tei, K., and Saigo, K. (2003). Short-interfering-RNA-mediated gene silencing in mammalian cells requires dicer and eIF2C translation initiation factors. *Curr Biol* **13**: 41-6.

Dome, J.S., and Coppes, M.J. (2002). Recent advances in Wilms tumor genetics. *Curr Opin Pediatr* **14**: 5-11.

Elbashir, S.M., Lendeckel, W., and Tuschl, T. (2001). RNA interference is mediated by 21- and 22-nucleotide RNAs. *Genes Dev* **15**: 188-200.

Elbashir, S.M., Harborth, J., Weber, K., and Tuschl, T. (2002). Analysis of gene function in somatic mammalian cells using small interfering RNAs. *Methods* **26**: 199-213.

Elledge, S.J. (1996). Cell cycle checkpoints: preventing an identity crisis. *Science* **274**: 1664-71.

Erlandsson, A., Enarsson, M., and Forsberg-Nilsson, K. (2001). Immature neurons from CNS stem cells proliferate in response to platelet-derived growth factor. *J Neurosci* **21**: 3483-91.

Escalier, D. (1999). Mammalian spermatogenesis investigated by genetic engineering. *Histol Histopathol* **14**: 945-58.

Feinberg, A.P., and Vogelstein, B. (1983). A technique for radiolabeling DNA restriction endonuclease fragments to high specific activity. *Anal Biochem* **132**: 6-13.

Findley, S.D., Tamanaha, M., Clegg, N.J., and Ruohola-Baker, H. (2003). Maelstrom, a Drosophila spindle-class gene, encodes a protein that colocalizes with Vasa and RDE1/AGO1 homolog, Aubergine, in nuage. *Development* **130**: 859-71.

Furuchi, T., Masuko, K., Nishimune, Y., Obinata, M., and Matsui, Y. (1996). Inhibition of testicular germ cell apoptosis and differentiation in mice misexpressing Bcl-2 in spermatogonia. *Development* **122**: 1703-19.

Gershoni, J.M., and Palade, G.E. (1982). Electrophoretic transfer of proteins from sodium dodecyl sulfate-polyacrylamide gels to a positively charged membrane filter. *Anal Biochem* **124**: 396-405.

Giuili, G., Tomljenovic, A., Labrecque, N., Oulad-Abdelghani, M., Rassoulzadegan, M., and Cuzin, F. (2002). Murine spermatogonial stem cells: targeted transgene expression and purification in an active state. *EMBO Rep* **3**: 753-9.

Goldschneider, I., Gordon, L.K., and Morris, R.J. (1978). Demonstration of Thy-1 antigen on pluripotent hemopoietic stem cells in the rat. *J Exp Med* **148**: 1351-66.

Gritsko, T., Williams, A., Turkson, J., Kaneko, S., Bowman, T., Huang, M., Nam, S., Eweis, I., Diaz, N., Sullivan, D., Yoder, S., Enkemann, S., Eschrich, S., Lee, J.H., Beam, C.A., Cheng, J., Minton, S., Muro-Cacho, C.A., and Jove, R. (2006). Persistent activation of stat3 signaling induces survivin gene expression and confers resistance to apoptosis in human breast cancer cells. *Clin Cancer Res* **12**: 11-9.

Gunning, W.T., Kramer, P.M., Steele, V.E., and Pereira, M.A.(2002). Chemoprevention by lipoxygenase and leukotriene pathway inhibitors of vinyl carbamate-induced lung tumors in mice. *Cancer Res* **62**: 4199-201.

Hadjiargyrou, M., and Patterson, P.H. (1995). An anti-CD9 monoclonal antibody promotes adhesion and induces proliferation of Schwann cells in vitro. *J Neurosci* **15**: 574-83.

Hannon, G.J. (2002). RNA interference. *Nature* **418**: 244–51.

Hartwell, L.H., and Weinert, T.A. (1989). Checkpoints: controls that ensure the order of cell cycle events. *Science* **246**: 629-34.

Hay, B.A., Maile, R., and Rubin, G.M. (1997). P element insertion-dependent gene activation in the *Drosophila* eye. *Proc Natl Acad Sci* **94:** 5195-200.

Hecht, J.L., and Aster, J.C. (2000). Molecular biology of Burkitt's lymphoma. *J Clin Oncol* **18**: 3707-21.

Hodge, R. (1994). Preparation of RNA gel blots. *Methods Mol Biol* **28**: 49-54.

Huckins, C. (1978). The morphology and kinetics of spermatogonial degeneration in normal adult rats: an analysis using a simplified classification of the germinal epithelium. *Anat Rec* **180**: 905-26.

Hu, G. (1993). DNA polymerase-catalyzed addition of nontemplated extra nucleotides to the 3' end of a DNA fragment. *DNA Cell Biol* **12**: 763-70.

Hutvagner, G., and Zamore, P.D. (2002). RNAi: nature abhors a double-strand. *Curr Opin Genet Dev* **12**: 225-32.

Ikeyama, S., Koyama, M., Yamaoko, M., Sasada, R., and Miyake, M. (1993). Suppression of cell motility and metastasis by transfection with human motility-related protein (MRP/CD9) DNA. *J Exp Med* **177**: 1231-7.

Ikuta, K., and Weissman, I.L. (1992). Evidence that hematopoietic stem cells express mouse c-kit but do not depend on steel factor for their generation. *Proc Natl Acad Sci U S A* **89**: 1502-6.

Jaronczyk, K., Carmichael, J.B., and Hobman, T.C. (2005). Exploring the functions of RNA interference pathway proteins: some functions are more RISCy than others? *Biochem J* **387**: 561-71.

Jiang, L.I., and Nadeau, J.H. (2001). 129/Sv mice-a model system for studying germ cell biology and testicular cancer. *Mamm Genome* **12**: 89-94.

Jiang, Y., Jahagirdar, B.N., Reinhardt, R.L., Schwartz, R.E., Keene, C.D., Ortiz-Gonzalez, X.R., Reyes, M., Lenvik, T., Lund, T., Blackstad, M., Du, J., Aldrich, S., Lisberg, A., Low, W.C., Largaespada, D.A., and Verfaillie, C.M. (2002). Pluripotency of mesenchymal stem cells derived from adult marrow. *Nature* **418**: 41-9.

Jost, M., Huggett, T.M., Kari, C., Boise, L.H., and Rodeck, U. (2001). Epidermal growth factor receptor-dependent control of keratinocyte survival and Bcl-xL expression through a MEK-dependent pathway. *J Biol Chem* **276**: 6320-26.

Kanatsu-Shinohara, M., Toyokuni, S., and Shinohara, T. (2004). CD9 is a surface marker on mouse and rat male germline stem cells. *Biol Reprod* **70**: 70-5.

Kataoka, Y., Takeichi, M., and Uemura, T. (2001). Developmental roles and molecular characterization of a Drosophila homologue of Arabidopsis Argonaute1, the founder of a novel gene superfamily. *Genes Cells* **6**: 313-25.

Kaul, D., and Sikand, K. (2004). Defective RNA-mediated c-myc gene silencing pathway in Burkitt's lymphoma. *Biochem Biophys Res Commun* **313**: 552-4.

Ke, H., Pei, J., Ni, Z., Xia, H., Qi, H., Woods, T., Kelekar, A., and Tao, W. (2004). Putative tumor suppressor Lats2 induces apoptosis through downregulation of Bcl-2 and Bcl-x(L). *Exp Cell Res* **298**: 329-38.

Kennedy, T.J., Chan, C.Y., Ding, X.Z., and Adrian, T.E. (2003). Lipoxygenase inhibitors for the treatment of pancreatic cancer. *Expert Rev Anticancer Ther* **3**: 525-36.

Kerr, J.B. (1992). Spontaneous degeneration of germ cells in normal rat testis: assessment of cell types and frequency during the spermatogenic cycle. *J Reprod Fertil* **95**: 825-30.

King, F.J., Szakmary, A., Cox, D.N., and Lin, H. (2001). Yb modulates the divisions of both germline and somatic stem cells through piwi- and hh-mediated mechanisms in the Drosophila ovary. *Mol Cell* **7**: 497-508.

King, K.L., and Cidlowski, J.A. (1995). Cell cycle and apoptosis: common pathways to life and death. *J Cell Biochem* **58**: 175-180.

Knaut, H., Pelegri, F., Bohmann, K., Schwarz, H., and Nusslein-Volhard, C. (2000). Zebrafish vasa RNA but not its protein is a component of the germ plasm and segregates asymmetrically before germline specification. *J Cell Biol* **149**: 875-88.

Koesters, R., Adams, V., Betts, D., Moos, R., Schmid, M., Siermann, A., Hassam, S., Weitz, S., Lichter, P., Heitz, P.U., von Knebel Doeberitz, and M., Briner, J. (1999). Human eukaryotic initiation factor EIF2C1 gene: cDNA sequence, genomic organization, localization to chromosomal bands 1p34-p35, and expression. *Genomics* **61**: 210-8.

Kubota, H., Avarbock, M.R., and Brinster, R.L. (2003). Spermatogonial stem cells share some, but not all, phenotypic and functional characteristics with other stem cells. *Proc Natl Acad Sci U S A* **100**: 6487-92.

Kubota, H., Avarbock, M.R., and Brinster, R.L. (2004). Growth factors essential for self-renewal and expansion of mouse spermatogonial stem cells. *Proc Natl Acad Sci U S A* **101**: 16489-94.

Kuramochi-Miyagawa, S., Kimura, T., Ijiri, T.W., Isobe, T., Asada, N., Fujita, Y., Ikawa, M., Iwai, N., Okabe, M., Deng, W., Lin, H., Matsuda, Y., and Nakano, T. (2004).

Mili, a mammalian member of piwi family gene, is essential for spermatogenesis. *Development* **4**: 839-49.

Kuramochi-Miyagawa, S., Kimura, T., Yomogida, K., Kuroiwa, A., Tadokoro, Y., Fujita, Y., Sato, M., Matsuda, Y., and Nakano, T. (2001). Two mouse piwi-related genes: miwi and mili. *Mech Dev* **108**: 121-33.

Laemmli, U.K. (1970). Cleavage of structural proteins during the assembly of the head of bacteriophage T4. *Nature* **227**: 680-5.

Laird, P.W., Zijderveld, A., Linders, K., Rudnicki, M.A., Jaenisch, R., and Berns, A. (1991). Simplified mammalian DNA isolation procedure. *Nucleic Acids Res* **19**: 4293.

Lammers, J.H., Offenberg, H.H., van Aalderen, M., Vink, A.C., Dietrich, A.J., and Heyting, C. (1994). The gene encoding a major component of the lateral elements of synaptonemal complexes of the rat is related to X-linked lymphocyte-regulated genes. *Mol Cell Biol* **14**: 1137-46.

Lam, M.Y., and Nadeau, J.H. (2003). Genetic control of susceptibility to spontaneous testicular germ cell tumors in mice. *APMIS* **111**: 184-90.

Lewis, B.P., Shih, I.H., Jones-Rhoades, M.W., Bartel, D.P., and Burge, C.B. (2003). Prediction of mammalian microRNA targets. *Cell* **115**: 787-98.

Ling, V., and Neben, S. (1997). In vitro differentiation of embryonic stem cells: immunophenotypic analysis of cultured embryoid bodies. *J Cell Physiol* **171**: 104-15.

Lin, H. (1998). The self-renewing mechanism of stem cells in the germline. *Curr Opin Cell Biol* **10**: 687-93.

Lin, H., and Spradling, A.C. (1997). A novel group of pumilio mutations affects the asymmetric division of germline stem cells in the Drosophila ovary. *Development* **124**: 2463-76.

Liu, J., Carmell, M.A., Rivas, F.V., Marsden, C.G., Thomson, J.M., Song, J.J., Hammond, S.M., Joshua-Tor, L., and Hannon, G.J. (2004). Argonaute2 is the catalytic engine of mammalian RNAi. *Science* **305**: 1437-41

Loewenstein, W.R. (1981). Junctional intercellular communication: the cell-to-cell membrane channel. *Physiol Rev* **61**: 829-913.

Lynn, K., Fernandez, A., Aida, M., Sedbrook, J., Tasaka, M., Masson, P., and Barton, M.K. (1999). The PINHEAD/ZWILLE gene acts pleiotropically in Arabidopsis development and has overlapping functions with the ARGONAUTE1 gene. *Development* **126**: 469-81.

Ma, J.B., Ye, K., and Patel, D.J. (2004). Structural basis for overhang-specific small interfering RNA recognition by the PAZ domain. *Nature* **429**: 318-22.

Masanobu, S., Shinichiro, C., Kayo, Y., Takashi, M., and Norio, N. (2005). RNA interference during spermatogenesis in mice. *Developmental Biology* **283**: 524-34

Masellis-Smith, A., and Shaw, A.R. (1994). CD9-regulated adhesion: anti-CD9 monoclonal antibody induces pre-B cell adhesion to bone marrow fibroblasts through de novo recognition of fibronectin. *J Immunol* **152**: 2768-77.

Masuda, M., Suzui, M., and Weinstein, I.B. (2001). Effects of epigallocatechin-3-gallate on growth, epidermal growth factor receptor signaling pathways, gene expression, and chemosensitivity in human head and neck squamous cell carcinoma cell lines. *Clin Cancer Res* **7**: 4220-9.

Matin, A., and Nadeau, J.H. (2002), Sensitized polygenic trait analysis. *Trends Genet* **17**: 727-31.

Matsuda, T., Nakamura, T., Nakao, K., Arai, T., Katsuki, M., Heike, T., and Yokota, T. (1999). STAT3 activation is sufficient to maintain an undifferentiated state of mouse embryonic stem cells. *EMBO J* **18**: 4261-19.

Mettus, R.V., Litvin, J., Wali, A., Toscani, A., Latham, K., Hatton, K., and Reddy, E.P. (1994). Murine A-myb: evidence for differential splicing and tissue-specific expression. *Oncogene* **9**: 3077-86.

Meuwissen, R.L., Offenberg, H.H., Dietrich, A.J., Riesewijk, A., van Iersel, M., and Heyting, C. (1992). A coiled-coil related protein specific for synapsed regions of meiotic prophase chromosomes. *EMBO J* **11**: 5091-100.

Miyado, K., Yamada, G., Yamada, S., Hasuwa, H., Nakamura, Y., Ryu, F., Suzuki, K., Kosai, K., Inoue, K., Ogura, A., Okabe, M., and Mekada, E. (2000). Requirement of CD9 on the egg plasma membrane for fertilization. *Science* **287**: 321-4.

Mizushima, S., and Nagata, S. (1990). pEF-BOS, a powerful mammalian expression vector. *Nucleic Acids Res* **18**: 5322.

Morel, J.B., Godon, C., Mourrain, P., Beclin, C., Boutet, S., Feuerbach, F., Proux, F., and Vaucheret, H. (2002). Fertile hypomorphic ARGONAUTE (ago1) mutants impaired in post-transcriptional gene silencing and virus resistance. *Plant Cell* **14**: 629-39.

Moussian, B., Schoof, H., Haecker, A., Jurgens, G., and Laux, T. (1998). Role of the ZWILLE gene in the regulation of central shoot meristem cell fate during Arabidopsis embryogenesis. *EMBO J* **17**: 1799-809.

Nayernia, K., Li, M., Jaroszynski, L., Khusainov, R., Wulf, G., Schwandt, I., Korabiowska, M., Michelmann, H.W., Meinhardt, A., and Engel, W. (2004). Stem cell based

therapeutical approach of male infertility by teratocarcinoma derived germ cells. *Human Molecular Genetics* **13**: 1451-60.

Neckers, L., and Whitesell, L. (1993). Antisense technology: biological utility and practical considerations. *Am J Physiol* **265**: 1-12.

Nicholson, P.W., and Harland, S.J. (1995). Inheritance and testicular cancer. *Br J Cancer* **71**: 421-6.

Niwa, H., Burdon, T., Chambers, I., and Smith, A. (1998). Self-renewal of pluripotent embryonic stem cells is mediated via activation of STAT3. *Genes Dev* **12**: 2048-60.

Olive, V., and Cuzin, F. (2005). The spermatogonial stem cell: from basic knowledge to transgenic technology. *Int J Biochem Cell Biol* **37**: 246-50.

Oulad-Abdelghani, M., Bouillet, P., Decimo, D., Gansmuller, A., Heyberger, S., Dolle, P., Bronner, S., Lutz, Y., and Chambon, P. (1996). Characterization of a premeiotic germ cell-specific cytoplasmic protein encoded by Stra8, a novel retinoic acid-responsive gene. *J Cell Biol* **135**: 469-77

Pantaleon, M., Ryan, J.P., Gi,l M., and Kaye, P.L. (2001). An unusual subcellular localization of GLUT1 and link with metabolism in oocytes and preimplantation mouse embryos. *Biol Reprod* **64**: 1247-54.

Park, K.R., Inoue, T., Ueda, M., Hirano, T., Higuchi, T., Maeda, M., Konishi, I., Fujiwara, H., and Fujii, S. (2000). CD9 is expressed on human endometrial epithelial cells in association with integrins α6, α3 and ß1. *Mol Hum Reprod* **6**: 252-7.

Paulovich, A.G., Toczyski, D.P., and Hartwell, L.H. (1997). When checkpoints fail. *Cell* **88**: 315-21.

Pesce, M., and Schöler, H.R. (2001). Oct-4: gatekeeper in the beginnings of mammalian development. *Stem Cells* **19**: 271-8.

Provost, P., Samuelsson, B., and Radmark, O. (1999). Interaction of 5-lipoxygenase with cellular proteins. *Proc Natl Acad Sci U S A* **96**: 1881-5.

Provost, P., Silverstein, R.A., Dishart, D., Walfridsson, J., Djupedal, I., Kniola, B., Wright, A., Samuelsson, B., Radmark, O., and Ekwall, K. (2002). Dicer is required for chromosome segregation and gene silencing in fission yeast cells. *Proc Natl Acad Sci U S A* **99**: 16648-53.

Puglianiello, A., Campagnolo, L., Farini, D., Cipollone, D., Russo, M.A., and Siracusa, G. (2004). Expression and role of PDGF-BB and PDGFR-beta during testis morphogenesis in the mouse embryo. *J Cell Sci* **117**: 1151-60.

Qiao, D., Zeeman, A.M., Deng, W., Looijenga, L.H., and Lin, H. (2002). Molecular characterization of hiwi, a human member of the piwi gene family whose overexpression is correlated to seminomas. *Oncogene* **21**: 3988-99.

Reed, J.C. (1998). Bcl-2 family proteins. *Oncogene* **17**: 3225-36.

Reventos, J., and Munell, F. (1997). Transgenic animal models in reproductive endocrine research. *Eur J Endocrinol* **136**: 566-80.

Rubin, L.L., Philpott, K.L., and Brooks, S.F. (1993). The cell cycle and cell death. *Curr Biol* **3**: 391-4.

Russell, L.D., Ettlin, R.A., Sinha Hihim, A.P., and Clegg, E.D. (1990). In Histological and Histpathological Evaluation of the Testis. Clearwater, FL: *Cache River Press* 19-161.

Saiki, R.K., Chang, C.A., Levenson, C.H., Warren, T.C., Boehm, C.D., Kazazian, H.H .Jr, and Erlich, H.A. (1988). Diagnosis of sickle cell anemia and beta-thalassemia with enzymatically amplified DNA and nonradioactive allele-specific oligonucleotide probes. *N Engl J Med* **319**: 537-41.

Sambrook, P.N., Cohen, M.L., Eisman, J.A., Pocock, N.A., Champion, G.D., and Yeates, M.G. (1989). Effects of low dose corticosteroids on bone mass in rheumatoid arthritis: a longitudinal study. *Ann Rheum Dis* **48**: 535-8.

Sanger, F., Nicklen, S., and Coulson, A.R. (1977). DNA sequencing with chain-terminating inhibitors. *Proc Natl Acad Sci U S A* **74**: 5463-7.

Sasaki, T., Shiohama, A., Minoshima, S., and Shimizu, N. (2003). Identification of eight members of the Argonaute family in the human genome. *Genomics* **82**: 323-30.

Sassone-Corsi, P. (1997). Transcriptional checkpoints determining the fate of male germ cells. *Cell* **88**: 163-6.

Sathya, P., Tomkins, D.J., Freeman, V., Paes, B., and Nowaczyk, M.J. (1999). De novo deletion 12q: report of a patient with 12q24.31q24.33 deletion. *Am J Med Genet* **84**: 116-9.

Scanlan, M.J., Simpson, A.J., and Old, L.J. (2004). The cancer/testis genes: review, standardization, and commentary. *Cancer Immun* **4**: 1-11.

Selva, D.M., Tirado, O.M., Toran, N., Suarez-Quian, C.A., Reventos, J., and Munell, F. (2000). Meiotic arrest and germ cell apoptosis in androgen-binding protein transgenic mice. *Endocrinology* **141**: 1168-77.

Sevilla, L., Aperlo, C., Dulic, V., Chambard, J.C., Boutonnet, C., Pasquier, O., Pognonec, P., and Boulukos, K.E. (1999). The Ets2 transcription factor inhibits apoptosis

induced by colony-stimulating factor 1 deprivation of macrophages through a Bcl-xL-dependent mechanism. *Mol Cell Biol* **19**: 2624-34.

Sharma, A.K., Nelson, M.C., Brandt, J.E., Wessman, M., Mahmud, N., Weller, K.P., and Hoffman, R. (2001). Human CD34 (+) stem cells express the hiwi gene, a human homologue of the Drosophila gene piwi. *Blood* **97**: 426-34.

Shinohara, T., Avarbock, M.R., and Brinster, R.L. (1999). beta1- and alpha6-integrin are surface markers on mouse spermatogonial stem cells. *Proc Natl Acad Sci U S A* **96**: 5504-9.

Shinohara, T., Orwig, K.E., Avarbock, M.R., and Brinster, R.L. (2000). Spermatogonial stem cell enrichment by multiparameter selection of mouse testis cells. *Proc Natl Acad Sci U S A* **97**: 8346-51.

Simpson, A.J., Caballero, O.L., Jungbluth, A., Chen, Y.T., and Old, L.J. (2005). Cancer/testis antigens, gametogenesis and cancer. *Nature Reviews Cancer* **5**: 615-25.

Skotheim, R.I., Kraggerud, S.M., Fossa, S.D., Stenwig, A.E., Gedde-Dahl, T. Jr., Danielsen, H.E., Jakobsen, K.S., and Lothe, R.A. (2001). Familial/bilateral and sporadic testicular germ cell tumors show frequent genetic changes at loci with suggestive linkage evidence. *Neoplasia* **3**: 196-203.

Song, J.J., Smith, S.K., Hannon, G.J., and Joshua-Tor, L. (2004). Crystal structure of Argonaute and its implications for RISC slicer activity. *Science* **305**: 1434-7.

Southern, E.M. (1975). Detection of specific sequences among DNA fragments separated by gel electrophoresis. *J Mol Biol* **98**: 503-17.

Spangrude, G.J., Heimfeld, S., and Weissman, I.L. (1988). Purification and characterization of mouse hematopoietic stem cells. *Science* **241**: 58-62.

Stephan, H., Polzar, B., Rauch, F., Zanotti, S., Ulke, C., and Mannherz, H.G. (1996). Distribution of deoxyribonuclease I (DNase I) and p53 in rat testis and their correlation with apoptosis. *Histochem Cell Biol* **106**: 383-93.

Stevens, L.C. (1967). The biology of teratomas. *Adv Morphog* **6**: 1-31.

Stevens, L.C. (1973). A new inbred subline of mice (129-terSv) with a high incidence of spontaneous congenital testicular teratomas. *J Natl Canc Inst* **50**: 235-42.

Summersgill, B., Osin, P., Lu, Y. J., Huddart, R., and Shipley, J. (2001). Chromosomal imbalances associated with carcinoma *in situ* and associated testicular germ cell tumours of adolescents and adults. *Br J Cancer* **85**: 213-20.

Tadokoro, Y., Yomogida, K., Ohta, H., Tohda, A., and Nishimune, Y. (2002). Homeostatic regulation of germinal stem cell proliferation by the GDNF/FSH pathway. *Mech*

Dev **113**: 29-39.

Trauth, K., Mutschler, B., Jenkins, N.A., Gilbert, D.J., Copeland, N.G., and Klempnauer, K.H. (1994). Mouse A-myb encodes a trans-activator and is expressed in mitotically active cells of the developing central nervous system, adult testis and B lymphocytes. *EMBO J* **13**: 5994-6005.

Uetsuki, T., Naito, A., Nagata, S., and Kaziro, Y. (1989). Isolation and characterization of the human chromosomal gene for polypeptide chain elongation factor-1 alpha. *J Biol Chem* **264**: 5791-8.

Umeda, J., Sano, S., Kogawa, K., Motoyama, N., Yoshikawa, K., Itami, S., Kondoh, G., Watanabe, T., and Takeda, J. (2003). In vivo cooperation between Bcl-xL and the phosphoinositide 3-kinase-Akt signaling pathway for the protection of epidermal keratinocytes from apoptosis. *FASEB J* **17**: 610-20.

van Kempen, M., van Ginneken, A., and de Grijs, I. (2003). Expression of the electrophysiological system during murine embryonic stem cell cardiac differentiation. *Cell Physiol Biochem* **13**: 263-70.

Vogelstein, B., and Gillespie, D. (1979). Preparative and analytical purification of DNA from agarose. *Proc Natl Acad Sci U S A* **76**: 615-9.

Volpe, T.A., Kidner, C., Hall, I.M., Teng, G., Grewal, S.I., and Martienssen, R.A. (2002). Regulation of heterochromatic silencing and histone H3 lysine-9 methylation by RNAi. *Science* **297**: 1833-7.

Watt, F.M. (2002). Role of integrins in regulating epidermal adhesion, growth and differentiation. *EMBO J* **21**: 3919-26.

Weissman, I.L. (2000). Stem cells: units of development, units of regeneration, and units in evolution. *Cell* **100**: 157-68.

Williams, D.A., Rios, M., Stephens, C., and Patel, V.P. (1991). Fibronectin and VLA4 in hematopoietic stem cell-microenvironment interactions. *Nature* **352**: 438-41.

Wright, M.D., and Tomlinson, M.G. (1994). The ins and outs of the transmembrane 4 superfamiliy. *Immunol Today* **15**: 588-94.

Xu, C., Inokuma, M.S., Denham, J., Golds, K., Kundu, P., Gold, J.D., and Carpenter, M.K. (2001). Feeder-free growth of undifferentiated human embryonic stem cells. *Nat Biotechnol* **19**: 971-4.

Yang, X.W., Wynder, C., Doughty, M.L., and Heintz, N. (1999). BAC-mediated gene-dosage analysis reveals a role for Zipro1 (Ru49/Zfp38) in progenitor cell proliferation in cerebellum and skin. *Nat Genet* **22:** 327-35.

Yoon, C., Kawakami, K., and Hopkins, N. (1997). Zebrafish vasa homologue RNA is localized to the cleavage planes of 2- and 4-cell-stage embryos and is expressed in the primordial germ cells. *Development* **124**: 3157-65.

Yoshida, K., Kondoh, G., Matsuda, Y., Habu, T., Nishimune, Y., and Morita, T. (1998). The mouse RecA-like gene Dmc1 is required for homologous chromosome synapsis during meiosis. *Mol Cell* **1**: 707-18.

Zamzami, N., Brenner, C., Marzo, I., Susin, S.A., and Kroemer, G. (1998). Subcellular and submitochondrial mode of action of Bcl-2-like oncoproteins. *Oncogene* **16**: 2265-82.

Zendman, A.J., Ruiter, D.J., Van Muijen, G.N. (2003). Cancer/testis-associated genes: identification, expression profile, and putative function. *J Cell Physiol* **194**: 272-88.

Zirkin, B.R., Santulli, R., Strandberg, J.D., Wright, W.W., and Ewing, L.L. (1993). Testicular steroidogenesis in the aging brown Norway rat. *J Androl* **14**: 118-23.

Zhao and Garbers. (2002). Male germ cell specification and differentiation. *Dev Cell* **2**: 537-47.

Curriculum vitae

I. Personal Data

Full Name:	Lee, Jae-Ho
E-mail:	vincent1225@daum.net; jlee2@gwdg.de
Date of Birth:	8th August, 1972
Sex:	Male
Present Address:	Zimmermannstr. 11, Nr.413, D-37075, Goettingen, Germany
Nationality:	Korean
Marital Status:	Single

II. Educational Background:

Mar. 1991 - Feb. 1998:	Bachelor of Science, Department of Molecular Biotechology, Hankuk University of Foreign Studies, Seoul
May. 1993 - Jul. 1995:	Military Service (Army)
Mar. 1999 - Feb. 2001:	Master of Science, Department of Biological Sciences, Seoul National University Thesis Topic: **"Characterization of a novel gene related to *dpp (decapentaplegic)* signaling in Drosophila wing formation"**
Feb. 2003 - May. 2006:	Doctorate of Philosophy (Ph.D), Institute of Human Genetics, Georg-August-Universität Göttingen, Germany Thesis Topic: **"Analysis of the role of Piwil2 gene in tumorigenesis and germline stem cell metabolisms"**

III. Occupation:

Oct. 2001 - Sep. 2002: Principal Research Scientist, "KeeGene" Life Science institute, Seoul

IV. Publications:

1. **Jae Ho Lee**, Wolfgang Engel, Karim Nayernia. Stem Cell Protein Piwil2 Modulates Expression of Murine Spermatogonial Stem Cell Expressed Genes. ***Molecular Reproduction and Development.*** 2006 Feb;73(2):173-9.

2. **Jae Ho Lee**, Dorothea Schütte, Gerald Wulf, Laszlo Füzesi, Heinz-Joachim Radzun, Stephan Schweyer, Wolfgang Engel, Karim Nayernia. Stem cell protein Piwil2 is widely expressed in tumors and inhibits apoptosis through activation of Stat3/Bcl-X_L pathway. ***Hum Mol Genet.*** 2006 Jan 15;15(2):201-11.

3. Kaomei Guan, Karim Nayernia, Lars S. Maier, Stefan Wagner, Ralf Dressel, **Jae Ho Lee**, Jessica Nolte, Frieder Wolf, Manyu Li, Wolfgang Engel, Gerd P. Hasenfuss. Pluripotency of spermatogonial stem cells from adult mouse testis. ***(Nature, In Press)***.

4. Nadja Drusenheimer, Gerald Wulf, Jessica Nolte, **Jae Ho Lee**, Jorg Gromoll, Jorg Schmidtke, Wolfgang Engel and Karim Nayernia. Putative human male germ cells from bone marrow stem cells. ***(Reproduction, In Press)***.

5. Karim Nayernia, **Jae Ho Lee**, Nadja Drusenheimer, Jessica Nolte, Gerald Wulf, Iris Schwandt, Christian Müller, Jörg Gromoll and Wolfgang Engel. Derivation of male germ cells from bone marrow stem cells. ***(Laboratory investigation, In Press)***.

6. Karim Nayernia, Jessica Nolte, Hans W. Michelmann, **Jae Ho Lee**, Nadja Drusenheimer, Iris Schwandt, Gerald Wulf, Ingrid E. Ehrmann, David J. Elliott, Ulrich

Zechner, Thomas Haaf, Andreas Meinhardt and Wolfgang Engel. Progeny from Embryonic Stem Cell-derived Male Gametes. ***(Revision resubmitted to Developmental Cell)***.

7. **Jae Ho Lee**, Cornelia Jung, Stephan Schweyer, Dorothea Schütte, Ralf Dressel, Laszlo Füszesi, Wolfgang Engel and Karim Nayernia. Establishment of diagnostic and therapeutical approaches for breast cancer using Piwil2. ***(International journal of cancer, In Preparation)***.

8. **Jae Ho Lee**, Jessica Nolte, Nadja Drusenheimer, Wolfgang Engel and Karim Nayernia. New sources of stem cells for reproductive medicine. **(*Current Medicinal Chemistry, In Preparation)***.

9. **Jae Ho Lee**, Dirk G. De Rooij, Stephan Schweyer, Andreas Meinhardt, Christian Müller, Stephan Wolf, Wolfgang Engel and Karim Nayernia. Impaired spermatogenesis in mice overexpressing stem cell protein Piwil2. ***(Molecular Reproduction and Development, In Preparation)***.

ACKNOWLEDGEMENTS

There are many people to whom I wish to thank and who helped me, taught me and encouraged me along the way. First of all, I appreciate God to keep my mind and draw me close to YOU through foreign life.

I would like to express my deepest gratitude to Prof. Dr. W. Engel for his support, encouragement, and excellent scientific supervision. It has been a pleasure working in such an inspiring and friendly atmosphere as he has created in the Institute of Human Genetics.

I wish to express sincere appreciation to my supervisor PD. Dr. Karim Nayernia for proofreading the manuscript, his help and friendly relationship throughout my study.

I sincerely thank PD Dr. S. Hoyer-Fender to be my co-referee. I also extend my sincere thanks to Prof. Dr. Stephan Robbert Gradstein and PD. Dr. Rolf Daniel for accepting to be my examiners.

I would like to thank all my institute colleagues for being so friendly and helpful during my stay for their numerous advices, constant support, and fantastic work atmosphere.

I would like to appreciate the current and former members of lab. 107: Iris, Christian, Arvind, Lukasz, Jessica, Loukas, Ute, Irakli, Nadja , Moneef, Rovena, Diana, Kristina, Cornelia, Zanabazar, Johannes, Jan, Sandra and lab 108: Oggy, Byambaa, Katy, Torsten, Ilona, Wolfgang, Ozanna, Meike and lab 114: Krishna, Tomoko, Ashraf and Jutta, Tae Won for the international atmosphere, opportunity to know your culture and countries better. You did not only create a very pleasant working atmosphere but also make it hard to leave.

Finally, I must express my deepest gratitude to my parents, brother and sisters for their emotional support and encouragement from home; you are so far away, but always deep in my heart.

Finally, and most importantly, this work would not have been possible without the love and my best friends: Chung Ah, Uh Jin, Jeong Im, Jong In, Seung Han, Ji Hye, Jung Yeol, Ji Hwan, Yun Yong, Sung Eun, Suk Yeol, Bo Ram, Joo Hee, So Mi, Seung Hee, Mi Jeong, Sin Hong, Hyo Jin, Sang Hwan, Ji Hyun, Su Sie and closest companions. Thank you for the encouragement and the understanding during all those stressful hours.